

Journal of Drug Delivery Science and Technology

Synthesis of pH-sensitive ternary hydrogel with synergetic antibacterial response for the release of ampicillin sodium

--Manuscript Draft--

Manuscript Number:	JDDST-D-24-03283R1
Article Type:	Research Paper
Keywords:	Chitosan; controlled release; ratan-jot extract; Ampicillin sodium; Antibacterial response
Corresponding Author:	Huma Andlib University of the Punjab Quaid-i-Azam Campus PAKISTAN
First Author:	Huma Andlib
Order of Authors:	Huma Andlib Muhammad Shafiq Aneela Sabir Sehrish Jabeen Timothy Douglas
Abstract:	<p>In the area of biomedicine, pH-responsive hydrogels have attracted a lot of attention. The smart novel polyelectrolyte complex carriers are made of chitosan, gum arabic and polyvinylpyrrolidone using various concentrations of ratan-jot plant extract for the release of sodium ampicillin antibiotic very first time. These hydrogels have been prepared by solution casting method and cross-linked by using 3-aminopropyl diethoxymethyl silane. According to swelling experiments, the cross linker concentration led to decreased swelling because the hydrogels were more tightly packed together. CPG-3A showed maximum swelling 54.5g/g in 210 minutes. When the swelling behaviour of hydrogels was tested under various pH circumstances, it was found that they swelled most noticeably in alkaline media and least noticeably in acidic and neutral pH settings. These hydrogels may be appropriate for injection-based controlled drug release due to their unique pH-responsive behaviour. Ampicillin sodium salt was utilised as a model drug to analyse drug release behaviour of engineered hydrogel at pH 7.4. The results indicate that these smart hydrogels could be used for injectable controlled drug release (ampicillin sodium) for the treatment of wound as well as for other biomedical applications.</p>
Suggested Reviewers:	Karl Jacob karl.jacob@mse.gatech.edu Wail Falath wfallata@kfupm.edu.sa Karen Gleason kkg@mit.edu Nafisa Gull nafisagull@gmail.com
Opposed Reviewers:	
Response to Reviewers:	

Editor,

Journal of Drug Delivery Science and Technology

Reference No: **JDDST-D-24-03283**

Dated: November 4, 2024

Sir,

The manuscript titled **“Synthesis of pH-sensitive ternary hydrogel with synergetic antibacterial response for the release of ampicillin sodium.”** has been revised in the light of referee’s suggestions. I hope, now the manuscript is acceptable for publication in **“Journal of Drug Delivery Science and Technology”**.

With best regards and wishes.

Yours sincerely,

Huma Andlib

Ph.D. scholar

Department of Polymer Engineering and Textile, University of the Punjab

Lahore, Pakistan

Phone: +92 3324534788

E-mail: hshah3421@gmail.com

Synthesis of pH-sensitive ternary hydrogel with synergetic antibacterial response for the release of ampicillin sodium

Huma Andlib^{1,*}, Muhammad Shafiq¹, Aneela Sabir¹, Sehrish Jabeen², Timothy Douglas³.

¹Institute of Polymer and Textile Engineering, University of the Punjab, Lahore, 54590, Pakistan

²Institute of Polymer Materials, Friedrich-Alexander-University Erlangen-Nuremberg, Martensstrasse 7,91058 Erlangen, Germany

³School of Engineering, Gillow Avenue, Lancaster University, Lancaster, LA1 4YW, United Kingdom

Corresponding author: Huma Andlib*, Email: hshah3421@gmail.com,

Phone: +923324534788

Abstract

In the area of biomedicine, pH-responsive hydrogels have attracted a lot of attention. The smart novel polyelectrolyte complex carriers are made of chitosan, gum arabic and polyvinylpyrrolidone using various concentrations of ratan-jot plant extract for the release of sodium ampicillin antibiotic very first time. These hydrogels have been prepared by solution casting method and cross-linked by using 3-aminopropyl diethoxymethyl silane. According to swelling experiments, the cross linker concentration led to decreased swelling because the hydrogels were more tightly packed together. CPG-3A showed maximum swelling 54.5g/g in 210 minutes. When the swelling behaviour of hydrogels was tested under various pH circumstances, it was found that they swelled most noticeably in alkaline media and least noticeably in acidic and neutral pH settings. These hydrogels may be appropriate for injection-based controlled drug release due to their unique pH-responsive behaviour. Ampicillin sodium salt was utilised as a model drug to analyse drug release behaviour of engineered hydrogel at pH 7.4. The results indicate that these smart hydrogels could be used for injectable controlled drug release (ampicillin sodium) for the treatment of wound as well as for other biomedical applications.

Keywords. Chitosan; Controlled release; Ratan-jot extract; Ampicillin sodium; Antibacterial response

Highlights

- A ternary biopolymer based hydrogel was fabricated via solution casting method.
- The synthesized ternary hydrogels were analysed by TGA, SEM, FTIR.
- Cytotoxicity and antibacterial behaviour of CPGs hydrogel was also investigated.
- Ampicillin sodium was released in controllable way and it was 98.717%.

1. Introduction

The production of precise and targeted dosage forms has become more important for efficiently treating illnesses and recovering patients well-being keeping in view of the alarming increase in diseases and health issues. Conventional way of drugs intake possess uncontrolled side effects, because administered drug also reached to the other parts of body and very minor proportion of drug reached to the infected area of body [1, 2].

Now a days, researchers are more attentive and eager for the development of new category of therapeutic materials to solve the emerging problems of bio-therapeutics and drug access to the targeted site without any adverse side effect [3-5]. To increase the specificity of drug distribution system and to decrease the toxicity of drugs, many devices are synthesized since last few

decades to overcome the severe attack of various diseases. To address these issues of drug delivery system we focused here the release of drug from bio-polymers based hydrogel system. Hydrogel is an emerging field and considered as structural backbone for development of novel and potent therapeutic agents [6].

Hydrogel, plays an indispensable role in our daily life due to their marvellous properties. Hydrogels show capacity to absorb the high quantity of water and having a three-dimensional(3D) cross linked, or a straight or a forked water loving structure. Hydrophilicity behaviour of hydrogel is produced because of the presence of some water loving groups like -OH, -COOH, -NH₂. They show swelling variation with changing in their structure and potential properties, in response to various stimulus [3, 6-10]. In this contemporary era, hydrogels can be synthesized through natural, synthetic as well as from semi synthetic polymers. Biopolymers made hydrogels are more effective because of their exceptional properties, like non-hazardous behaviour, good biocompatibility, excellent biodegradability and economical suitability etc. This is the reason they play significant role in the relief of pain as well as to overcome diseases and many more other biomedical applications [11, 12]. Among biopolymers, the chitosan and its derivative are cationic polymers with antioxidant, anti-bacterial (against many microorganisms with a high mortality rate) and antifungal properties making it unique for targeted drug delivery platform [7, 13, 14]. Chitosan is derivative of chitin and generated by its deacetylation This is the second most prevalent biopolymer in the world after cellulose and exist in exoskeleton of insects and crustaceans like crabs, lobsters etc., [15-17]. Gum arabic is one of the ancient gum well-known due to its numerous application approximately for more than 5000 years. Gum arabic is composed of polysaccharides as well as glycoproteins mainly the polymers of galactose and arabinose. Gum Arabic shows excellent properties like water solubility, antioxidant properties, antibacterial, haemostatic and non-haemolytic properties. Non digestible properties make it more attractive in the field of pharmaceutical industries [18-20]. Although, the biopolymers show good compatibility to human body but on the other hand, mechanical strength of biopolymer-based hydrogel is usually low. This problem can be controlled by unification of biopolymer with a synthetic polymer or even with some other appropriate biopolymer. This strategy will not only improve the sustainability of hydrogels but also plays an important role to keep their structure intact for the period of drug delivery by enhancing the hydrogels thermal stability [21]. These combined biomaterials with non-natural polymers like polyvinyl pyrrolidone (PVP), also known as polyvidone (C₆H₉NO)_n have proved excellent in achieving extraordinary mechanical strength. PVP is amorphous polymer, it shows good water solubility as it is hydrophilic in nature but it

is also soluble in organic solvents [22]. PVP is considered as a potential polymer because it attracts pharmacist due to its distinctive properties like cytocompatibility, non-toxicity, cheap and biodegradability [23-26]. Silane based cross linkers are getting more attraction by scientists as these possess countless unique properties. Cross linker increases mechanical strength of hydrogels as well as control high swelling rate by making chemical bonds with their reactive groups to the polymer functional groups. In this study, we pick out a 3-aminopropyl (diethoxy)methyl-silane cross linker due to its bio functional properties as well as its environmental friendly behaviour. The mechanical strength and drug loading capacity of a hydrogel is increased by dual crosslinking ability of 3-aminopropyl (diethoxy) methyl-silane through its amino and silane groups. Hydrogen and covalent bonds are formed between amino group of 3-APDEMS and polymeric groups [27]. Plethora of plants extracts are also used in hydrogel synthesis as polyphenols, carotenoids due to their anti-oxidant and anti-bacterial properties. Extraction from the roots of alkanet plant are used to produce a red dye. One of the famous name of red dye is ratan-jot. This red dye is basically herbal drug that is famous for its anthelmintic, antipyretic and antiseptic behaviour. It plays an undeniable role in various types of wounds treatment. However, naphthoquinones, is the main component of drug (extracted from roots of plant) that is responsible for its red colour. In fact, therapeutic behaviour of drug is due to naphthoquinone [28-30].

The broad-spectrum antibiotic ampicillin is a white crystalline powder that dissolves in water easily. It is frequently used to treat bacterial infections and works well for a variety of problems, such as gonorrhoea, respiratory and urinary tract bacterial infections and several illnesses of the gastrointestinal and neurological systems. Because of its good adaptability, ampicillin is a good choice for treating a range of bacterial infections.

This study comprises, synthesis of novel ternary polysaccharide based hydrogel made of chitosan (CS), polyvinylpyrrolidone (PVP) and gum arabic(GA) in the presence of cross linker 3-aminopropyldiethoxymethylsilane (3-APDEMS) with variable concentrations of ratan-jot (RJ) ethanolic extract. Ampicillin sodium salt was added to the hydrogel as a model drug in order to study its antibiotic release characteristic. This formulation was not used yet according to best of our knowledge. The fabricated hydrogel was analysed by FTIR, TGA, SEM, Biodegradation, water swelling, cytotoxicity and by antibacterial test.

2. Experimental details

2.1 Materials

CS (Mw = 406,039 g/mol, degree of deacetylation (DDA) 90%). Polyvinylpyrrolidone (PVP) (Mw = 40,000–70,000 g/mol), Acetic acid (CH₃COOH) (100%) extra pure was purchased from

Merck, Germany. respectively, 3-Aminopropyldiethoxymethylsilane (97%) were obtained from Sigma Aldrich. Gum arabic (Mw = 250,000 Da), purchased from Sigma Aldrich (USA). Ratan-jot ethanoic extract was made at indigenous level in the laboratory. Sodium dihydrogen phosphate (Na_2HPO_4), Boric acid, NaCl (Sodium chloride), KCl (Potassium chloride), CaCl_2 (Calcium chloride) and Potassium dihydrogen phosphate (KH_2PO_4) were also obtained from Sigma-Aldrich. Sodium acetate (CH_3COONa) and sodium hydroxide (NaOH) were obtained from Riedel-de Haen. HCl (hydrochloric acid) and Ethanol ($\text{C}_2\text{H}_5\text{OH}$) were purchased from BDH laboratory supplies and J.T. Baker, respectively. We used analytical-grade chemicals in our studies, using them directly without any need for purification.

2.2 Methodology

2.2.1 Extraction of ratan-jot (Alkanna tinctoria) extract

Ethanolic extract of ratan-jot has been prepared by conventional method. In this study the roots of the plant were washed properly to remove mud completely. The roots were then blotted and dried by filter paper by changing the filter paper regularly after few intervals. These were further dried in sunlight for 7 days, in oven at 50 °C and finally dried in a vacuum desiccator. The completely dried roots were, thereafter, grinded and sieved to get a fine powder and was stored in air tight bottle. 10 grams of this powder was weighed and added in 50 ml of ethanol in a sample bottle and was stored in dark place for 14 days. Finally, after 14 days all the extract got infuse in the ethanol.

2.2.2 Preparation of Hydrogel

Chitosan (0.6 g or 60 wt%) was dispersed in 50 ml of 0.5 % acetic acid solution at temperature of 60°C with stirring continuously for 3 hours to get complete dissolution. Gum arabic (0.1 g or 10 wt%) was dissolved in 40 ml double distilled water with magnetic stirring at 50°C until it became a smooth solution. Gum arabic solution was mixed with chitosan solution and was put again on magnetic stirring at 50°C for another 2 hours to get homogeneous blend. PVP (0.3 g or 30 wt%) was solvated in 50 ml of double distilled water with magnetic stirring at 95°C on hot plate. Then PVP solution was blended with chitosan and GA solution by magnetic stirring for 2 hours on hot plate at 50°C. The ethanolic extract of ratan-jot was added in ternary blend (CS/GA/PVP) and was stirred for 1 hour. The 3-APDEMS cross linker was first added in 5 ml of ethanol and then added drop wise in CS/GA/PVP/RJ blend. This later solution was vortexed and then stirred for minimum 4 hours for maximum crosslinking at same temperature. The prepared solution was added to petri dishes before being dried in a vacuum oven (LVO-2040, Lab Tech, Korea) at 60°C. **The ethanol was evaporated when the hydrogel film dried and the remaining residues of acetic acid were removed by washing it with distilled water.**

Through use of the same processes, four formulations were made, each with a varied rattan-jot concentration ranging from 0 to 300 μL and a constant cross-linker concentration of 50 μL . The control hydrogel was synthesized with neither cross linker nor rattan-jot and named CPG. Hydrogel with just cross linker code as CPG-3A. The hydrogel with 50 μL cross linker and with 100 μL quantity for rattan-jot code as CPG-3AR1. Further, hydrogel with same the volume of cross linker and 300 μL of rattan-Jot code as CPG-3AR2. Table.1. exhibits the hydrogels composition along their specific code.

Table .1 Chemical compositions of prepared hydrogels.

Sample code	Chitosan (g)	Gum Arabic (g)	PVP(g)	Ratan-jot(μL)	3-APDEMS(μL)
CPG	0.6	0.1	0.3	0.0	0.0
CPG-3A	0.6	0.1	0.3	0.0	50
CPG- 3AR1	0.6	0.1	0.3	100	50
CPG -3AR2	0.6	0.1	0.3	300	50

The possible interactions taking place within the hydrogel components are depicted in Figure.1.

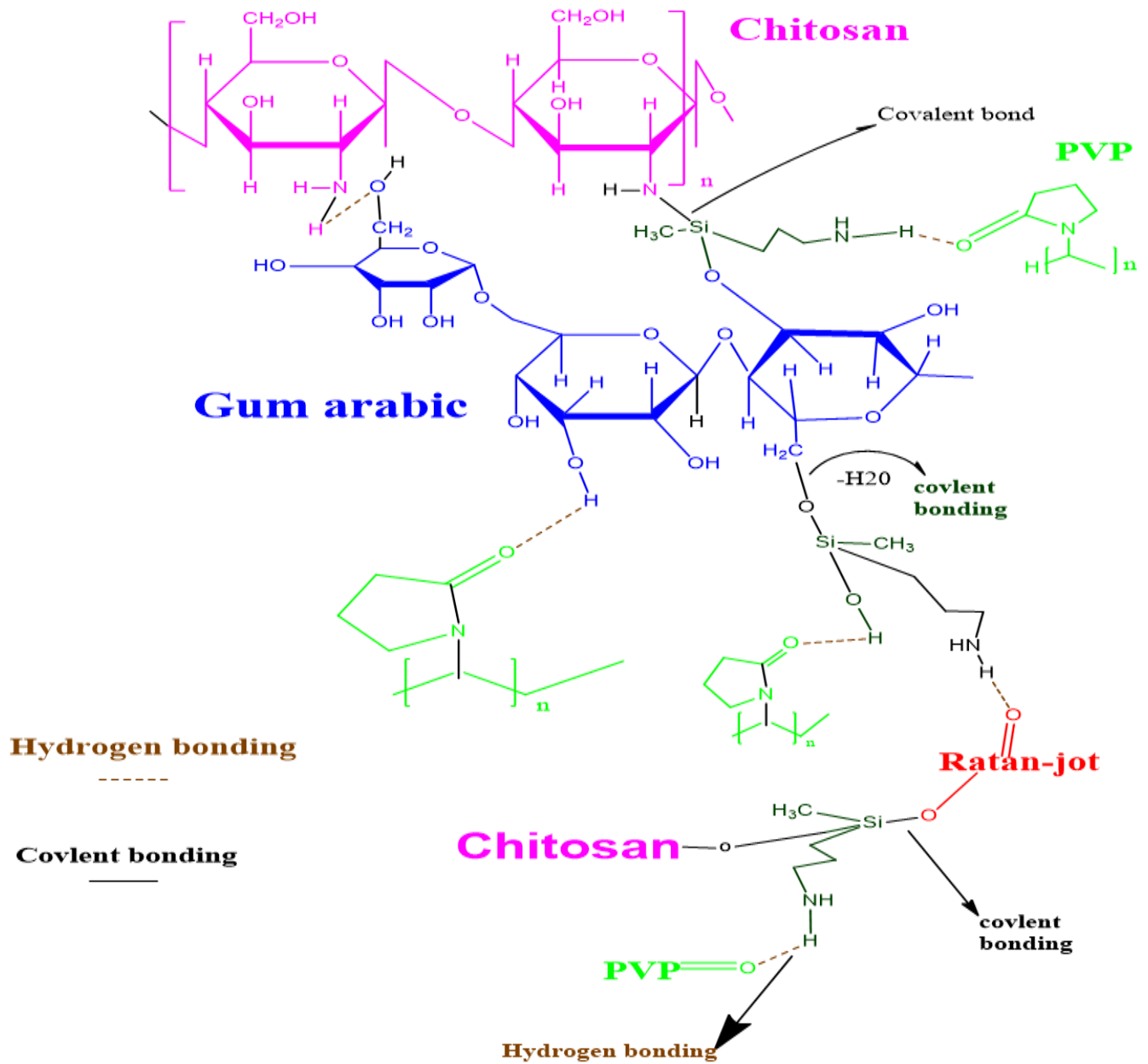


Fig.1 Schematic interactions between the components of the CPGs hydrogel.

2.3 Antibiotic-loaded hydrogel synthesis

Chitosan (0.6 g or 60 wt%) was dispersed in 50 ml of 0.5% acetic acid solution at temperature 60°C with stirring continuously for 3 hours to get complete dissolution. Gum arabic (0.1 g or 10 wt%) was dissolved in 40 ml double distil water with magnetic stirring at 50°C until it became a smooth solution. Gum arabic solution was mixed with chitosan solution and put it again on magnetic stirring at 50°C for another 2 hours to get homogeneous blend. PVP (0.3 g or 30 wt%) was solvated in 50 ml of double distilled water with magnetic stirring at 95°C on hot plate. The polyvinylpyrrolidone (PVP) solution was blended with chitosan and GA blend by

magnetic stirring for 2 hours on hot plate at 50°C. Ethanol extract of ratan-jot 300 µL was added in synthesized ternary blend (CS/GA/PVP) and stirred for 1 hour. Afterward 50 mg of ampicillin sodium drug was dissolved in distilled water and added to the blend.

The 3-APDEMS cross linker was first added in 5 ml of ethanol and thereafter added drop wise in CS/GA/PVP/RJ + Drug blend. This later solution was put on stirring for 4 hours for maximum crosslinking at same temperature. The fabricated solution was cast in petri dishes and desiccated. by using a drying oven (LVO-2040, Lab Tech, Korea) at 60°C under vacuum desiccator.

3. Characterizations

3.1 Fourier transform infrared microscopy

To confirm the existence of particular functional groups and to clarify interactions between the hydrogel components, FTIR spectra were obtained for all hydrogel samples (CPG, CPG-3A, CPG-3AR1, CPG-3AR2). The FTIR spectra were collected using FTIR spectrophotometer with a resolution of 2 cm⁻¹, a scan rate of 32 scans per spectrum and a programmed range of 4000 to 400 cm⁻¹ (Model: Tensor II, Bruker).

3.2 Swelling studies

3.2.1 Swelling trend in distilled water

The fully dried hydrogel was initially divided into tiny 25 mg pieces in order to assess the hydrogels response when swollen in distilled water. Next, 40 ml of double-distilled water was poured into a plastic petri dish with these hydrogel fragments. After predetermined time, the water was drained from the petri dish. (for instance, 10 minutes) and the petri dish was then gently cleaned with tissue paper to remove any remaining water. The swelled hydrogel sample weights were calculated accordingly. This process was continued until equilibrium was attained. Each hydrogel was subjected to this complete experiment three times in order to achieve the mean value for more accurate findings. The swelling ratio was determined by using following formula

$$Swelling \left(\frac{g}{g} \right) = \frac{W_s - W_d}{W_d} \quad (1)$$

Here W_d is the weight of vacuum dried hydrogel at a specific time interval and W_s denotes the weight of swelled hydrogel at time [31].

3.2.2 Swelling trend in pH solutions

Individually prepared buffer solutions with different pH values (1.2, 2, 4, 6, 7, 8, 10) were submerged with pre-measured hydrogel samples, and they were let to approach equilibrium. The buffer solution was then removed, and the hydrogel samples were delicately patted with

paper to remove the surface solvent. The weight of the swelled hydrogel was measured, and the degree of swelling was estimated using the formula given before. To increase the accuracy of the results, this process was performed three times.

3.2.3 Swelling trend in ionic solutions.

The evaluation of electrolyte solution swelling was done. In particular, prepared electrolyte solutions containing NaCl and CaCl₂ at different concentrations (0.2, 0.4, 0.6, 0.8, and 1.0 M) were made in accordance with known procedures. Utilising the same technique described in Section 3.2.1, the swelling indices of the hydrogels made in various electrolyte solutions were calculated.

3.3 Thermogravimetric analysis

TGA of hydrogels was carried out on Thermal analysis instrument SDT build 95 module DSC-TGA standard, USA, with nitrogen flow of (15 ml/min). The temperature range was kept at 20 °C per-min from ambient room temperature to 600 °C.

3.4 *In-vitro* biodegradation

CPG samples were cross-linked with fixed concentration of 3-APDEMS and different ratan-jot extract concentrations before being dipped into a PBS solution at 37 °C. At certain intervals (1, 2,3,4, 5 and 6 days), the degradation of the samples was monitored. The samples were removed from the solution, thoroughly dried with blotting paper to eliminate any excess solution, weighed, and afterward submerged in new PBS solution once more. To avoid any contamination from bacteria or fungi, all studies were conducted in sterilised environments. Using the following equation (2), the biodegradability of the hydrogel samples was calculated

$$\text{Biodegradation (\%)} = \frac{W_d - W_i}{W_i} \times 100 \quad (2)$$

where W_d is the weight of the CPG samples following degradation and W_i is the weight of the CPG specimens at their initial composition [32, 33].

3.5 Antimicrobial profile

CPGs were tested against Escherichia coli (*E. coli*) and *B.Subtilis* to determine their antibacterial efficacy. The sterile Luria-Bertani (LB) medium was used to monitor the growth of the bacterial strain. It was made by dissolving 10 g of tryptone, 5 g of yeast, and 10 g of NaCl in 800 ml of distilled water while keeping the pH neutral. Following volume adjustment to 1000 ml, the solution was autoclave sterilized for one hour. During the sample preparation process, a hydrogel sample (5 × 5 mm) was added after mixing 20 ml of LB media and 20 ml of bacterial strain (*E. coli* or *B.Subtilis*). The control group underwent the same process again. Using a

spectrophotometer (Double beam, PerkinElmer, Model Lambda25, USA) set to measure optical densities at 600 nm, the antibacterial efficacy was evaluated [34].

3.6 Cytotoxicity Evaluation *in-vitro*

Using the brine shrimp lethality assay, a typical method for preliminary toxicity screening, *in vitro* cytotoxicity study was carried out. Brine shrimp eggs were incubated for 48 hours at room temperature in sterile sea water with constant aeration in order to conduct the experiment. Active nauplii were taken after hatching and moved to a deep well microliter plate from the brighter area of the hatching vessel. Each well of the plate was 1.8 cm in diameter, 2 cm deep, and contained 0.2 ml of saltwater. In the wells containing active nauplii, hydrogel samples were inserted in triplicate and the immature larvae were counted. The experiment involved keeping the well plate at normal temperature and in the dark. Following a 24-hour observation period, observations of surviving nauplii were made under a microscope (GXM, XPL33230; GT Vision, Haverhill, UK) and tallied to determine mortality using Equation (3)

$$M(\%) = \frac{A-B-N}{G-N} \times 100 \quad (3)$$

Where: After 24 hours, M is the proportion of dead larvae.

A is the quantity of dead larvae after 24 hours.

B represents the typical number of dead larvae in the control samples after a day.

G = the total number of larvae,

N = the number of dead larvae before the test.

This formula made it possible to calculate the proportion of dead larvae after 24 hours while taking into account the control samples and beginning larval population [35].

3.7 Porosity

Using the solvent displacement method, the synthetic hydrogels' porosity was evaluated. As a standard, 100% ethanol was employed as the displacing solvent. An electronic Vernier calliper, the Fowler 6/150 mm Pro-Max Electronic Calliper 54-200-777-1, was used to measure the length, width, and volume of dry hydrogel films. To successfully permeate the hydrogel pores, pre-weighed hydrogel samples were submerged in the displacement solvent for 24 hours. The samples that had been soaked were taken out of the solvent after 24 hours and weighed again. Each sample went through this procedure three times. Equation 4 was used to calculate the percentage of porosity [36].

$$\text{Porosity \%} = \frac{M_2 - M_1}{\rho V} \times 100 \quad (4)$$

Here, M_1 is the weight of sample before dipped in ethanol and M_2 is the weight of the hydrogel sample after it has been soaked in ethanol. V is the volume of sample and ρ is the density of ethanol.

3.8 Scanning electron microscopy

Scanning electron microscopic analysis (SEM) was used for Surface morphology of the hydrogel. Hydrogels were inspected through SEM, Model JEOL/EO JSM 6480 (LA) Akishima, Tokyo, Japan. At different magnification the SEM images of hydrogels were recorded. A 48-hour freeze-drying procedure in liquid nitrogen under vacuum conditions was used to retain the hydrogel's porous cross-linked structure without compromising it. Approximately 0.2 mm was the thickness of the samples.

3.9 Contact angle

The wettability of the hydrogel surfaces after hydration was evaluated using the Contact Angle (CA) measurement. We used a Dataphysics Model OCA20 (Filderstadt, Germany) to do this assessment at room temperature. Before being placed on a glass cover slide, the hydrated hydrogel samples were divided into 2 cm² pieces. Using a micrometric syringe, ten microliters of deionized water were injected onto the sample surface. After taking a still picture, the inbuilt software was used to calculate the contact angle. We recorded the average values of each sample after it was tested ten times ($n = 10$).

3.10 Drug release profile

Phosphate buffer saline (PBS) solution of pH 7.4 was used to study drug release. In 500 ml of deionized water, 4.0 g of NaCl, 0.12 g of KH₂PO₄, 0.1 g of KCl, and 0.72 g of Na₂HPO₄ were mixed to make the PBS solution. At 37 °C, 100 ml of the PBS solution was used to submerge the drug-loaded hydrogel. In order to keep the beakers total volume at 100 mL, 5.0 ml of the solution was taken out and replaced every 10 minutes with an equal amount of brand-new PBS solution. A UV-Vis spectrophotometer (more precisely, a double-beam Perkin Elmer Model Lambda 25 USA) with a wavelength of 205 nm was used to analyse the samples over the course of three hours. For comparison, ampicillin sodium reference solution with a 100 ppm concentration was also made.

$$\text{Cumulative release (\%)} = \left(\frac{M_t}{M_0} \right) 100\% \quad (5)$$

In this context, M_t stands for the amount of ampicillin that was liberated from the hydrogel at a given time t , whereas M_0 stands for the initial amount of ampicillin that was injected into the hydrogels [37].

4. Results and discussion

4.1 FTIR

FTIR spectra of all the hydrogel samples (CPG, CPG-3AR1, CPG-3AR2, CPG-3A) are given in Figure 2. For chitosan the absorption peaks of amide I was confirmed at 1674 cm^{-1} . The bands detected at 890 cm^{-1} and 1167 cm^{-1} were due to the existence of chitosan pyranose ring and saccharine. The symmetric and asymmetric C-H stretching in chitosan, gum arabic showed peaks at $2916\text{--}2873\text{ cm}^{-1}$. The hydrogen bond between polymeric chains, both intra- and intermolecular bonds, were confirmed by the broad peak value at $3556\text{--}3080\text{ cm}^{-1}$ that confirms the -OH stretching of all prepared hydrogels. The stretching vibration of C-N of PVP within the hydrogel networks are observed at peaks $1200\text{--}1400\text{ cm}^{-1}$. The Si-N peak appeared in the range of $934\text{--}940\text{ cm}^{-1}$. Carbonyl peak range (1655 cm^{-1} - 1649 cm^{-1}) confirmed that it shifted to lower wavenumber (1649 cm^{-1}) because of the formation of hydrogen bonding. The presence of Si-O-Si and Si-O-C that confirmed the crosslinking due to silanol groups showed the peaks, at of $1128\text{--}1016\text{ cm}^{-1}$ [38, 39].

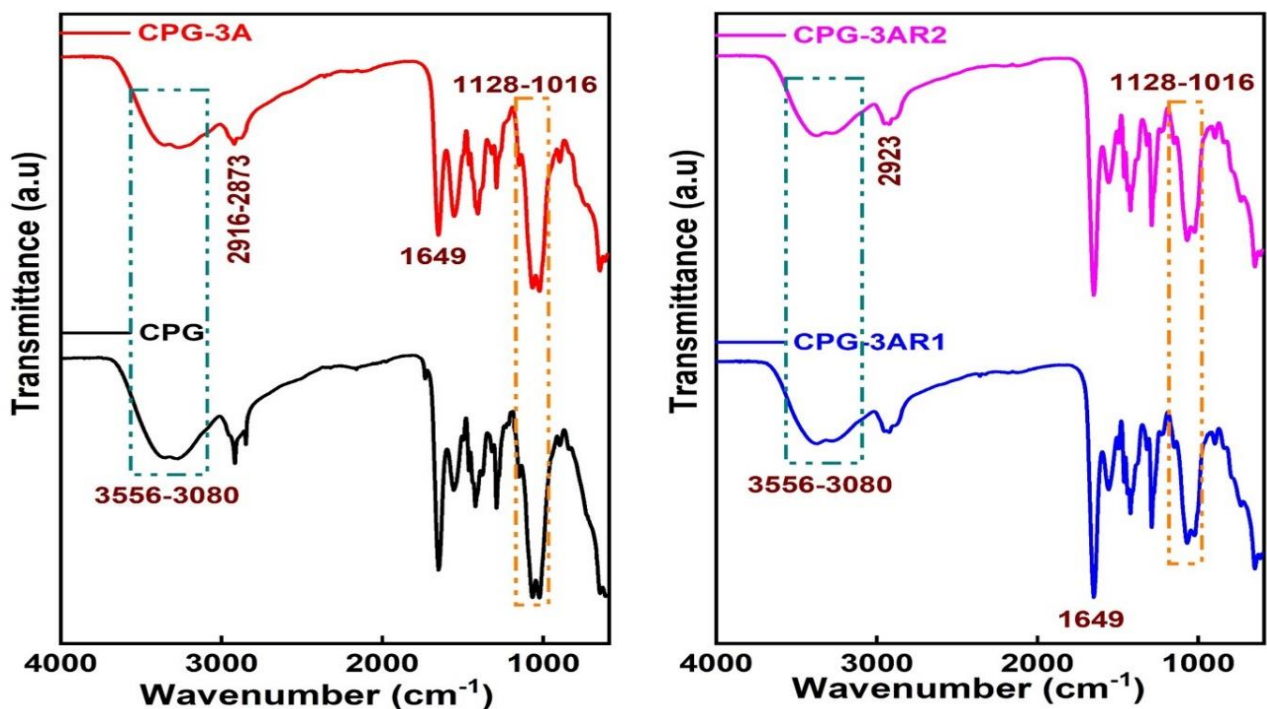


Fig.2 FTIR spectra of the CPGs hydrogels.

4.2 Swelling studies

4.2.1 Swelling trend in distilled water

The hydrogels swelling in water over time is illustrated in Figure 3. All the hydrogel samples exhibited a smooth progress of swelling over time but equilibrium time of all hydrogels was

different. This is crystal clear and can be observed from Figure 3. that crosslinking is inversely proportional to swelling. Hydrogels showed low swelling with the addition of cross linker. Addition of cross linker decreased the water entry as the cross linker not only increased the number of pores but also decreased the pore size due to development of a number of inter and intramolecular interactions. Consequently, it decreases the swelling of hydrogels with increase in equilibrium time. The controlled sample swelling increased with the passage of time but it showed less stability than other cross-linked hydrogels so it gets dissolved early. The equilibrium time for controlled (CPG) hydrogel was observed 150 minutes and exhibited the highest swelling (42 g/g) because of the absence of cross linker and its structure was less dense than other cross-linked structures. CPG-3A showed abrupt increase in swelling at 180 minutes it showed swelling 50.9 g/g and the equilibrium swelling time of CPG-3A was 210 min and its swelling was 54.5 g/g. Because of the presence of cross linker, it showed stability than all CPGs hydrogels. While swelling time was displayed by CPG-3AR1 and that of CPG-3AR2 was 180 min with swelling values 43.05 g/g and 44.95 g/g, respectively. Their equilibrium time decreases than CPG-3A because of the presence of ethanolic extract of ratan-jot that causes hydrolysis in hydrogels. On the other hand CPG-3AR2 showed more smooth linear curve rather than CPG-3AR hydrogel may be due to highest volume of ethanolic extract in it[14].

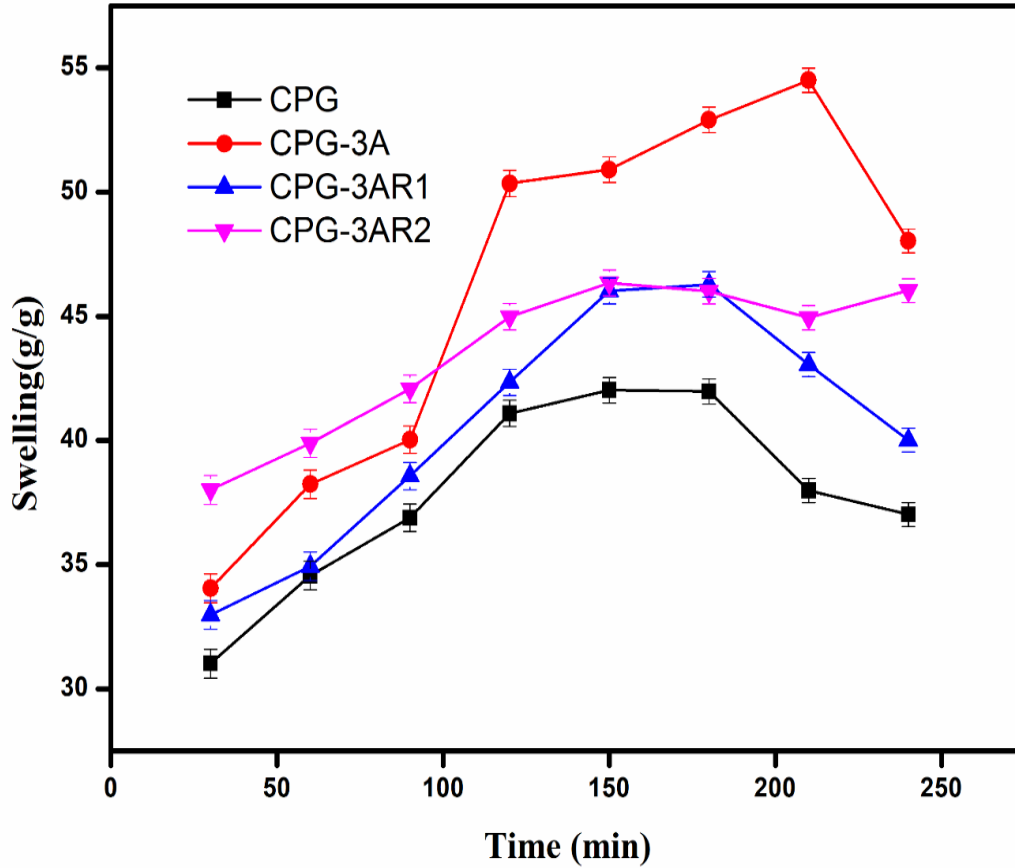


Fig.3 Swelling response of the prepared CPGs in distilled water.

4.2.1.1 Water diffusion method

The solvents migration from the surrounding extracellular matrix into the hydrogels internal structure affects the hydrogel's ability to expand. Researchers frequently use the following equation to shed light on the water diffusion mechanism that causes this swelling phenomenon:

$$F = kt^n \quad (6)$$

Understanding the transport of solvent inside hydrogels depends heavily on the swelling rate constant (k), F is the fractional swelling represented by the ratio of W_{eq} to W_t and the swelling exponent n [40]. Researchers may determine the values of n and k by computing the swelling data of hydrogels in distilled water. The value of n offers information on the solvent transport method in hydrogels. A Fickian Transport Mechanism indicates if $n \leq 0.5$, whereas a non-Fickian Mechanism indicates if $n \geq 0.5$ but less than 1.

By using swelling values of developed hydrogels (CPG, CPG-3RA1, CPG-3AR2, CPG-3A) a relationship between $(\ln t)$ and $(\ln F)$ is shown in Figure 4. In Table 2 the values of diffusion parameter are calculated and given. From the given data, it was determined that in fabricated

hydrogels CPG exhibited Non-Fickian diffusion mechanism as the n value was greater than 0.5. While all remaining hydrogels exhibited Fickian diffusion mechanism as the n value was less than 0.5.

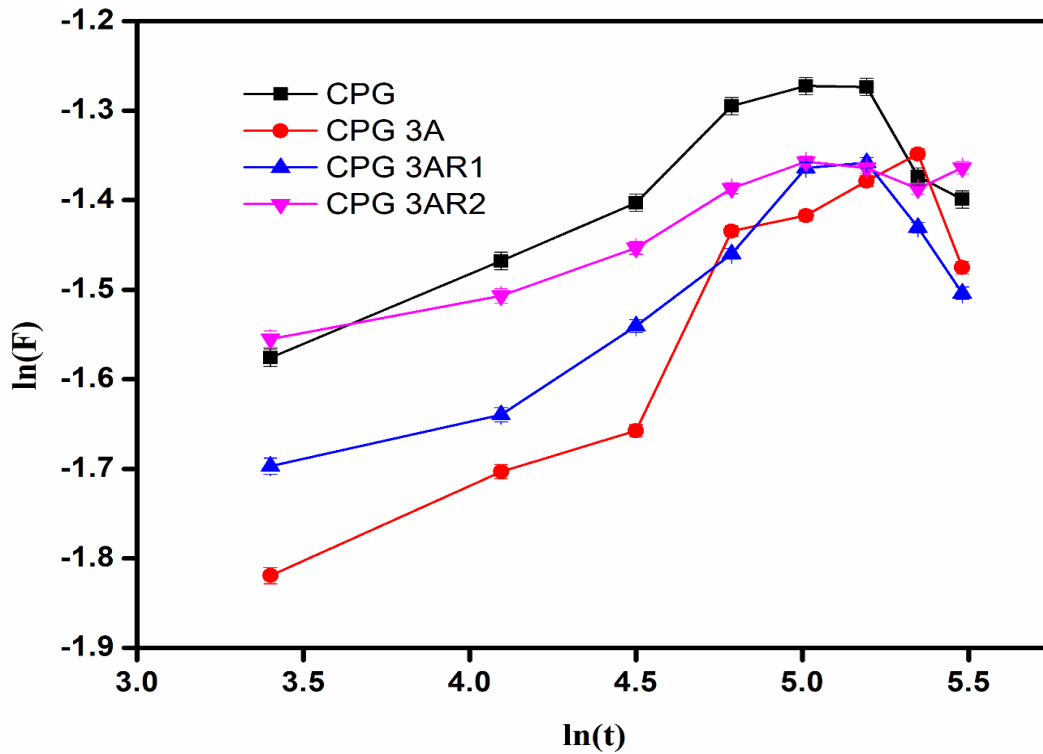


Fig. 4 CPGs hydrogels ln(F) vs. ln(t) plots.

Table.2 Diffusion parameter of the CPGs hydrogels

Parameters	CPG	CPG-3A	CPG-3AR1	CPG-3AR2
n	0.814	0.262	0.205	0.125
Intercept	-2.209	-2.747	-2.436	-1.999
K	0.109	0.064	0.087	0.135
Regression(%)	96	91.9	91.9	92.9

4.2.2 Swelling in pH solutions

To investigate the behaviour of the generated hydrogel, a series of buffers with various pH values (10, 8, 7, 6, 4, 2 and 1.2) were created. Figure 5. shows how the hydrogel films swell over time in different buffers. It was shown that all the samples show pronounced swelling in an alkaline environment but this trend decreased in a neutral and acidic pH. Interestingly, the hydrogels started to swell once again around pH 8 to 10. The CPG (Control) sample exhibited the most swelling out of all the samples, which can be attributed to the large voids inside its

polymer network because it is uncrosslinked. As a result of greater covalent and physical bonding in other hydrogel samples, the network was denser and more compact, which reduced swelling. At pH values of 4, 6 and 7 the swelling response of all fabricated hydrogels was stable. The $-NH_2$ of chitosan and carboxylate group of gum arabic were the main interaction groups in the produced hydrogels. Notably, at pH 1.2 and 2 the hydrogels rapidly disintegrated completely. The high protonation of the chitosan's amino groups ($-NH_2$) into ammonium ions ($-NH_3^+$) is the reason that causes the high swelling in lower acidic media. As the pH increases swelling decreases because of amine group deprotonation. Chitosan amine group ($-NH_3^+$) started to deprotonate again when exposed to high pH environments. Resultantly, at pH 4, 6, and 7 there develop physical networks in CPGs hydrogels. While at higher pH like 8,10 hydrogels showing its greatest expansion in alkaline pH solutions due to carboxylate group of gum arabic[41, 42].

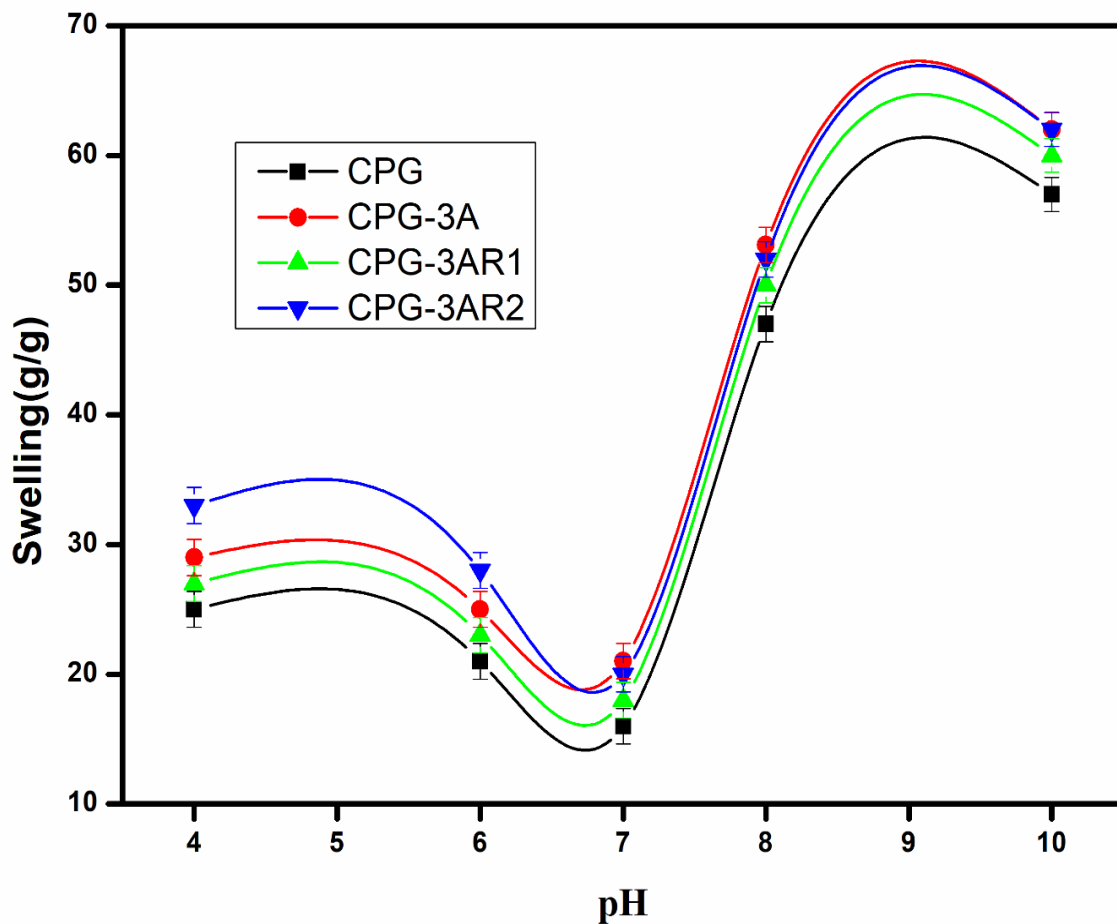


Fig.5 Swelling indices of the CPGs in buffer solutions.

4.2.3. Swelling in ionic solutions

A wide variety of electrolytes with complex compositions can be found in the human body. As typical electrolytes for the investigation, NaCl and CaCl₂ were used. Because Na⁺ ions are

monovalent and Ca^{++} ions are divalent, their charge-to-size ratios differ, substantially. The kind and concentration of salt used will determine how much hydrogels swell in ionic solutions. Using solutions with various concentrations of NaCl and CaCl_2 , the swelling behaviour of the CPGs series was assessed. Both salts have the same anions (Cl^-), but they have different cations (Na^+ and Ca^{2+}). According to Peppas et al. report from 2000, the concentration of these salts significantly affected how much the hydrogel swelled. Complex structures took place at lower salt concentrations, which caused the holes in the hydrogel to widen. According to Wang et al. explanation, as the amount of salt grew, the osmotic pressure between the external solution and the hydrogel dropped, hence limiting the extent of hydrogel swelling. Each hydrogels equilibrium time for the CPGs series swelling was calculated, as shown in Figure 6 [43].

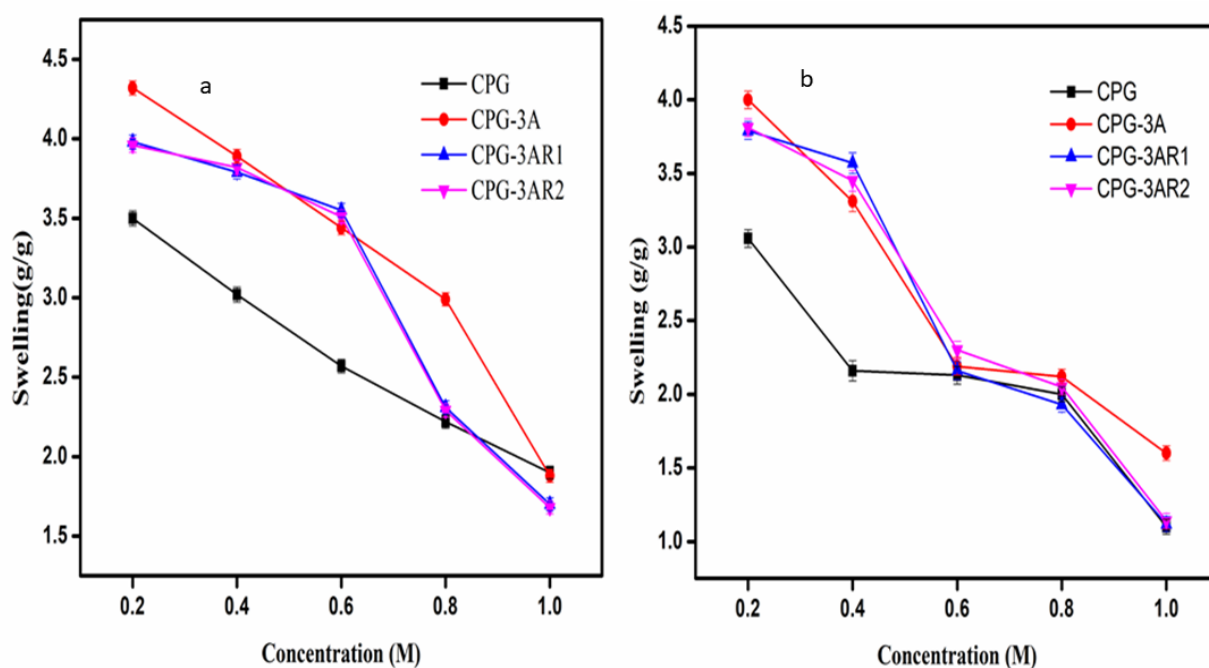


Fig.6 CPGs swelling indices in ionic solutions of CaCl_2 (b) and NaCl (a).

4.3 Thermogravimetric analysis (TGA)

Utilizing TGA, it was determined how the crosslinker affected the produced hydrogels thermal stability with a focus on the effect of 3-APDEMS concentration. Figure 7. shows 4 separate stages of thermal degradation together with the weight loss behaviour of the hydrogel samples. At first, weight loss up to 100°C was noticed, which was attributed to moisture loss and at about 200°C , the degradation process occurs. At temperature 320°C , side chains or functional groups began to separate. At 470°C , more deterioration of the primary polymers backbone was seen. In the last stage, up to 500°C no weight loss was observed indicating residual or ash contents. All hydrogels completely degraded after 470°C showing similar pattern of degradation.

Although, it can be seen from the graph that thermal stability increases with the addition of cross linker amount. The thermogram of CPG hydrogel with no cross linker showed 22% weight loss at 240 °C. while at 400°C 50% weight loss was observed respectively. While for CPG-3A, weight loss was 20%.at 240 °C whereas it was 50% at 404°C. On the other hand, the CPG-3AR1, CPG-3AR2 both showed 21 %, weight loss at 240°C but CPG-3AR2 showed 50% weight loss at 403°C while CPG-3AR1 showed 50% weight loss at temperature 401°C. It is therefore, crystal clear that CPG-3AR among all crosslinked hydrogels is more thermally stable. At 470°C the remaining residues of all hydrogels were CPG 23%,CPG-3A 26.52%, CPG-3AR1 24.18% and CPG-3AR2 24.29% respectively [35, 42, 44].

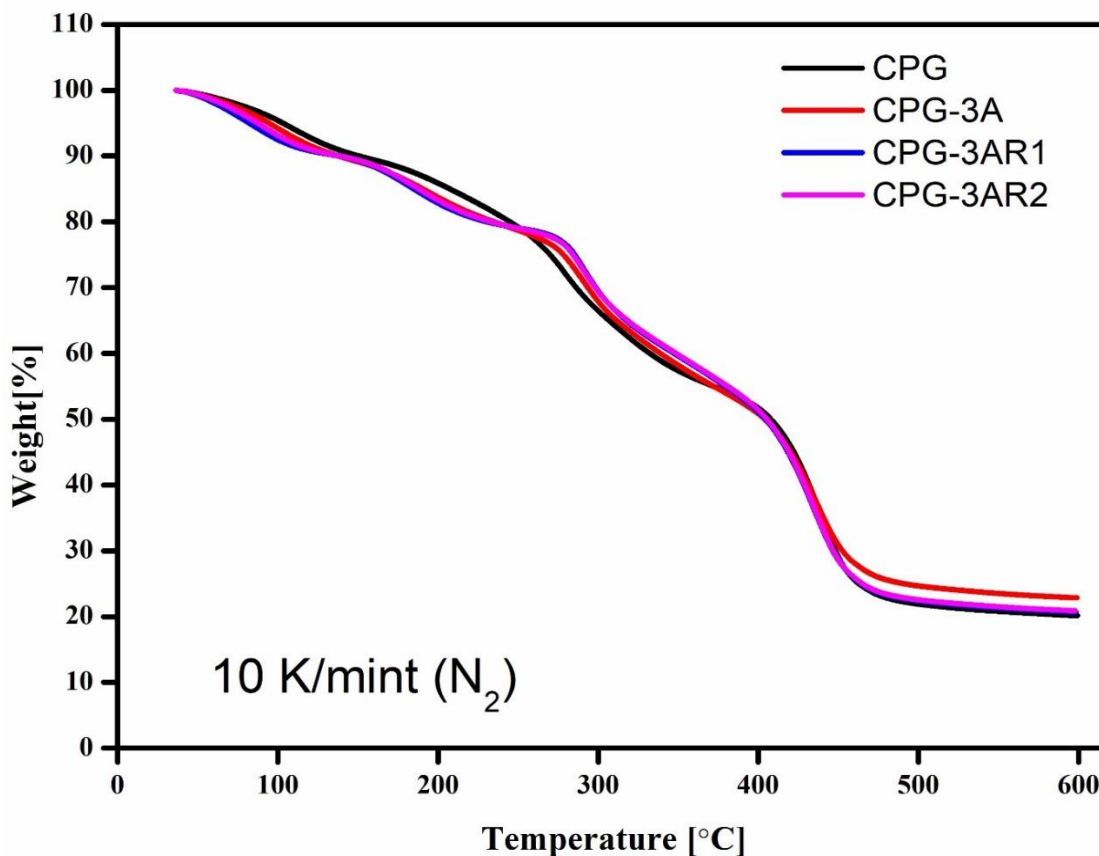


Fig.7 TGA thermograms of the CPGs hydrogels.

4.4 Scanning electron microscopy (SEM)

Figure 8 shows the morphology of the hydrogels made from chitosan, PVP and gum arabic. Without a crosslinker, the hydrogels showed surface abnormalities, including observable depressions (Figure.8). However, the hydrogels showed a more uniform and smooth surface when 3-APDEMS was introduced as a crosslinker (SEM pictures). These photos unmistakably show that the prepared hydrogels have a distinct porous structure, the crosslinker and ethanolic ratan-jot extract addition significantly contributing to the creation of pores in CPG-

3A, CPG-3AR1 and CPG-3AR2. These micrographs show that the addition of a particular amount of crosslinker (50 μL) caused the creation of many pores that were uniformly spaced across the surface (Figure .9). In fact, the extra OH groups produced by the addition of the right quantity of crosslinker as well as extract encouraged the growth and expansion of the hydrogel network between the polymer chains. The improved water absorption seen in CGPs gels with a crosslinker likely results from this improvement, which also makes the gels appropriate for gas exchange and encapsulating biological agents [34] .

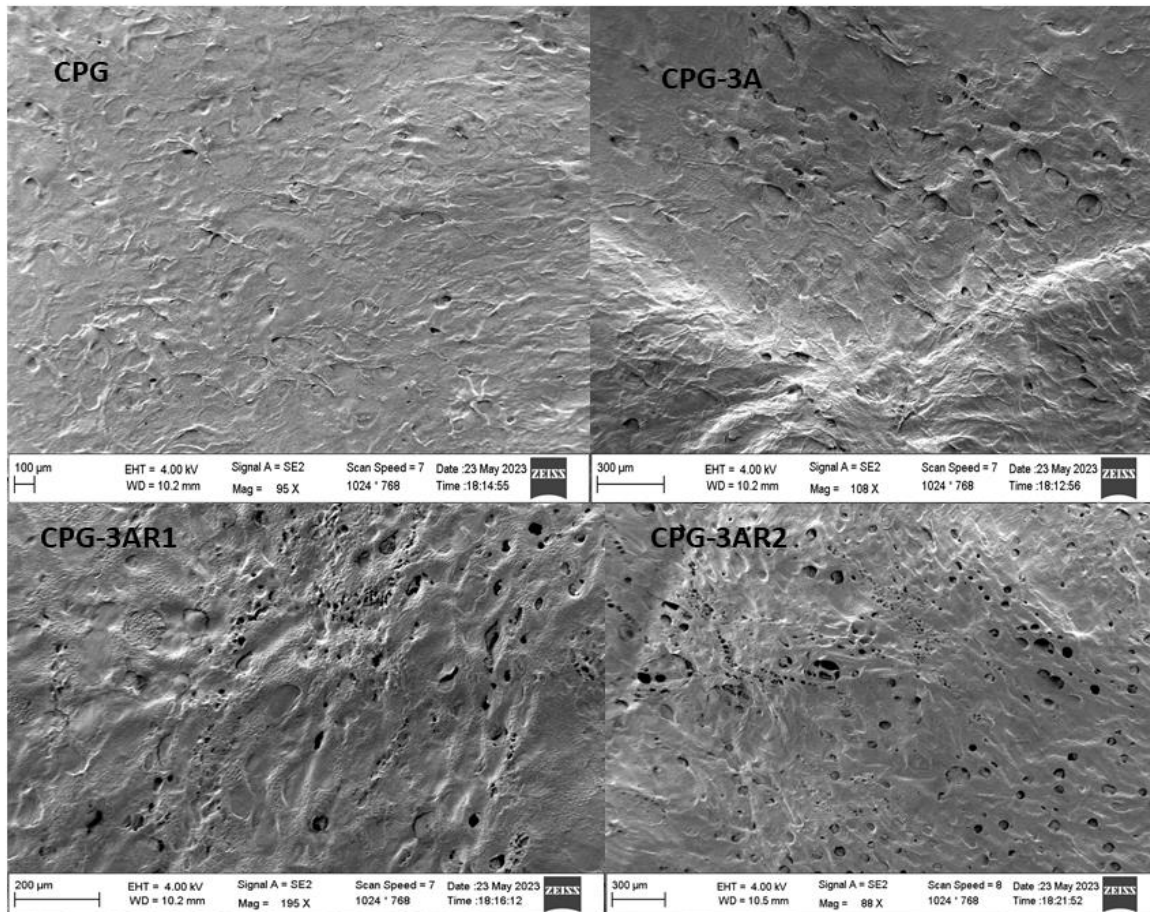


Fig.8 SEM micrographs of CPG (control), CPG-3A, CPG-3AR1 and CPG-3AR2.

4.5 *In-vitro* biodegradation analysis

Figure 9. illustrates the relationship between incubation period and degradation by showing the biodegradation profile of the CPGs. It has been noted that the crosslinking agent increases the stability of the hydrogels and that the rate of degradation increases without any concentration of 3-APDEMS. When the concentration of 3-APDEMS is utilised, the degradation rate gradually drops over the time. Furthermore, degradation also rises when ratan-jot extract is added because it results in hydrolysis in the hydrogel. Although, gum Arabic is natural polymer but here, the degrading behaviour is mostly related to the presence of CS, a biopolymer that

breaks down into oligosaccharide units of various lengths and dissolves glycosidic linkages. This degradation is basically caused by the dissociation of secondary and primary interactions in fabricated hydrogel. These interactions developed due to CS,GA,PVP and 3-APDEMS functional groups (-OH,-NH₂).Smaller polymeric chains are created from these weak connections and are subsequently broken down by mtabolic processes [45].

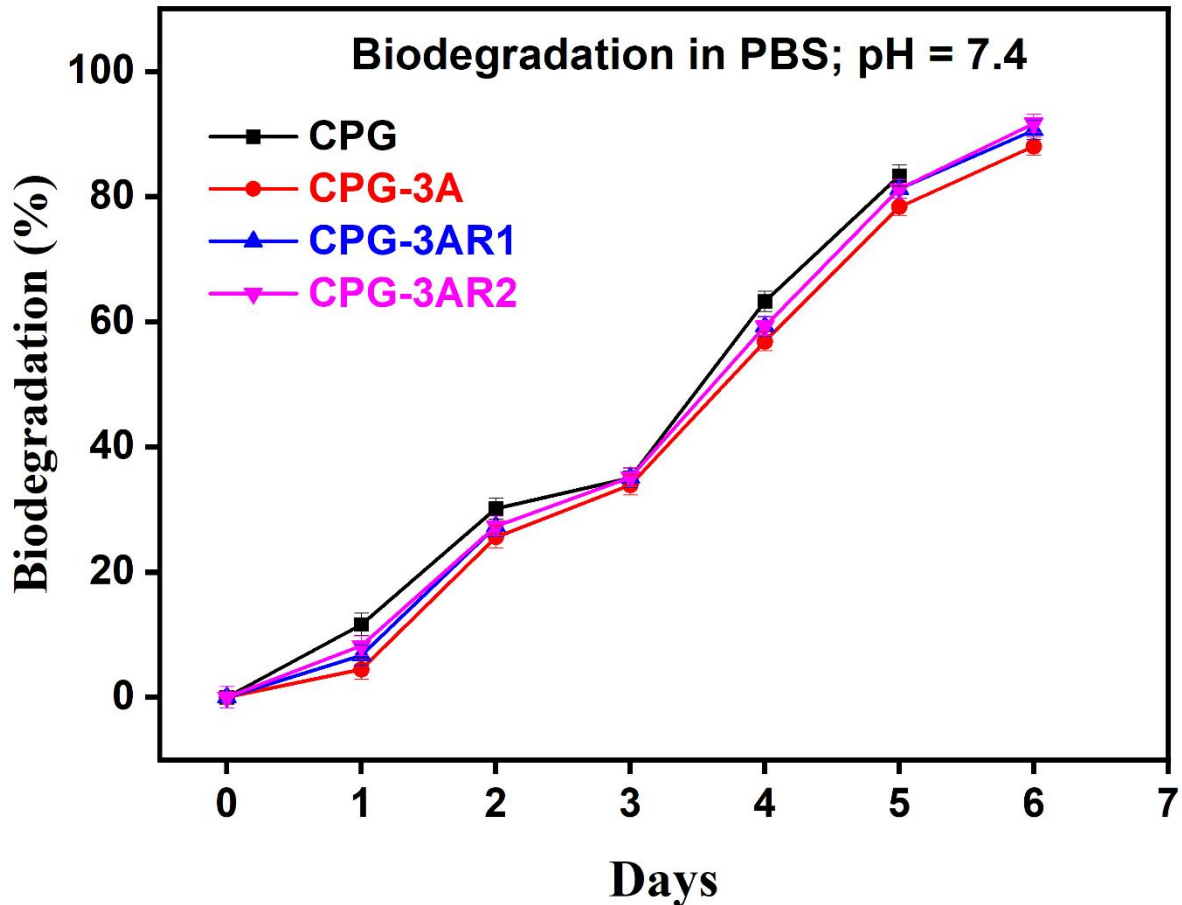


Fig.9 Degradation (%) of the CPGs in the PBS solution

4.6 Microbial resistance

Figure 10. presents the results of the liquid diffusion method used to evaluate the hydrogels antibacterial properties. The control solutions absorbance value was found to be 1.34 for *E. Coli* and 1.287 for *B. Subtilis* . On the other hand, the test sample absorbance values were less than 1.34 and 1.287 which suggests efficient inhibition. The inhibition of bacterial growth is mainly caused by 3-APDEMS crosslinker and ratan-jot extracts. Interestingly, CPG-3AR2 demonstrated an especially remarkable capacity to inhibit bacteria's growth. The negatively charged bacterial cell wall interacted with the test samples, which contained cationic (positively charged) chitosan. Due to the interaction, the *E. Coli* cell wall was disrupted, the bacterial cell was penetrated and the growth of the bacteria was inhibited by preventing the conversion of

DNA into RNA. Through hydrogen bonding and physical interactions with the bacterial cell wall, PVP and GA play a critical role in controlling the growth of gram positive bacteria. The hydroxyl groups in GA, the C=O and NH groups in PVP make interactions with bacterial cell wall. These interactions cause the bacterial cell walls structural integrity to be weakened, which prevents bacteria from growing. On the other side, because of double quantity of antibacterial resistant ratan-jot extract in this gel, it shows excellent antibacterial activity. The CPGs demonstrated greater antibacterial activity against *B. subtilis*. because of its thick peptidoglycan layer, which makes it more vulnerable to the antimicrobial chemicals inside the hydrogel. *E. coli*, on the other hand, has an outer membrane made of lipopolysaccharides that acts as a barrier to protect it from antibacterial substances. This discrepancy in antibacterial efficacy is explained by this structural difference [46, 47].

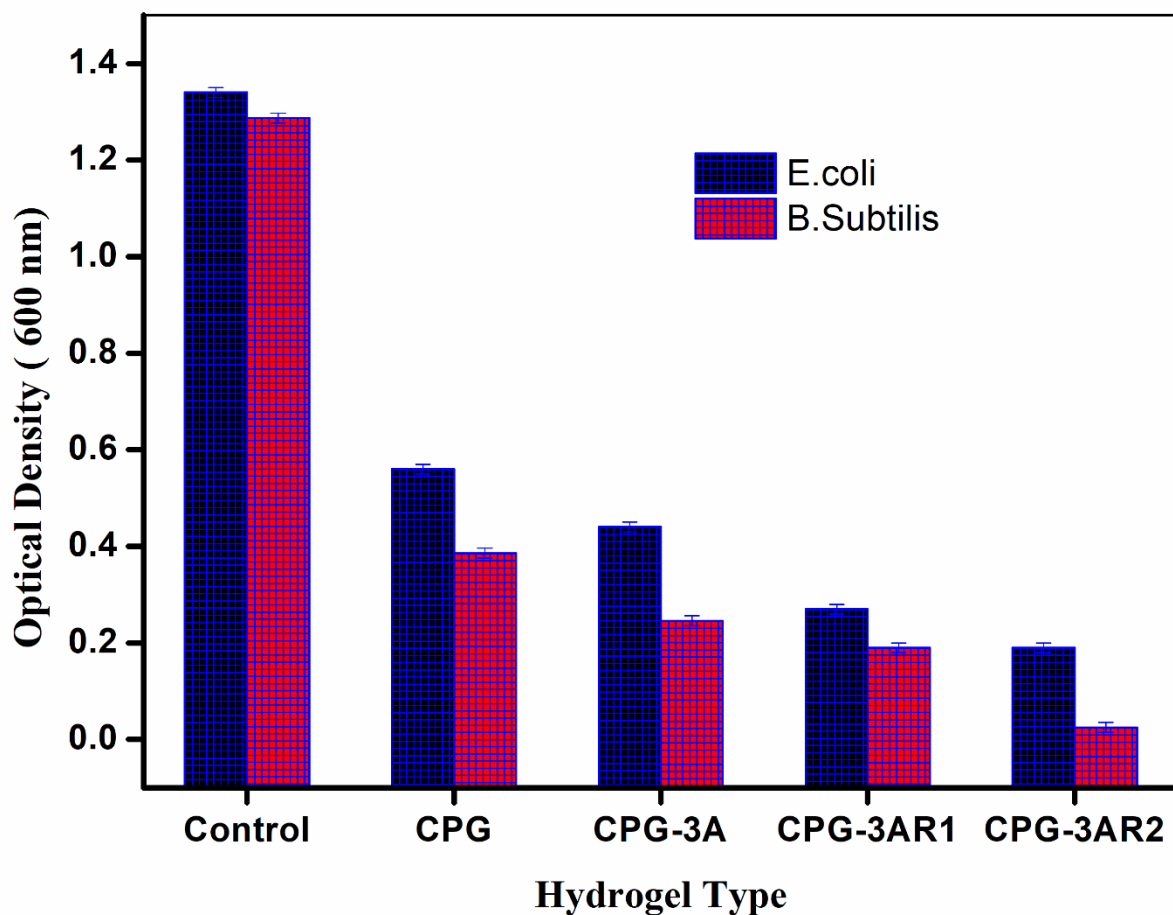


Fig.10 Antibacterial resistance of CPGs hydrogels.

4.7 Cytotoxicity analysis

Analysing cytotoxicity is a useful technique for identifying potential problems with local tissue response. It enables assessment of cell toxicity and offers information on how cells and tissues react. By using the equation 3 from Section 3.6 and looking at both living and dead nauplii

under a light microscope, in-vitro cytotoxicity examination of the hydrogel samples was carried out. Numerous reasons, including chemical cytotoxicity, dissolved oxygen deficit in sea water and the development of a viscous film on the nauplii gills, can be blamed for the death of nauplii. The low proportion of mortality seen at lower fix cross linker doses in this investigation indicates that the likelihood of nauplii dying from toxicity is extremely low (Table. 3). It is also important to note that when the concentration of ratan-jot extract exceeds to 300 μ L, the percentage of nauplii death also decreases by diminishing the toxic effects due to prevention of bacterial growth, retaining the sterile environment and cellular growth. The hydrogel samples utilised in the study were made with CS, GA, PVP, 3-APDEMS and ratan jot extract all of which are FDA-approved and recognised as being biocompatible. This is very important to keep in mind that the development of viscous layers on the gills of the nauplii may be responsible for this low mortality. These layers may prevent oxygen from passing through, killing the nauplii in the process [47, 48].

Table.3 Percentage of *A. Salina* deaths following 24-hour exposure to CPGs

Types of Hydrogels	Mortality (%)
CPG	1.72
CPG-3A	1.56
CPG-3AR1	1.51
CPG-3AR2	1.47

4.8 Porosity

In the context of hydrogel applications for drug release, porosity is essential since it improves the hydrogel matrix ability to absorb pharmaceuticals and makes their dispersion more uniform. This study focused on porosity evaluation, particularly with regard to CPG hydrogels. In Table. 4. the outcomes of porosity are shown, which indicates that the presence of cross-linker along with the higher concentration of ethanolic ratan-jot plant extract, both these lead to the hydrogels increased porosity. 3-APDEMS is essential in increasing porosity, the crosslinker encouraging the creation of connected channels. The increased concentration of hydroxyl groups in CPG hydrogels facilitates the formation of additional hydrogen and covalent bonds. As a result, this network structure strengthening is responsible for the initial rise in porosity.

Hydrogel expansion further encouraged by the addition of ethanolic ratan-jot plant extract. By increasing the plant extract concentration, more gaps are created inside the structure that causes

hydrogels to expand more. Remarkably, the ethanolic ratan-jot extract and 3-APDEMS both played a significant role in enhancing the porosity of CPG hydrogels from 53% to 58% [49].

Table.4 Porosity of prepared hydrogels.

Sample code	Porosity (%)
CPG	53.07+0.87
CPG-3A	57.03+0.71
CPG-3AR1	58.41+0.21
CPG-3AR2	58.89+1.02

4.9 Contact angle

Curious discoveries were made when CPGs hydrogels contact angles were studied. These are shown in Figure 11. CPG(control) had the largest contact angle (73°) among all the CPGs hydrogels when CPGs hydrogels with different concentrations of ratan-jot extract and specific amount of cross-linker were compared. Contact Angle values decreased as a result of the addition of 3-APDEMS as well as plant extract concentration. The contact angle approaches 0° when water droplets spread out across the hydrogel sheet due to strong adhesion. Angles of contact between 0° and 90° indicating that the hydrogel is hydrophilic, while angles larger than 90° indicate that it is hydrophobic. Results shows that all fabricated hydrogels are hydrophilic[50, 51].

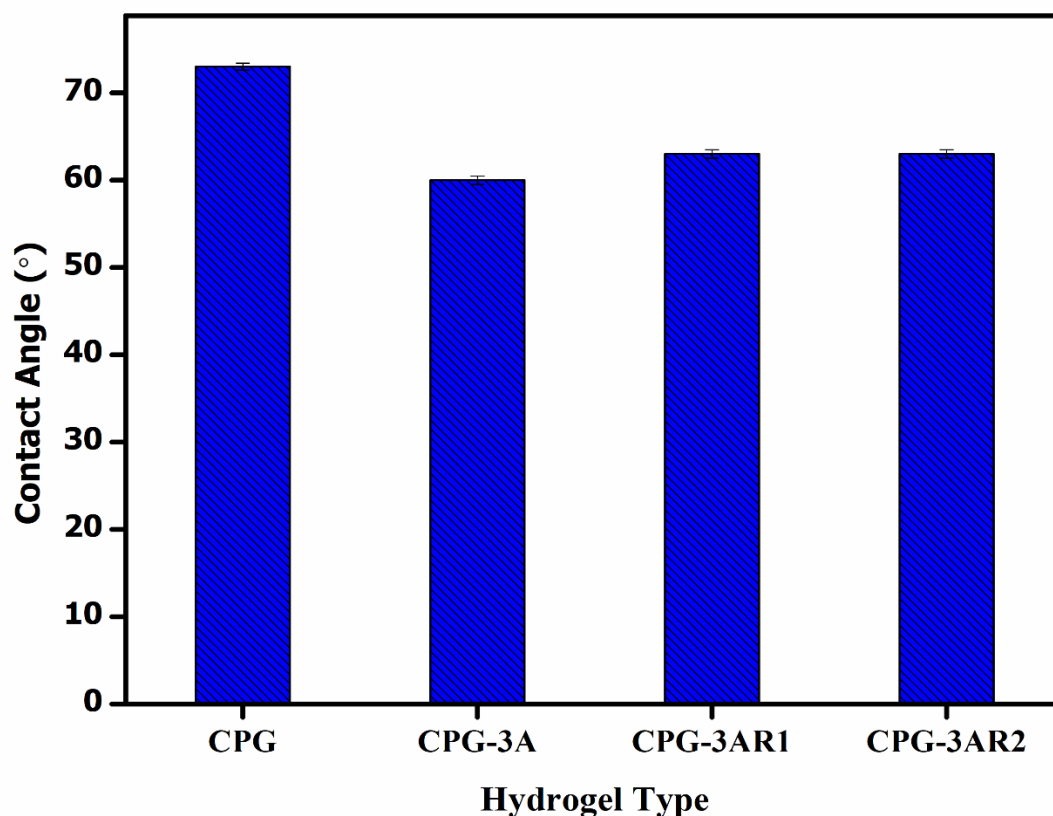


Fig.11 Hydrophilicity response of the CPGs hydrogels.

4.10 Drug release analysis and its kinetics

Using CPG-3AR2 as the carrier, the release % of ampicillin sodium was investigated over a time in a PBS solution (pH 7.4) at 37°C. Notably, the CPGs hydrogels showed noticeable swelling in an acidic as well as in basic environment showing that they may release the medication quickly in that setting. The drug release from the loaded samples was, therefore, assessed using a pH 7.4 (PBS) solution. This decision was made due to the reason that regulated release would be difficult to achieve if the medicine was administered orally because of how quickly it would be released in the stomach acidic environment. Contrarily, medicine release was regulated at blood pH levels, favouring injectable administration. In about 2 hour and 40 minutes, the drug release efficiency was precisely attained, reaching 80.82% and at about 180 minutes its release was 98.717%. (Figure 12). In study 2024, Andlib et al. created a chitosan-based carrier with a 90-minute drug release rate of over 98.236% [37]. The value of the exponent coefficient (n) in equation (6) plays a critical role in defining the diffusion way by which the medication is released from the hydrogel. The value of n for CPG-3AR2 hydrogel observed as 0.63 confirming the Non-Fickian diffusion process.

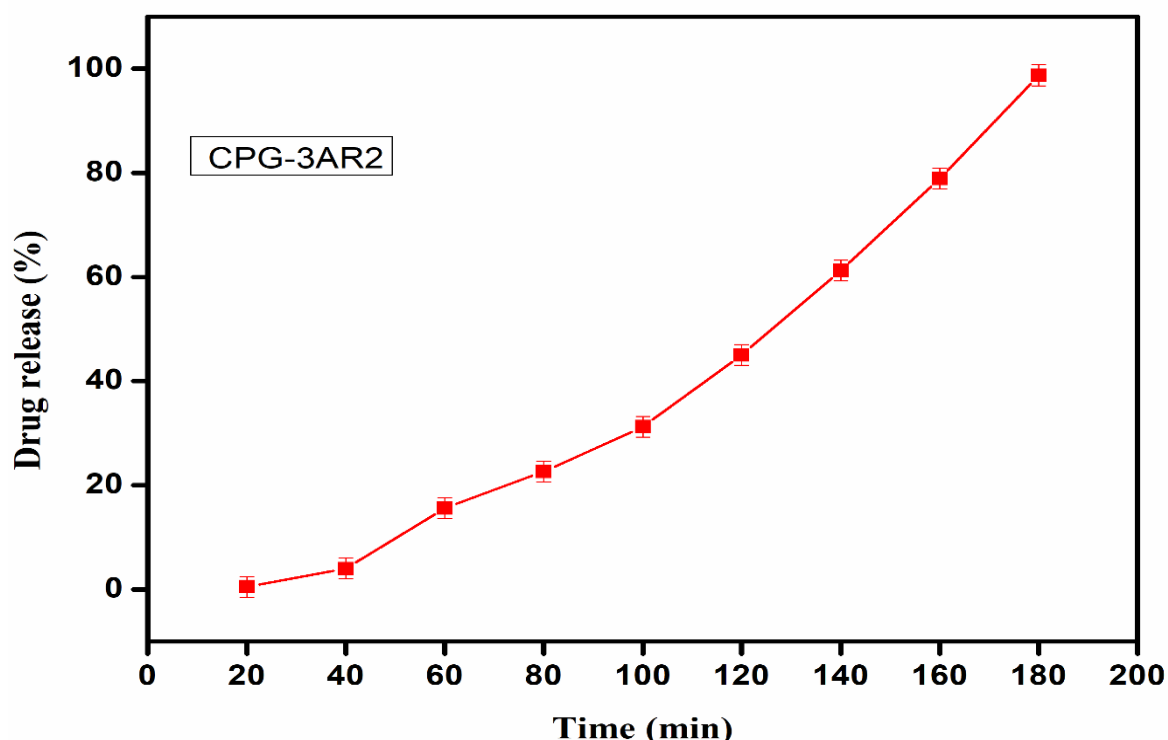


Fig.12 Drug release profile of engineered CPG-3AR2 sample in PBS solution

5. Conclusions

Through solution casting method, a new pH-sensitive cross-linked hydrogels were made by utilising biopolymers. Chitosan (CS), gum arabic(GA), polyvinylpyrrolidone (PVP) and 3-aminopropyl-diethoxymethylsilane (APDEMS) were expertly combined with anti-inflammatory ratan-jot extract to create these unusual hydrogels. FTIR spectroscopy was used to verify that the hydrogel components successfully interacted with one another. The CPGs gels with excellent biodegradation, pH sensitivity, antibacterial as well as cytotoxic behaviour makes it a good option for injectable drug delivery application. To determine the significance of the produced CPGs, the controlled release behaviour of CPG-3AR2 loaded with Ampicillin sodium was checked, attaining release rates of 98.717% in PBS, respectively, over 180 minutes. CPG showed the largest swelling capability, reaching 54.5g/g. However, the level of edema in distilled water reduced as the amount of 3-APDEMS rose. CPG-3A had the greatest thermal stability of all the samples. These hydrogels did not demonstrate hazardous effects on cell growth, according to an in vitro cytotoxicity analysis, which allowed cells to behave normally and follow their usual life cycles. **The developed hydrogels are very promising for the controlled release of drug but however these are only studied with ampicillin sodium as a model drug for drug**

release experiment. Also the controlled release time of ampicillin sodium from the hydrogel is 180 minutes. We have performed only in in-vitro analysis but for more clinical and in-vivo studies more analysis will be performed in future.

References

1. Sur, S., et al., *Recent developments in functionalized polymer nanoparticles for efficient drug delivery system*. Nano-Structures & Nano-Objects, 2019. **20**: p. 100397.
2. Huang, H., et al., *Thermo-sensitive hydrogels for delivering biotherapeutic molecules: A review*. Saudi Pharmaceutical Journal, 2019. **27**(7): p. 990-999.
3. Pacheco, C., et al., *Recent advances in long-acting drug delivery systems for anticancer drug*. Advanced Drug Delivery Reviews, 2023. **194**: p. 114724.
4. Huang, H., et al., *Thermo-sensitive hydrogels for delivering biotherapeutic molecules: A review*. Saudi Pharmaceutical Journal, 2019.
5. Zhang, Q., et al., *Recent advances in protein hydrogels: From design, structural and functional regulations to healthcare applications*. Chemical Engineering Journal, 2023. **451**: p. 138494.
6. Malik, M.K., et al., *Significance of chemically derivatized starch as drug carrier in developing novel drug delivery devices*. The Natural Products Journal, 2023. **13**(6): p. 40-53.
7. Fan, X., et al., *Mussel-induced nano-silver antibacterial, self-healing, self-adhesive, anti-freezing, and moisturizing dual-network organohydrogel based on SA-PBA/PVA/CNTs as flexible wearable strain sensors*. Polymer, 2022. **256**: p. 125270.
8. Luo, Y., et al., *From crosslinking strategies to biomedical applications of hyaluronic acid-based hydrogels: A review*. International Journal of Biological Macromolecules, 2023. **231**: p. 123308.
9. Yu, W., et al., *Hydrogel-mediated drug delivery for treating stroke*. Chinese Chemical Letters, 2023: p. 108205.
10. Barberi, G., et al., *Thermosensitive and mucoadhesive Xanthan gum-based hydrogel for local release of anti-Candida peptide*. Journal of Drug Delivery Science and Technology, 2024. **100**: p. 106054.
11. Hernandez Rivera, G., et al., *PVA-gelatine based hydrogel loaded with astaxanthin and mesoporous bioactive glass nanoparticles for wound healing*. Journal of Drug Delivery Science and Technology, 2024: p. 106235.
12. Li, T., et al., *Biocompatible puerarin injectable-hydrogel using self-assembly tetrapeptide for local treatment of osteoarthritis in rats*. Journal of Drug Delivery Science and Technology, 2022. **78**: p. 103909.
13. Zulaikha, W., M. Zaki Hassan, and S.a. Abdul Aziz, *Nanoparticle-embedded hydrogels as a functional polymeric composite for biomedical applications*. Materials Today: Proceedings, 2023.
14. Qureshi, M.A.u.R., N. Arshad, and A. Rasool, *Graphene oxide reinforced biopolymeric (chitosan) hydrogels for controlled cephadrine release*. International Journal of Biological Macromolecules, 2023. **242**: p. 124948.
15. Shariatinia, Z. and A.M. Jalali, *Chitosan-based hydrogels: Preparation, properties and applications*. International Journal of Biological Macromolecules, 2018. **115**: p. 194-220.
16. Mohite, P., et al., *Chitosan-Based Hydrogel in the Management of Dermal Infections: A Review*. Gels, 2023. **9**(7): p. 594.
17. Sudheer, S., S. Bandyopadhyay, and R. Bhat, *Sustainable polysaccharide and protein hydrogel-based packaging materials for food products: A review*. International Journal of Biological Macromolecules, 2023. **248**: p. 125845.

18. Ahmad, S., et al., *Antimicrobial gum based hydrogels as adsorbents for the removal of organic and inorganic pollutants*. Journal of Water Process Engineering, 2023. **51**: p. 103377.
19. Amaya-Chantaca, N.J., et al., *Semi-IPN hydrogels of collagen and gum arabic with antibacterial capacity and controlled release of drugs for potential application in wound healing*. Progress in Biomaterials, 2023. **12**(1): p. 25-40.
20. Cai, L., et al., *Polypeptide-based self-healing hydrogels: Design and biomedical applications*. Acta Biomaterialia, 2020. **113**: p. 84-100.
21. Nisar, S., et al., *5 - Recent advances in natural polymer based hydrogels for wound healing applications*, in *Advances in Healthcare and Protective Textiles*, S. ul-Islam, A. Majumdar, and B. Butola, Editors. 2023, Woodhead Publishing. p. 115-149.
22. Kurakula, M. and G.K. Rao, *Moving polyvinyl pyrrolidone electrospun nanofibers and bioprinted scaffolds toward multidisciplinary biomedical applications*. European Polymer Journal, 2020. **136**: p. 109919.
23. Gupta, B., et al., *Cellulosic polymers for enhancing drug bioavailability in ocular drug delivery systems*. Pharmaceuticals, 2021. **14**(11): p. 1201.
24. Franco, P. and I. De Marco, *The Use of Poly(N-vinyl pyrrolidone) in the Delivery of Drugs: A Review*. Polymers, 2020. **12**(5): p. 1114.
25. Rasekh, M., et al., *Electrospun PVP–indomethacin constituents for transdermal dressings and drug delivery devices*. International Journal of Pharmaceutics, 2014. **473**(1-2): p. 95-104.
26. Demeter, M., et al., *Biocompatible and antimicrobial chitosan/PVP/PEO/PAA/AgNP composite hydrogels synthesized by e-beam cross-linking*. Radiation Physics and Chemistry, 2024. **216**: p. 111391.
27. Kanwal, M., et al., *Cytocompatible and stimuli-responsive chitosan based carrier with 3-aminopropyl(diethoxy)methylsilane for controlled release of cefixime*. Chemical Papers, 2023. **77**(9): p. 5571-5586.
28. Zahoor, S., et al., *Diabetic wound healing potential of silk sericin protein based hydrogels enriched with plant extracts*. International Journal of Biological Macromolecules, 2023. **242**: p. 125184.
29. Yahia, S., I.A. Khalil, and I.M. El-Sherbiny, *Dual antituberculosis drugs-loaded gelatin hydrogel bioimplant for treating spinal tuberculosis*. International Journal of Pharmaceutics, 2023. **633**: p. 122609.
30. Bisht, A., V. Kamboj, and A. Bisht. *Reviewing Medicinal Plants of Treasure Land: The Indian Himalayan Range*. in *Environmental Pollution and Natural Resource Management*. 2022. Cham: Springer International Publishing.
31. Farooq, A., et al., *Designing Kappa-carrageenan/guar gum/polyvinyl alcohol-based pH-responsive silane-crosslinked hydrogels for controlled release of cephadrine*. Journal of Drug Delivery Science and Technology, 2022. **67**: p. 102969.
32. Bashir, A., et al., *Co-concentration effect of silane with natural extract on biodegradable polymeric films for food packaging*. International Journal of Biological Macromolecules, 2018. **106**: p. 351-359.
33. Rehmat, S., et al., *Novel Stimuli-Responsive Pectin-PVP-Functionalized Clay Based Smart Hydrogels for Drug Delivery and Controlled Release Application*. Frontiers in Materials, 2022. **9**.
34. Jabeen, S., et al., *Development of a novel pH sensitive silane crosslinked injectable hydrogel for controlled release of neomycin sulfate*. International Journal of Biological Macromolecules, 2017. **97**: p. 218-227.
35. Gull, N., et al., *Inflammation targeted chitosan-based hydrogel for controlled release of diclofenac sodium*. International Journal of Biological Macromolecules, 2020. **162**: p. 175-187.

36. Qu, Q., et al., *Strength and targeted-sustained release properties of sodium alginate-polyacrylamide hydrogel for anti-wrinkle eye-patch*. Journal of Drug Delivery Science and Technology, 2024. **100**: p. 106065.
37. Andlib, H., M. Shafiq, and A. Sabir, *Sodium Ampicillin release from biocompatible hydrogel with enhanced antibacterial characteristics*. Journal of Drug Delivery Science and Technology, 2024: p. 106086.
38. Jadoon, A., et al., *Probing the role of hydrolytically stable, 3-aminopropyl triethoxysilane crosslinked chitosan/graphene oxide membrane towards Congo red dye adsorption*. Current Applied Physics, 2022. **40**: p. 110-118.
39. Ghauri, Z.H., et al., *Development and evaluation of pH-sensitive biodegradable ternary blended hydrogel films (chitosan/guar gum/PVP) for drug delivery application*. Scientific Reports, 2021. **11**(1): p. 21255.
40. Andlib, H., M. Shafiq, and A. Sabir, *Development of pomegranate peel extract amalgamated ternary hydrogel with synergistic antibacterial efficacy against Escherichia Coli (E. Coli)*. 2024.
41. Felinto, M.C., et al., *The swelling behavior of chitosan hydrogels membranes obtained by UV- and γ -radiation*. Nuclear Instruments and Methods in Physics Research Section B: Beam Interactions with Materials and Atoms, 2007. **265**(1): p. 418-424.
42. Feyissa, Z., et al., *Fabrication of pH-Responsive Chitosan/Polyvinylpyrrolidone Hydrogels for Controlled Release of Metronidazole and Antibacterial Properties*. International Journal of Polymer Science, 2023. **2023**: p. 1205092.
43. Risbud, M., et al., *pH-sensitive freeze-dried Chitosan-polyvinyl hydrogels as controlled release system for antibiotic delivery*. Journal of controlled release : official journal of the Controlled Release Society, 2000. **68**: p. 23-30.
44. Sabbagh, H.A.K., et al., *A statistical study on the development of metronidazole-chitosan-alginate nanocomposite formulation using the full factorial design*. Polymers, 2020. **12**(4): p. 772.
45. Azaza, Y.B., et al., *Chitosan/collagen-based hydrogels for sustainable development: Phycocyanin controlled release*. Sustainable Chemistry and Pharmacy, 2023. **31**: p. 100905.
46. Sarmah, D., et al., *Self-cross-linked starch/chitosan hydrogel as a biocompatible vehicle for controlled release of drug*. International Journal of Biological Macromolecules, 2023. **237**: p. 124206.
47. Gull, N., et al., *In vitro study of chitosan-based multi-responsive hydrogels as drug release vehicles: a preclinical study*. RSC Advances, 2019. **9**(53): p. 31078-31091.
48. Suneka, S. and T. Manoranjan, *Brine shrimp lethality assay with selected medicinal plants extracts*. Vignanam Journal of Science, 2021.
49. Pan, H., et al., *Non-stick hemostasis hydrogels as dressings with bacterial barrier activity for cutaneous wound healing*. Materials Science and Engineering: C, 2019. **105**: p. 110118.
50. Ahmad, F., et al., *An eco-friendly hydroentangled cotton non-woven membrane with alginate hydrogel for water filtration*. International Journal of Biological Macromolecules, 2024. **256**: p. 128422.
51. Hafeez, S., et al., *Fabrication of pectin-based stimuli responsive hydrogel for the controlled release of ceftriaxone*. Chemical Papers, 2023. **77**(4): p. 1809-1819.

Response to Reviewer's Comments

Manuscript #: JDDST-D-24-03283

Reviewer: 1

Comment 1	P10 Fig.2: In the schematic representation of the prepared hydrogel, the arrows overlap with the chemical structures. The labeling needs to be clearer and more precise.
Reply	Thank you for your helpful feedback on the schematic representation of the hydrogel. We have revised the schematic representation along with labelling to improve clarity in the revised manuscript.
Comment 2	P8 Sec.2.2.2: The hydrogel composition includes acetic acid for dissolving chitosan, but the manuscript does not mention its removal. The authors should clarify how the system is suitable for biomedical applications, considering the potential presence of acetic acid.
Reply	Thank you for your valuable comment. The low concentration of acetic acid in diluted form used to dissolve chitosan. The traces of acetic acid residues were removed by washing the hydrogel film with distilled water. While acetic acid in diluted form poses no harm, as its recognized as safe by the FDA. Our hydrogel has been tested for biocompatibility, ensuring it remains safe for biomedical applications [1] .
Comment 3	The authors must provide appropriate references for all mathematical formulas used, such as those for swelling, biodegradation, and other calculations.
Reply	It has been done in the revised manuscript.
Comment 4	P23 Sec.4.6: Before discussing the antimicrobial activity of the prepared hydrogel, the authors need to clarify whether the hydrogel still contains acetic acid and ethanol, as both solvents can kill bacteria, and they were used in the hydrogel preparation.

Reply	During hydrogel preparation, ethanol ensures that it was evaporated during the drying process. The negligible residues of acetic acid were removed by washing the hydrogel film with distilled water according to the standard procedure. Therefore, there is no acetic acid and ethanol in film while testing it for bacterial activity.
Comment 5	P12 Sec.3.5: The authors should reference the procedure for determining the antimicrobial profile, citing relevant literature.
Reply	It has been done in the revised manuscript.
Comment 6	Authors need to clarify the specificity of the drug ampicillin sodium for the prepared hydrogel. Have they performed experiments with other drugs?
Reply	Ampicillin sodium targets and inhibit the growth of the bacteria's. It is used to treat gonorrhea, respiratory, urinary tract, gastrointestinal and neurological systems bacterial infections. As ampicillin sodium is used as model drug at this stage and we will perform for other drugs in future along with in-vivo analysis.

Reviewer: 2

Comment 1	How authors claim this hydrogel for injectable release? Please identify the problem through literature.
Reply	CPG hydrogel exhibits less swelling, especially at pH 7 values, which makes it perfect for physiological settings such as for blood. It provides controlled release of drug without premature degradation due to its stability in PBS (7.4) environments. CPGs is a great option for injectable drug administration because of its swelling profile, which guarantees long-lasting therapeutic benefits without compromising structural integrity [2].
Comment 2	What is new and novel in this study beyond the already reported literature?

Reply	The novelty of this work is the use of CS, GA, PVP and ratan-jot ethanolic extract to fabricate the hydrogel with dual antibacterial nature, which was then crosslinked by using 3-APDEMS crosslinker for the controlled release of Ampicillin Sodium salt. This formulation was not used yet according to best of our knowledge. This novelty is also added in revised manuscript.
Comment 3	Figure is not suitable for manuscript. It can be removed.
Reply	Thank you for your comment. It has been removed from the manuscript.
Comment 4	In Figure 2, some bond lengths are too large. It should be shorten.
Reply	It has been revised in the manuscript.
Comment 5	Si-N should be confirmed by FTIR. C=O bond also showing H-bonding which should be confirmed by FTIR.
Reply	Si-N peak of these hydrogels appear in $934-940\text{cm}^{-1}$ range while hydrogen bonded carbonyl shows peak at 1649cm^{-1} . The carbonyl peak shifted to lower wavenumber of 1649cm^{-1} due to the formation pf hydrogen bonding. It has been revised in manuscript.
Comment 6	Why TGA was performed up to 600 C while its application was drug release?
Reply	TGA ($600\text{ }^{\circ}\text{C}$) was performed because we have firstly prepared our hydrogels and then check its properties because hydrogels were prepared by using polymers. So initially we have checked thermal properties of polymeric hydrogels.
Comment 7	Present the biodegradation in percentage.
Reply	It has been revised in the manuscript.
Comment 8	Please check the antibacterial properties against gram positive bacteria and then compare with both types of bacteria
Reply	It has been revised in the manuscript.
Comment 9	Cytotoxicity should be measured against cell lines.

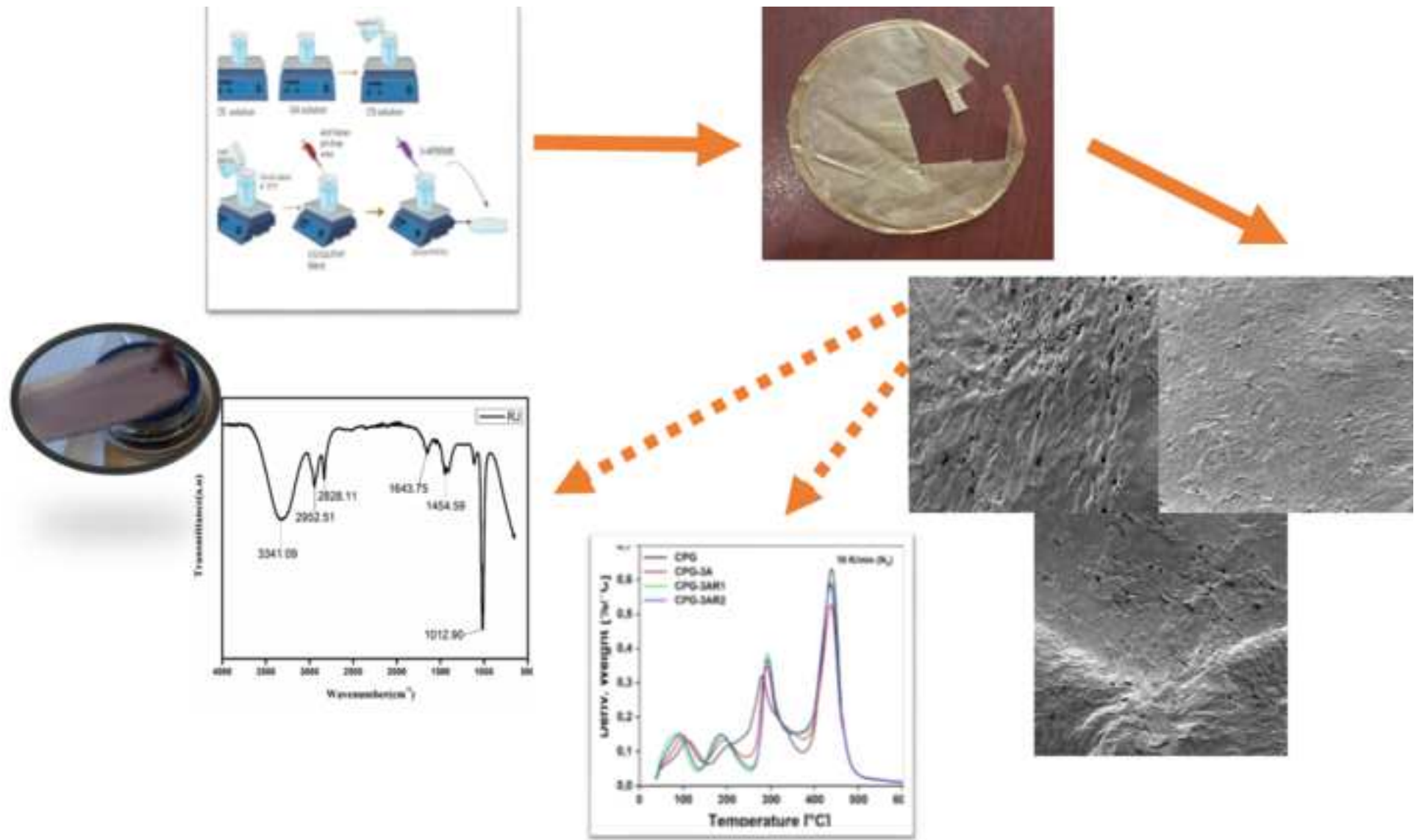
Reply	We have performed cytotoxicity available test with brine shrimp's larvae that is also a standard method. Unfortunately, we have no availability of cell lines .
Comment 10	Why contact angle was increased after CPG-3A sample?
Reply	The increase in contact angle after CPG-3A is likely due to the presence of hydrophobic compounds in the <i>ratan-jot</i> plant extract which counteract the hydrophilicity of the polymer matrix. More extract leads to a greater accumulation of hydrophobic molecules at the surface, reducing water affinity.
Comment 11	Please include limitations of your study in conclusion section.
Reply	Thank you for your guidance .It has been done in revised manuscript.
Comment 12	Cite some more relevant latest papers of "Journal of Drug Delivery Science and Technology".
Reply	It has been revised in the manuscript.

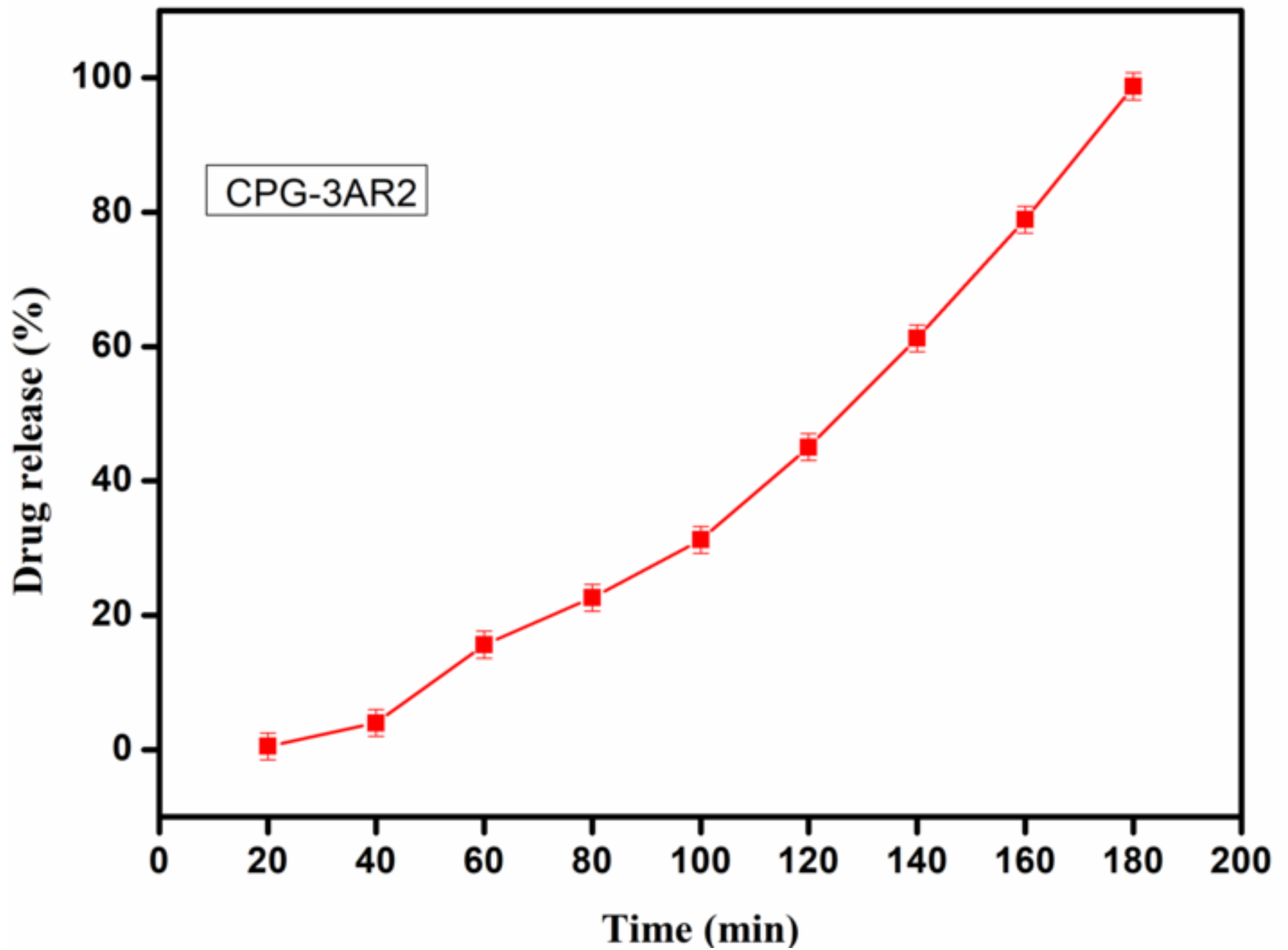
References

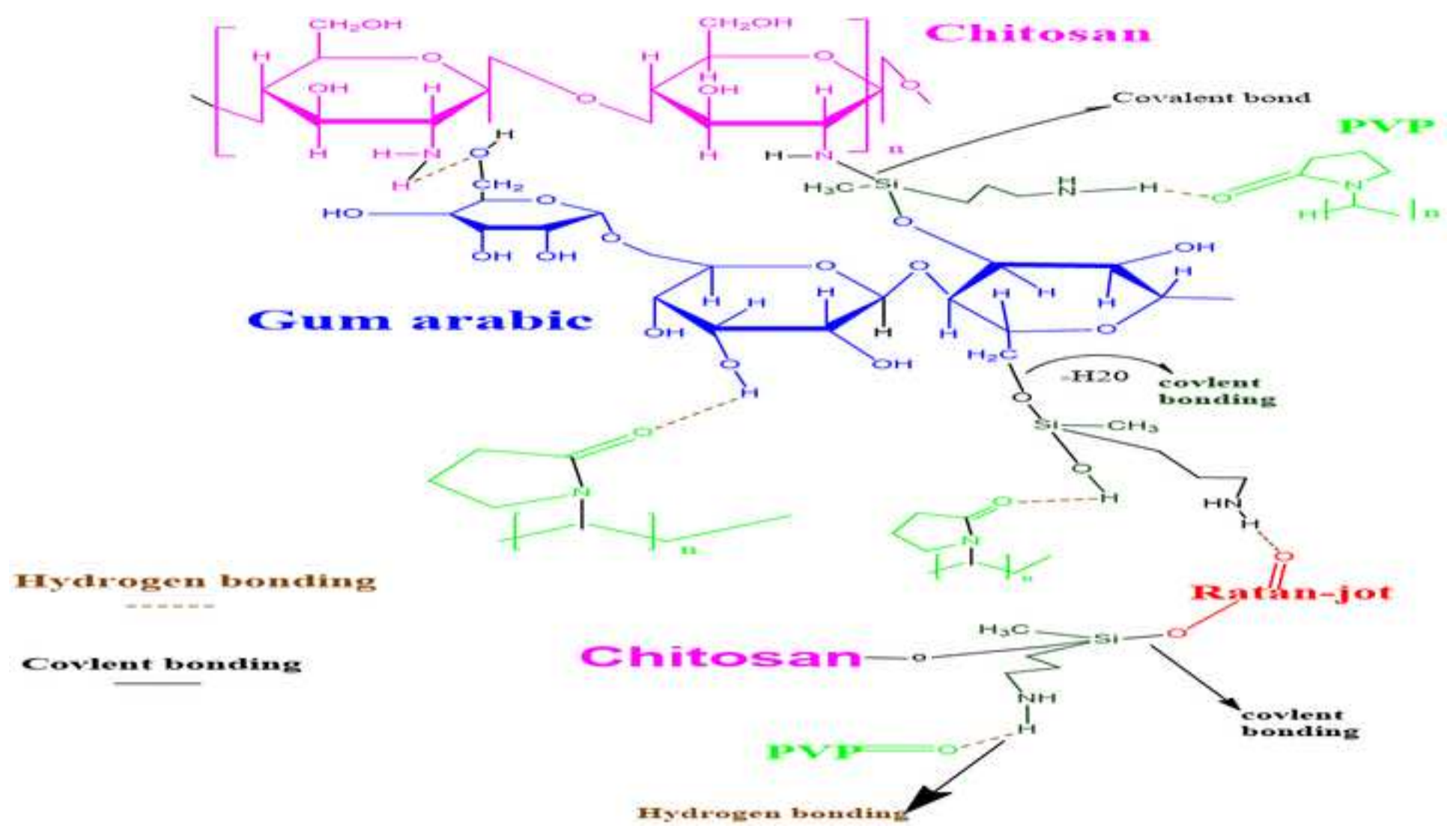
1. Moreira, T.F.M., et al., *Hydrogels based on gelatin: Effect of lactic and acetic acids on microstructural modifications, water absorption mechanisms and antibacterial activity*. LWT, 2019. **103**: p. 69-77.
2. Jabeen, S., et al., *Development of a novel pH sensitive silane crosslinked injectable hydrogel for controlled release of neomycin sulfate*. International Journal of Biological Macromolecules, 2017. **97**: p. 218-227.

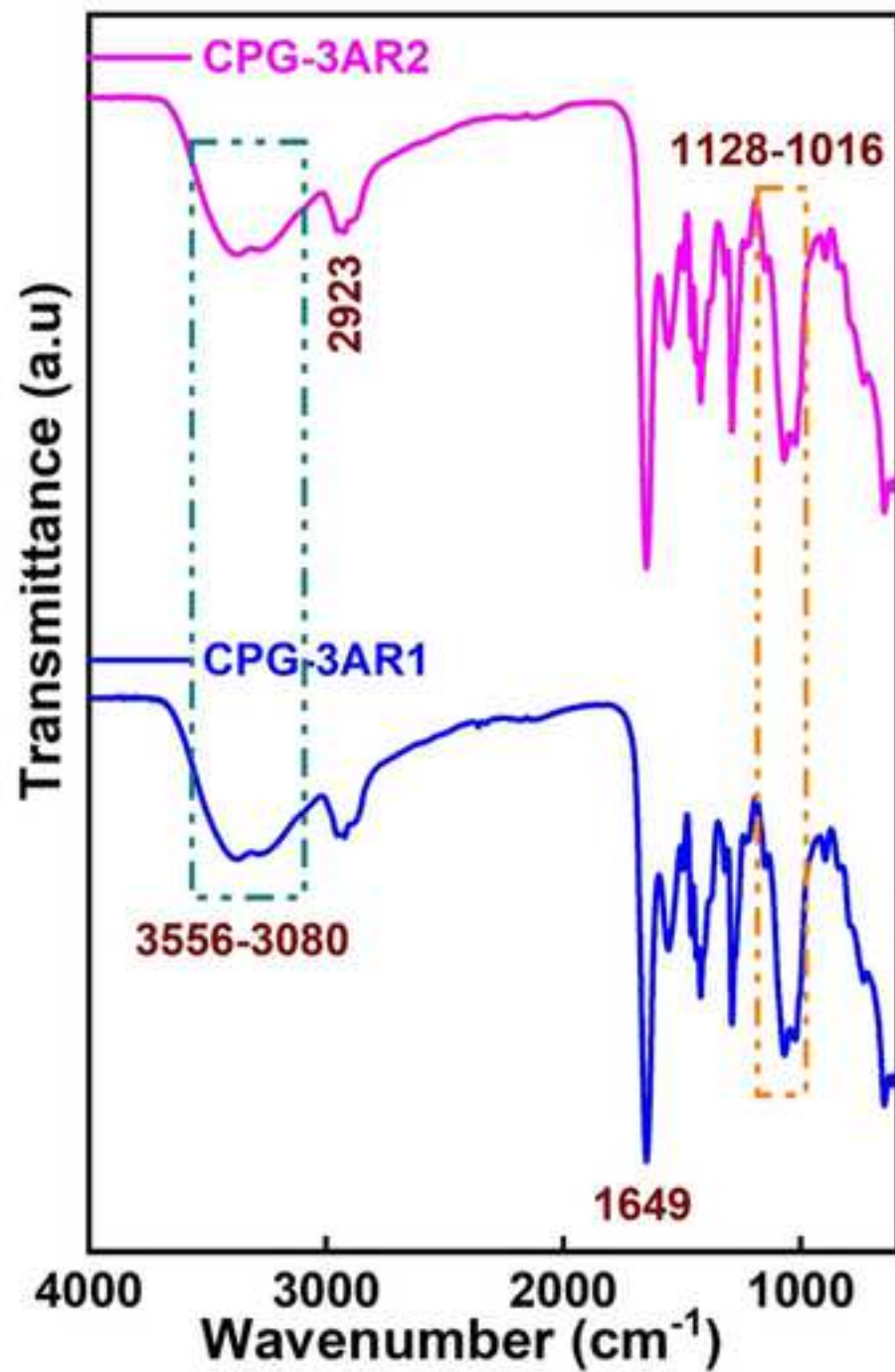
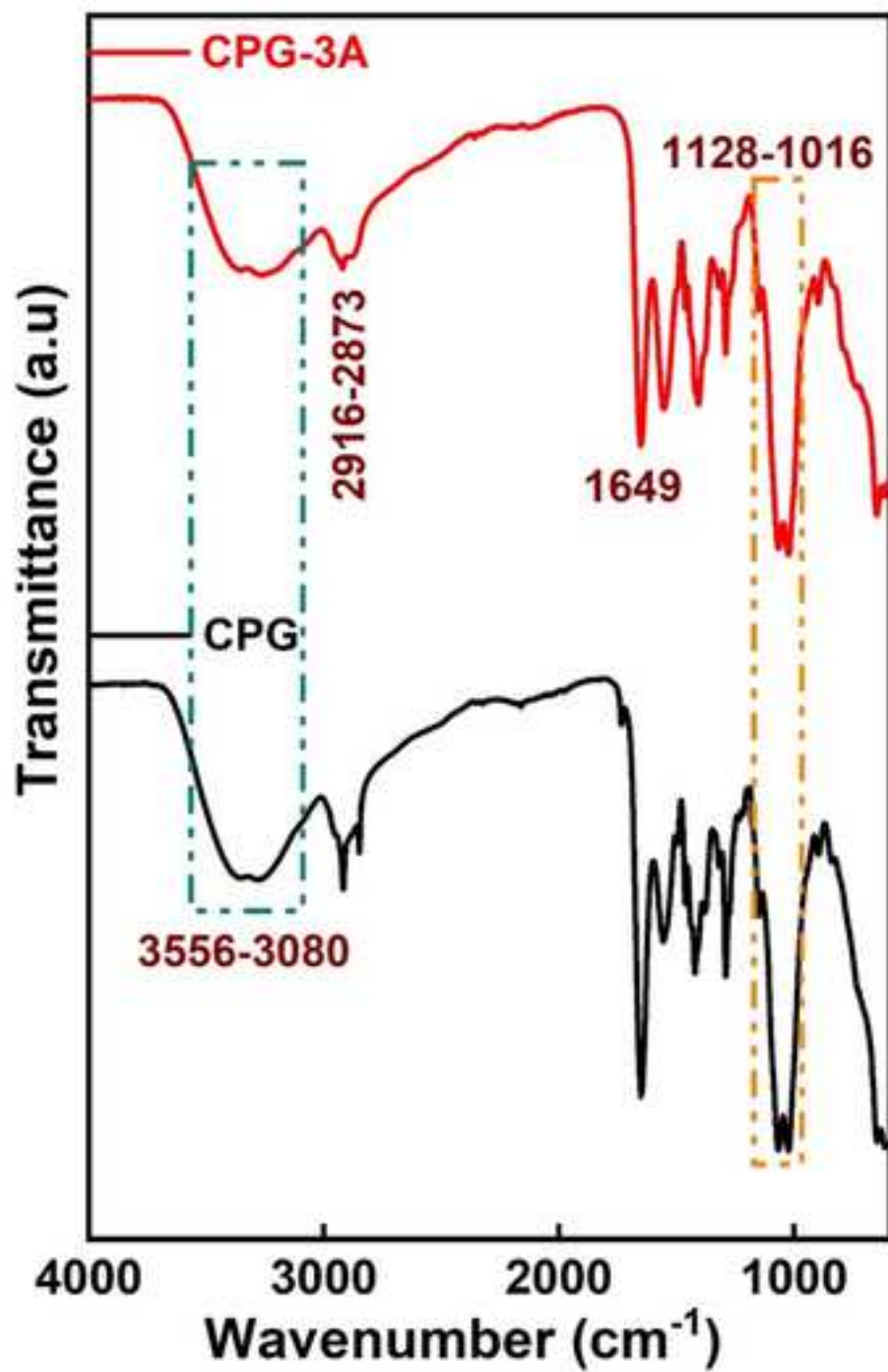
Highlights

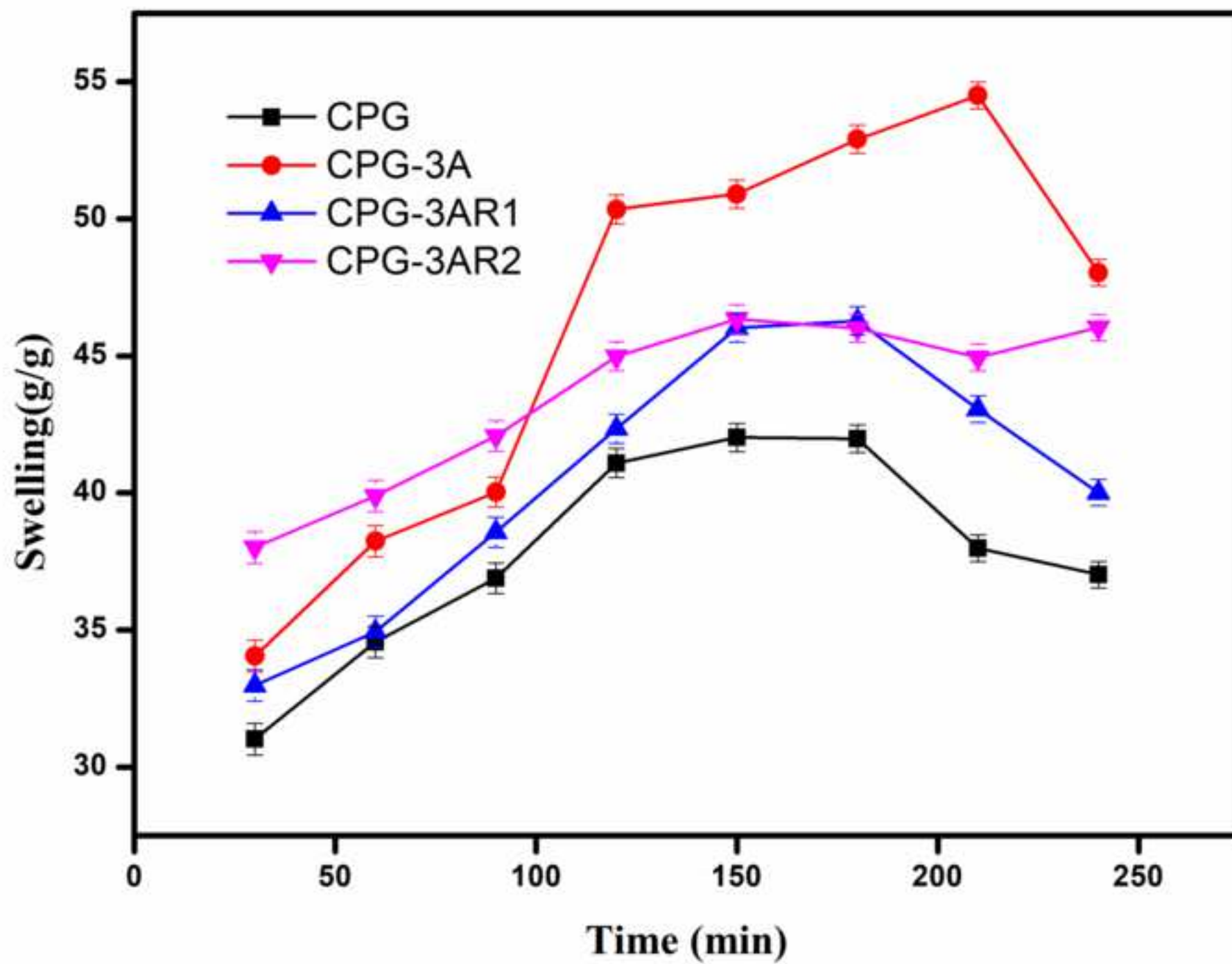
- A ternary biopolymer based hydrogel was fabricated via solution casting method.
- The synthesized ternary hydrogels were analysed by TGA, SEM, FTIR.
- Cytotoxicity and antibacterial behaviour of CPGs hydrogel was also investigated.
- Ampicillin sodium was released in controllable way and it was 98.717%.

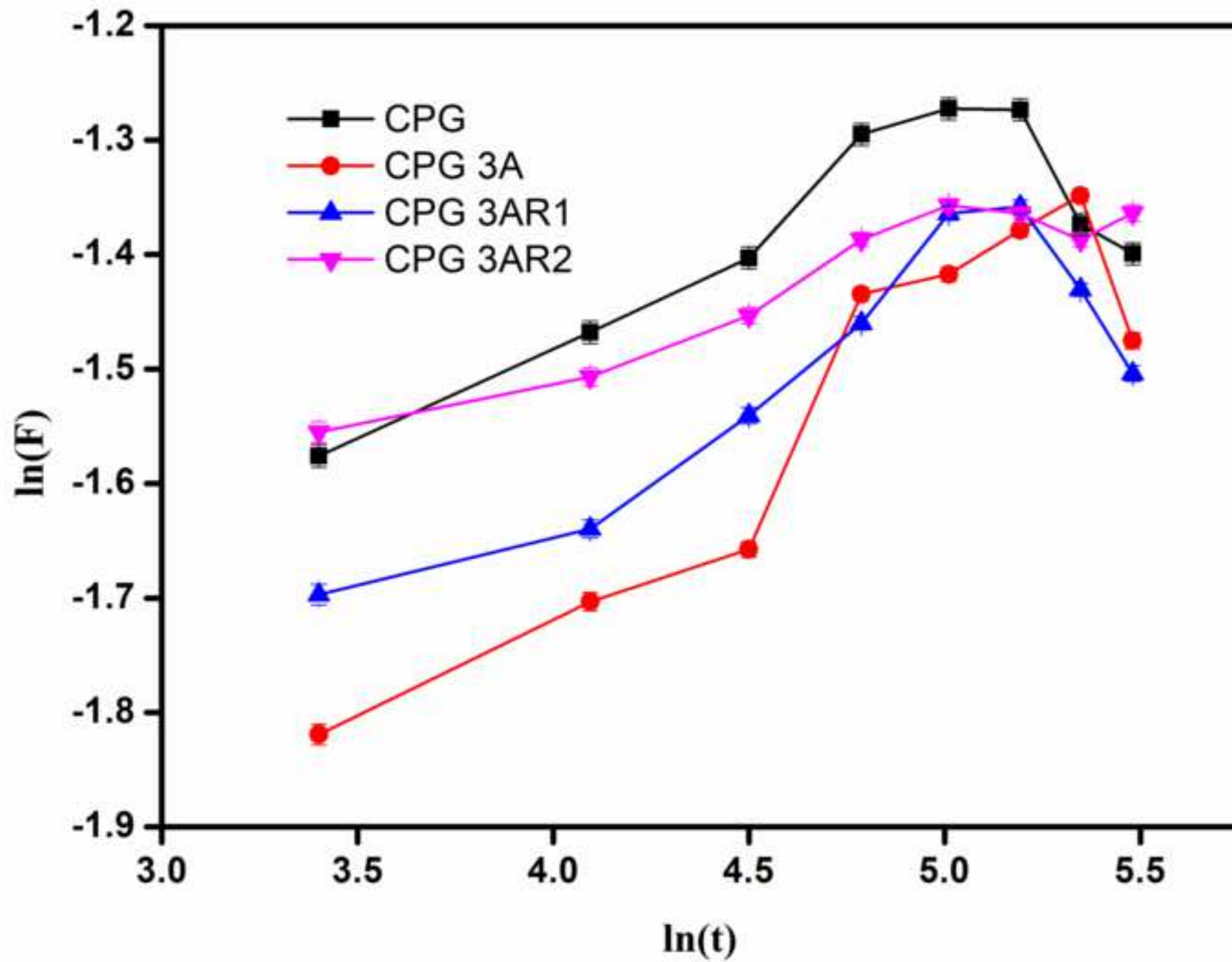


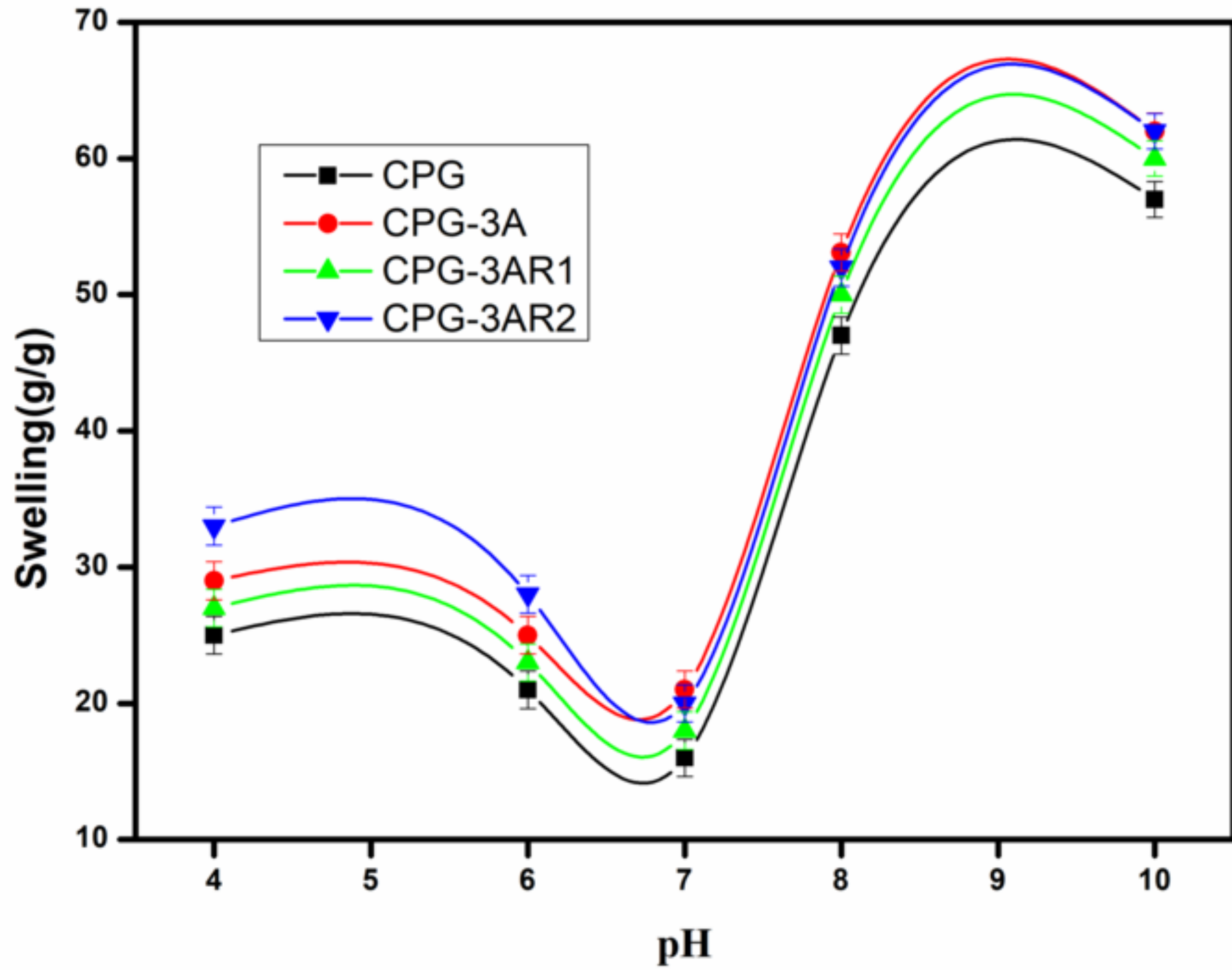


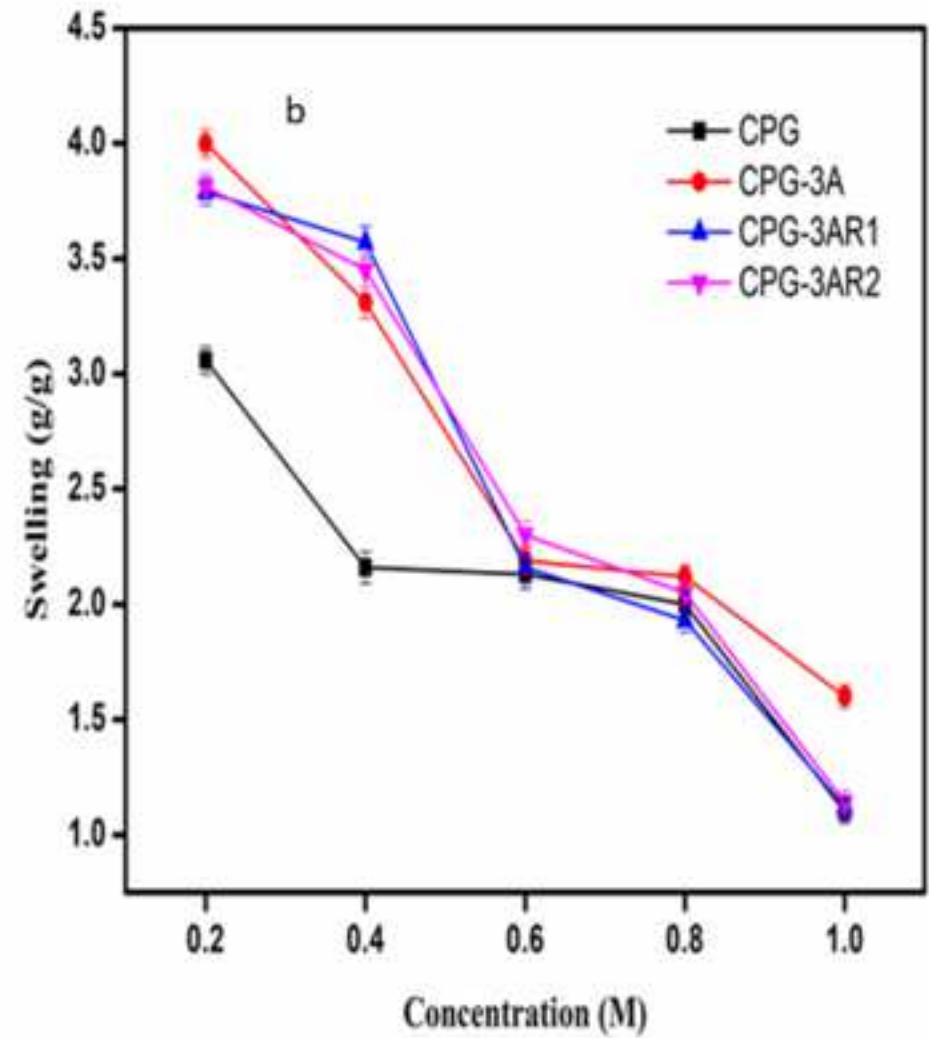
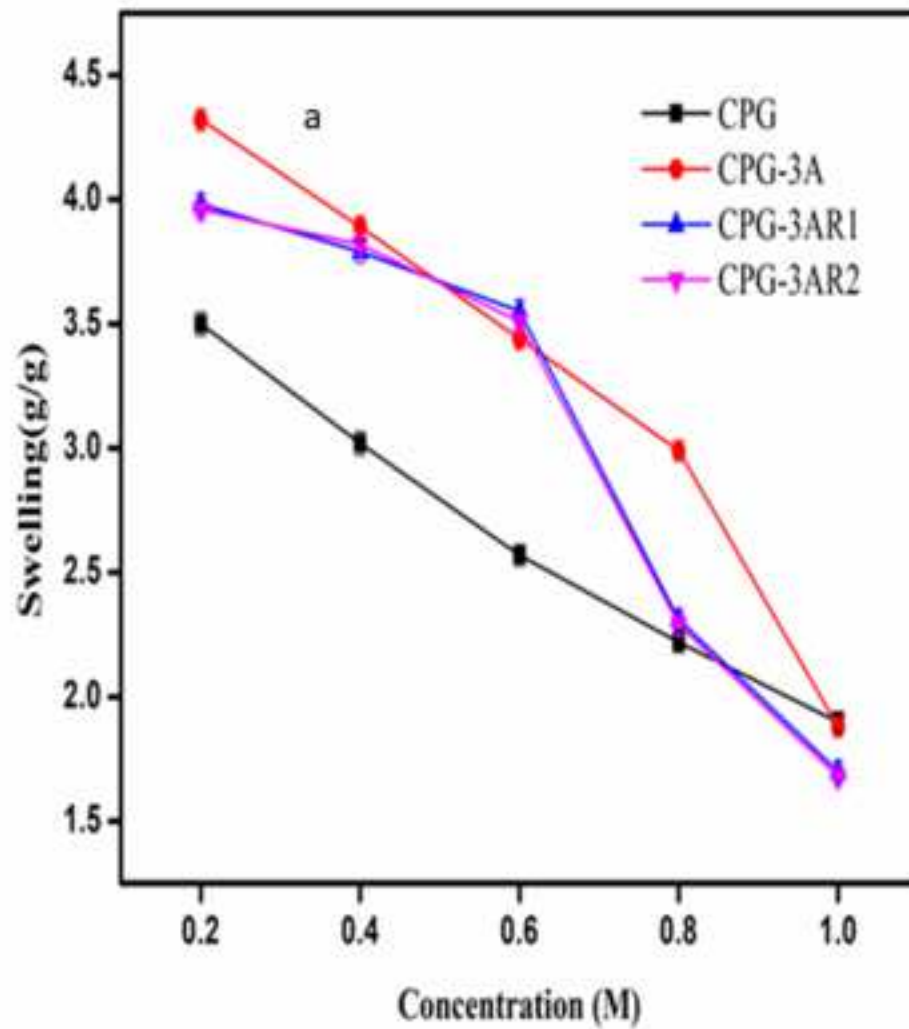


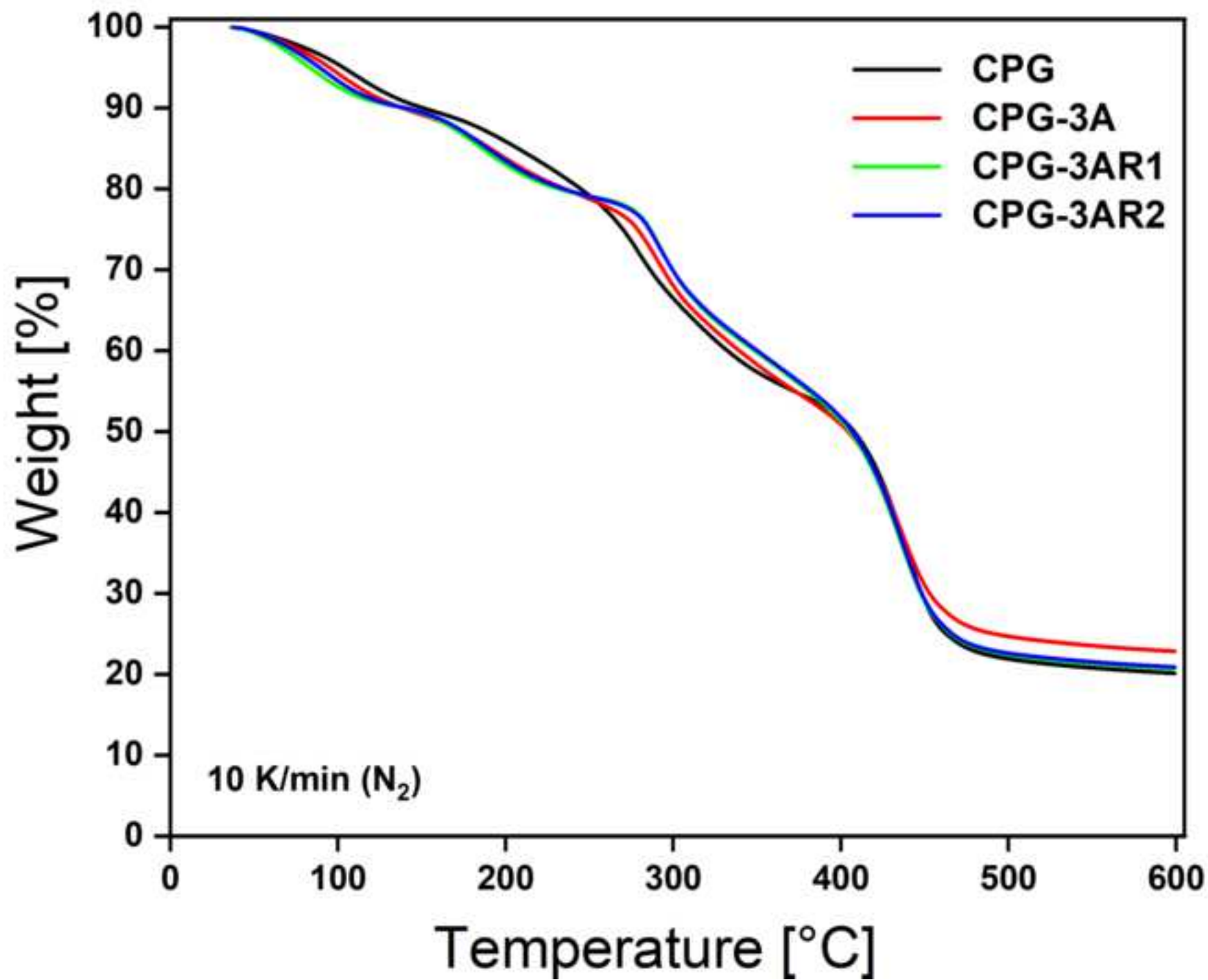


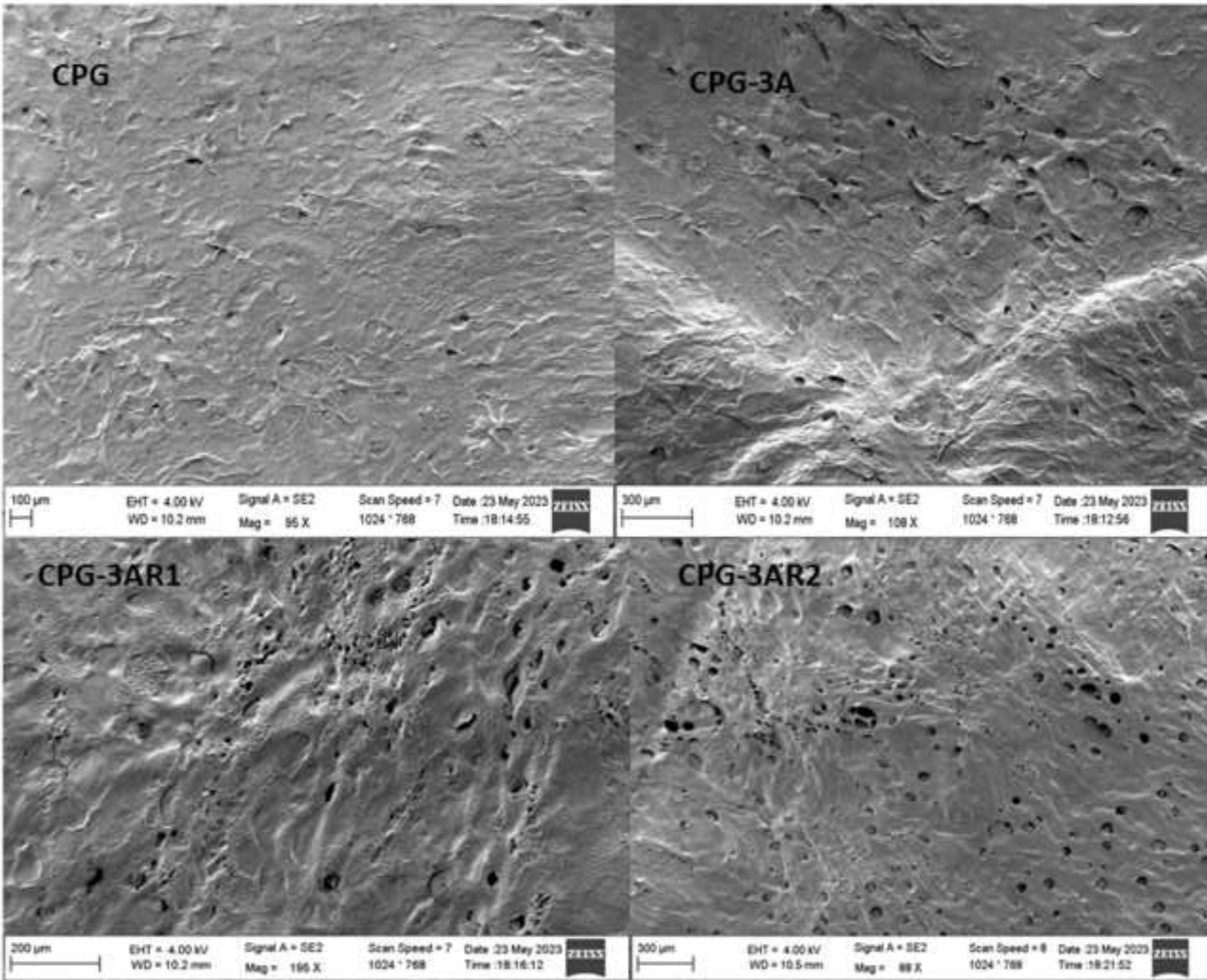


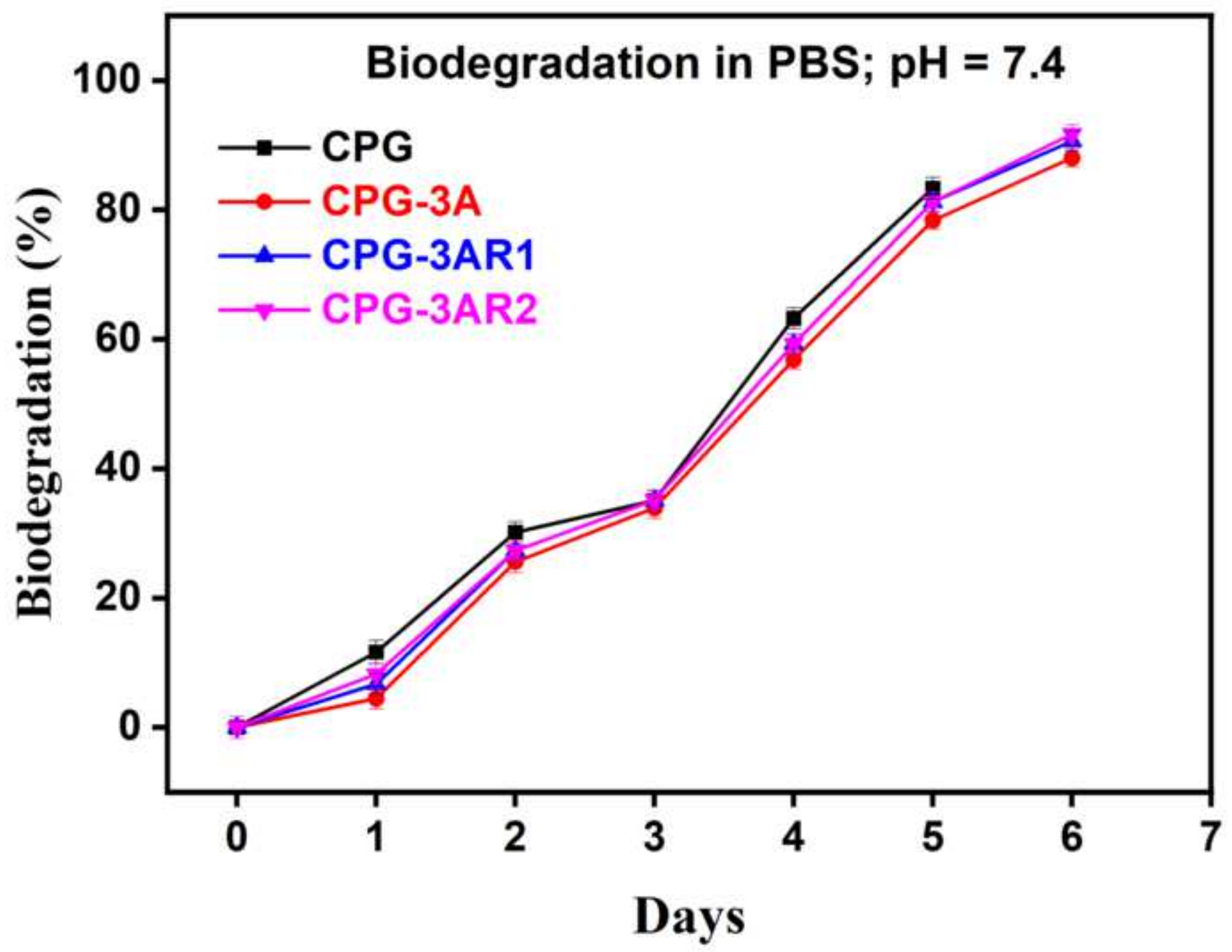


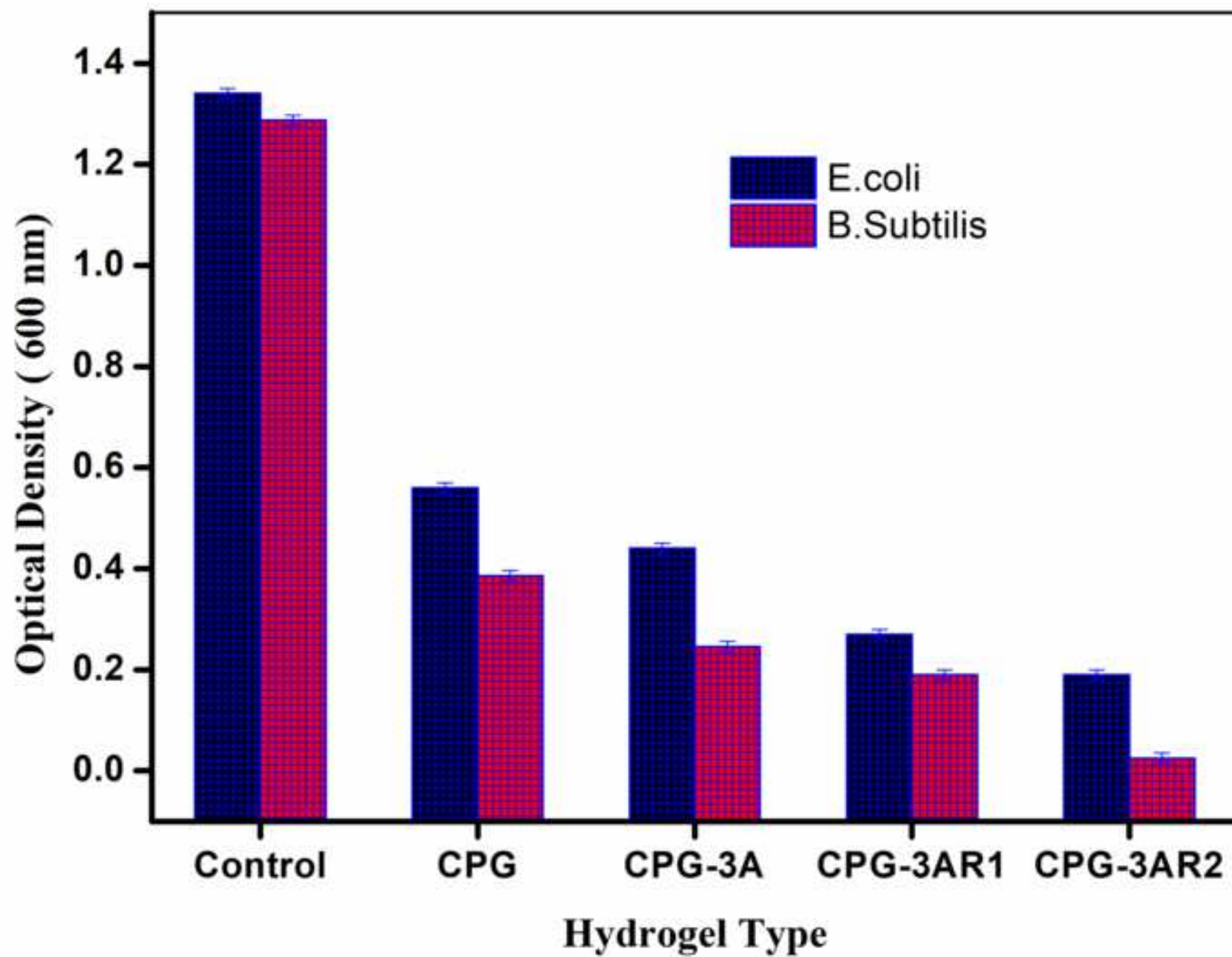












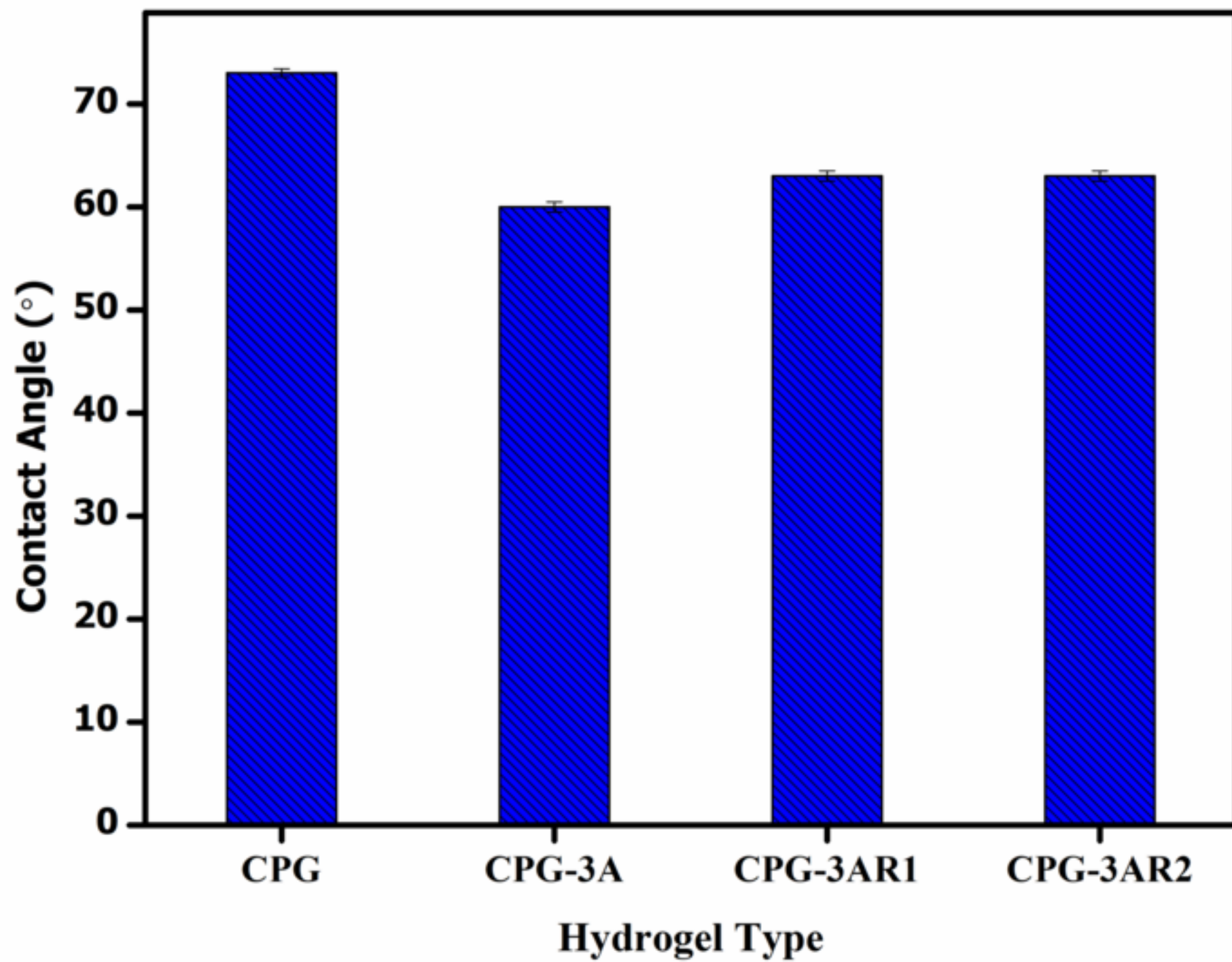


Table .1 Chemical compositions of prepared hydrogels.

Sample code	Chitosan (g)	Gum Arabic (g)	PVP(g)	Ratan-jot(μL)	Crosslinker (μL)
CPG	0.6	0.1	0.3	0.0	0.0
CPG-3A	0.6	0.1	0.3	0.0	50
CPG- 3AR1	0.6	0.1	0.3	100	50
CPG -3AR2	0.6	0.1	0.3	300	50

Table 2 Diffusion parameter of the CPGs hydrogels

Parameters	CPG	CPG-3A	CPG-3AR1	CPG-3AR2
n	0.814	0.262	0.205	0.125
Intercept	-2.209	-2.747	-2.436	-1.999
k	0.109	0.064	0.087	0.135
Regression(%)	96	91.9	91.9	92.9

Table.3 Percentage of *A. Salina* deaths following 24-hour exposure to CPGs

Types of Hydrogels	Mortality (%)
CPG	1.72
CPG-3A	1.56
CPG-3AR1	1.51
CPG-3AR2	1.47

Table 4 Porosity % of prepared hydrogels.

Sample code	Porosity (%)
CPG	53.07+0.87
CPG-3A	57.03+0.71
CPG-3AR1	58.41+0.21
CPG-3AR2	58.89+1.02

Declaration of interests

The authors declare that they have no known competing financial interests or personal relationships that could have appeared to influence the work reported in this paper.

The authors declare the following financial interests/personal relationships which may be considered as potential competing interests:

Credit statement

Huma Andlib: Writing - Original Draft, Methodology, Software, Data Curation, Analysis
Aneela Sabir: Supervision, Resources, Project administration **Muhammad Shafiq:** Supervision,
Project administration. **Sehrish Jabeen:** Formal analysis, Resources **Timothy Douglas:**
Supervision

Synthesis of pH-sensitive ternary hydrogel with synergetic antibacterial response for the release of ampicillin sodium

Huma Andlib^{1,*}, Muhammad Shafiq¹, Aneela Sabir¹, Sehrish Jabeen², Timothy Douglas³.

¹Institute of Polymer and Textile Engineering, University of the Punjab, Lahore, 54590, Pakistan

²Institute of Polymer Materials, Friedrich-Alexander-University Erlangen-Nuremberg, Martensstrasse 7,91058 Erlangen, Germany

³School of Engineering, Gillow Avenue, Lancaster University, Lancaster, LA1 4YW, United Kingdom

Corresponding author: Huma Andlib*, Email: hshah3421@gmail.com,

Phone: +923324534788

Abstract

In the area of biomedicine, pH-responsive hydrogels have attracted a lot of attention. The smart novel polyelectrolyte complex carriers are made of chitosan, gum arabic and polyvinylpyrrolidone using various concentrations of ratan-jot plant extract for the release of sodium ampicillin antibiotic very first time. These hydrogels have been prepared by solution casting method and cross-linked by using 3-aminopropyltriethoxymethyl silane. According to swelling experiments, the cross linker concentration led to decreased swelling because the hydrogels were more tightly packed together. CPG-3A showed maximum swelling 54.5g/g in 210 minutes. When the swelling behaviour of hydrogels was tested under various pH circumstances, it was found that they swelled most noticeably in alkaline media and least noticeably in acidic and neutral pH settings. These hydrogels may be appropriate for injection-based controlled drug release due to their unique pH-responsive behaviour. Ampicillin sodium salt was utilised as a model drug to analyse drug release behaviour of engineered hydrogel at pH 7.4. The results indicate that these smart hydrogels could be used for injectable controlled drug release (ampicillin sodium) for the treatment of wound as well as for other biomedical applications.

Keywords. Chitosan; Controlled release; ratan-jot extract; Ampicillin sodium; Antibacterial response

Highlights

- A ternary biopolymer based hydrogel was fabricated via solution casting method.
- The synthesized ternary hydrogels were analysed by TGA, SEM, FTIR.
- Cytotoxicity and antibacterial behaviour of CPGs hydrogel was also investigated.
- Ampicillin sodium was released in controllable way and it was 98.717%.

1. Introduction

The production of precise and targeted dosage forms has become more important for efficiently treating illnesses and recovering patients well-being keeping in view of the alarming increase in diseases and health issues. Conventional way of drugs intake possess uncontrolled side effects, because administered drug also reached to the other parts of body and very minor proportion of drug reached to the infected area of body [1, 2].

Now a days , researchers are more attentive and eager for the development of new category of therapeutic materials to solve the emerging problems of bio-therapeutics and drug access to the targeted site without any adverse side effect [3-5]. To increase the specificity of drug distribution system and to decrease the toxicity of drugs, many devices are synthesized since last few decades to overcome the sever attack of various diseases. To address these issues of drug

1 delivery system we focused here the release of drug from bio-polymers based hydrogel system.
2 Hydrogel is immerging field and considered as structural backbone for development of novel
3 and potent therapeutic agents [6].
4

5 Hydrogel, plays an indispensable role in our daily life due to their marvellous properties.
6 Hydrogels show capacity to absorb the high quantity of water and having a three-
7 dimensional(3D) cross linked, or a straight or a forked water loving structure. Hydrophilicity
8 behaviour of hydrogel is produced because of the presence of some water loving groups like -
9 OH, -COOH, -NH₂. They show swelling variation with changing in their structure and potential
10 properties, in response to various stimulus [3, 6-10]. In this contemporary era, hydrogels can
11 be synthesized through natural, synthetic as well as from semi synthetic polymers.
12 Biopolymers made hydrogels are more effective because of their exceptional properties, like
13 non-hazardous behaviour, good biocompatibility, excellent biodegradability and economical
14 suitability etc. This is the reason they play significant role in the relief of pain as well as to
15 overcome diseases and many more other biomedical applications [11, 12]. Among bio-
16 polymers, the chitosan and its derivative are cationic polymers with antioxidant, anti-bacterial
17 (against many microorganisms with a high mortality rate) and antifungal properties making it
18 unique for targeted drug delivery platform [7, 13, 14]. Chitosan is derivative of chitin and
19 generated by its deacetylation This is the second most prevalent biopolymer in the world after
20 cellulose and exist in exoskeleton of insects and crustaceans like crabs, lobsters etc., [15-17].
21 Gum arabic is one of the ancient gum well-known due to its numerous application
22 approximately for more than 5000 years. Gum arabic is composed of polysaccharides as well
23 as glycoproteins mainly the polymers of galactose and arabinose. Gum Arabic shows excellent
24 properties like water solubility, antioxidant properties, antibacterial, haemostatic and non-
25 haemolytic properties. Non digestible properties make it more attractive in the field of
26 pharmaceutical industries [18-20]. Although, the biopolymers show good compatibility to
27 human body but on the other hand, mechanical strength of biopolymer-based hydrogel is
28 usually low. This problem can be controlled by unification of biopolymer with a synthetic
29 polymer or even with some other appropriate biopolymer. This strategy will not only improve
30 the sustainability of hydrogels but also plays an important role to keep their structure intact for
31 the period of drug delivery by enhancing the hydrogels thermal stability [21]. These combined
32 biomaterials with non-natural polymers like polyvinyl pyrrolidone (PVP), also known as
33 polyvidone (C₆H₉NO)_n have proved excellent in achieving extraordinary mechanical strength.
34 PVP is amorphous polymer, it shows good water solubility as it is hydrophilic in nature but it
35 is also soluble in organic solvents [22]. PVP is considered as a potential polymer because it
36
37
38
39
40
41
42
43
44
45
46
47
48
49
50
51
52
53
54
55
56
57
58
59
60
61
62
63
64
65

1 attracts pharmacist due to its distinctive properties like cytocompatibility, non-toxicity, cheap
2 and biodegradability [23-26]. Silane based cross linkers are getting more attraction by scientists
3 as these possess countless unique properties. Cross linker increases mechanical strength of
4 hydrogels as well as control high swelling rate by making chemical bonds with their reactive
5 groups to the polymer functional groups. In this study, we pick out a 3-aminopropyl
6 (diethoxy)methyl-silane cross linker due to its bio functional properties as well as its
7 environmental friendly behaviour. The mechanical strength and drug loading capacity of a
8 hydrogel is increased by dual crosslinking ability of 3-aminopropyl (diethoxy) methyl-silane
9 through its amino and silane groups. Hydrogen and covalent bonds are formed between amino
10 group of 3-APDEMS and polymeric groups [27]. Plethora of plants extracts are also used in
11 hydrogel synthesis as polyphenols, carotenoids due to their anti-oxidant and anti-bacterial
12 properties. Extraction from the roots of alkanet plant are used to produce a red dye. One of the
13 famous name of red dye is ratan-jot. This red dye is basically herbal drug that is famous for its
14 anthelmintic, antipyretic and antiseptic behaviour. It plays an undeniable role in various types of
15 wounds treatment. However, naphthoquinones, is the main component of drug (extracted from roots
16 of plant) that is responsible for its red colour. In fact, therapeutic behaviour of drug is due to
17 naphthoquinone [28-30].

18 The broad-spectrum antibiotic ampicillin is a white crystalline powder that dissolves in water
19 easily. It is frequently used to treat bacterial infections and works well for a variety of problems,
20 such as gonorrhoea, respiratory and urinary tract bacterial infections and several illnesses of the
21 gastrointestinal and neurological systems. Because of its good adaptability, ampicillin is a good
22 choice for treating a range of bacterial infections.

23 This study comprises, synthesis of novel ternary polysaccharide based hydrogel made of
24 chitosan (CS), polyvinylpyrrolidone (PVP) and gum arabic(GA) in the presence of cross linker
25 3-aminopropyldiethoxymethylsilane (3-APDEMS) with variable concentrations of ratan-jot
26 (RJ) ethanolic extract. Ampicillin sodium salt was added to the hydrogel as a model drug in
27 order to study this antibiotic release characteristic. This formulation was not used yet according
28 to best of our knowledge. The fabricated hydrogel was analysed by FTIR, TGA, SEM,
29 Biodegradation, water swelling, cytotoxicity and by antibacterial test.

30 **2. Experimental details**

31 **2.1 Materials**

32 CS (Mw = 406,039 g/mol, degree of deacetylation (DDA) 90%). Polyvinylpyrrolidone (PVP)
33 (Mw = 40,000–70,000 g/mol), Acetic acid (CH₃COOH) (100%) extra pure was purchased from
34 Merck, Germany. respectively, 3-Aminopropyldiethoxymethylsilane (97%) were obtained
35
36
37
38
39
40
41
42
43
44
45
46
47
48
49
50
51
52
53
54
55
56
57
58
59
60
61
62
63
64
65

1 from Sigma Aldrich. Gum arabic (Mw = 250,000 Da), purchased from Sigma Aldrich (USA).
2 Ratan-jot ethanoic extract was made at indigenous level in the laboratory. Sodium dihydrogen
3 phosphate (Na₂HPO₄), Boric acid, NaCl (Sodium chloride), KCl (Potassium chloride), CaCl₂
4 (Calcium chloride) and Potassium dihydrogen phosphate (KH₂PO₄) were also obtained from
5 Sigma-Aldrich. Sodium acetate (CH₃COONa) and sodium hydroxide (NaOH) were obtained
6 from Riedel-de Haen. HCl (hydrochloric acid) and Ethanol (C₂H₅OH) were purchased from
7 BDH laboratory supplies and J.T. Baker, respectively. We used analytical-grade chemicals in
8 our studies, using them directly without any need for purification.
9

14 **2.2 Methodology**

16 **2.2.1 Extraction of ratan-jot (*Alkanna tinctoria*) extract**

18 Ethanolic extract of ratan-jot has been prepared by conventional method. In this study the roots
19 of the plant were washed properly to remove mud completely. The roots were then blotted and
20 dried by filter paper by changing the filter paper regularly after few intervals. These were further
21 dried in sunlight for 7 days, in oven at 50 °C and finally dried in a vacuum desiccator. The
22 completely dried roots were, thereafter, grinded and sieved to get a fine powder and was stored
23 in air tight bottle. 10 grams of this powder was weighed and added in 50 ml of ethanol in a
24 sample bottle and was stored in dark place for 14 days. Finally, after 14 days all the extract got
25 infuse in the ethanol.
26

32 **2.2.2 Preparation of Hydrogel**

34 Chitosan (0.6 g or 60 wt%) was dispersed in 50 ml of 0.5 % acetic acid solution at temperature
35 of 60°C with stirring continuously for 3 hours to get complete dissolution. Gum arabic (0.1 g
36 or 10 wt%) was dissolved in 40 ml double distilled water with magnetic stirring at 50°C until
37 it became a smooth solution. Gum arabic solution was mixed with chitosan solution and was
38 put again on magnetic stirring at 50°C for another 2 hours to get homogeneous blend. PVP (0.3
39 g or 30 wt%) was solvated in 50 ml of double distilled water with magnetic stirring at 95°C on
40 hot plate. Then PVP solution was blended with chitosan and GA solution by magnetic stirring
41 for 2 hours on hot plate at 50°C. The ethanolic extract of ratan-jot was added in ternary blend
42 (CS/GA/PVP) and was stirred for 1 hour. The 3-APDEMS cross linker was first added in 5 ml
43 of ethanol and then added drop wise in CS/GA/PVP/RJ blend. This later solution was vortexed
44 and then stirred for minimum 4 hours for maximum crosslinking at same temperature. The
45 prepared solution was added to petri dishes before being dried in a vacuum oven (LVO-2040,
46 Lab Tech, Korea) at 60°C. The ethanol was evaporated when the hydrogel film dried and the
47 remaining residues of acetic acid were removed by washing it with distilled water.
48
49
50
51
52
53
54
55
56
57
58
59
60
61
62
63
64
65

Through use of the same processes, four formulations were made, each with a varied rattan-jot concentration ranging from 0 to 300 μL and a constant cross-linker concentration of 50 μL . The control hydrogel was synthesized with neither cross linker nor rattan-jot and named CPG. Hydrogel with just cross linker code as CPG-3A. The hydrogel with 50 μL cross linker and with 100 μL quantity for rattan-jot code as CPG-3AR1. Further, hydrogel with same the volume of cross linker and 300 μL of rattan-Jot code as CPG-3AR2. Table.1. exhibits the hydrogels composition along their specific code.

Table .1 Chemical compositions of prepared hydrogels.

Sample code	Chitosan (g)	Gum Arabic (g)	PVP(g)	Ratan-jot(μL)	3-APDEMS(μL)
CPG	0.6	0.1	0.3	0.0	0.0
CPG-3A	0.6	0.1	0.3	0.0	50
CPG- 3AR1	0.6	0.1	0.3	100	50
CPG -3AR2	0.6	0.1	0.3	300	50

The possible interactions taking place within the hydrogel components are depicted in Figure.1.

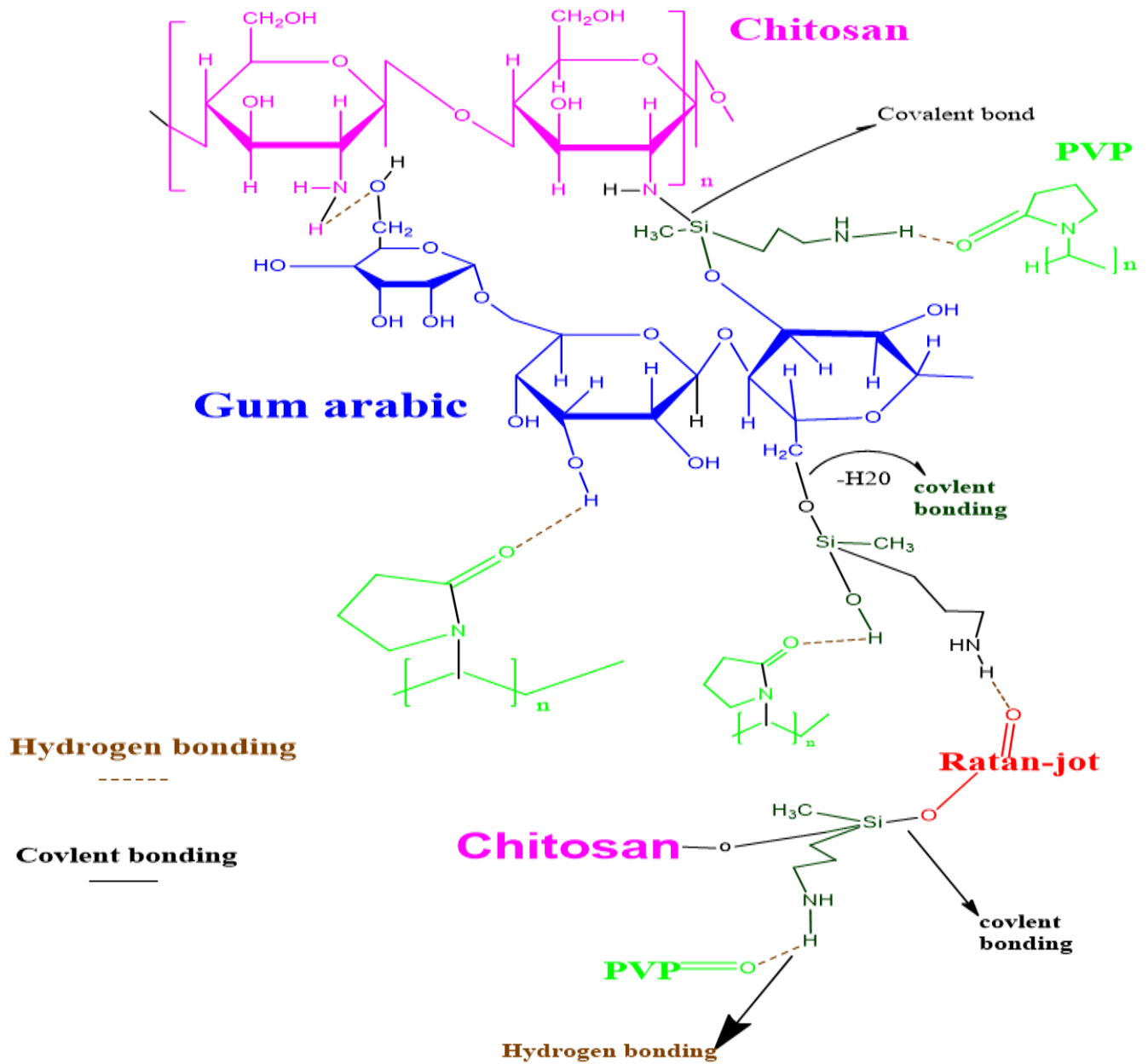


Fig.1 Schematic interactions between the components of the CPGs hydrogel.

2.3 Antibiotic-loaded hydrogel synthesis

Chitosan (0.6 g or 60 wt%) was dispersed in 50 ml of 0.5% acetic acid solution at temperature 60°C with stirring continuously for 3 hours to get complete dissolution. Gum arabic (0.1 g or 10 wt%) was dissolved in 40 ml double distil water with magnetic stirring at 50°C until it became a smooth solution. Gum arabic solution was mixed with chitosan solution and put it again on magnetic stirring at 50°C for another 2 hours to get homogeneous blend. PVP (0.3 g or 30 wt%) was solvated in 50 ml of double distilled water with magnetic stirring at 95°C on hot plate. The polyvinylpyrrolidone (PVP) solution was blended with chitosan and GA blend by

1 magnetic stirring for 2 hours on hot plate at 50°C. Ethanol extract of ratan-jot 300 µL was
2 added in synthesized ternary blend (CS/GA/PVP) and stirred for 1 hour. Afterward 50 mg of
3 ampicillin sodium drug was dissolved in distilled water and added to the blend.
4

5 The 3-APDEMS cross linker was first added in 5 ml of ethanol and thereafter added drop wise
6 in CS/GA/PVP/RJ + Drug blend. This later solution was put on stirring for 4 hours for
7 maximum crosslinking at same temperature. The fabricated solution was cast in petri dishes
8 and desiccated. by using a drying oven (LVO-2040, Lab Tech, Korea) at 60°C under vacuum
9 desiccator.
10
11
12
13

14 **3. Characterizations**

15 **3.1 Fourier transform infrared microscopy**

16 To confirm the existence of particular functional groups and to clarify interactions between the
17 hydrogel components, FTIR spectra were obtained for all hydrogel samples (CPG, CPG-3A, CPG-
18 3AR1, CPG-3AR2). The FTIR spectra were collected using FTIR spectrophotometer with a resolution
19 of 2 cm⁻¹, a scan rate of 32 scans per spectrum and a programmed range of 4000 to 400 cm⁻¹ (Model:
20 Tensor II, Bruker).
21
22
23
24
25
26

27 **3.2 Swelling studies**

28 **3.2.1 Swelling trend in distilled water**

29 The fully dried hydrogel was initially divided into tiny 25 mg pieces in order to assess the
30 hydrogels response when swollen in distilled water. Next, 40 ml of double-distilled water was
31 poured into a plastic petri dish with these hydrogel fragments. After predetermined time, the
32 water was drained from the petri dish. (for instance, 10 minutes) and the petri dish was then
33 gently cleaned with tissue paper to remove any remaining water. The swelled hydrogel sample
34 weights were calculated accordingly. This process was continued until equilibrium was
35 attained. Each hydrogel was subjected to this complete experiment three times in order to
36 achieve the mean value for more accurate findings. The swelling ratio was determined by using
37 following formula
38
39
40
41
42
43
44
45
46

$$47 \text{ Swelling } \left(\frac{g}{g}\right) = \frac{W_s - W_d}{W_d} \quad (1)$$

48 Here W_d is the weight of vacuum dried hydrogel at a specific time interval and W_s denotes the
49 weight of swelled hydrogel at time [31].
50
51
52

53 **3.2.2 Swelling trend in pH solutions**

54 Individually prepared buffer solutions with different pH values (1.2, 2, 4, 6, 7, 8, 10) were
55 submerged with pre-measured hydrogel samples, and they were let to approach equilibrium.
56 The buffer solution was then removed, and the hydrogel samples were delicately patted with
57
58
59
60
61
62
63
64
65

1 paper to remove the surface solvent. The weight of the swelled hydrogel was measured, and the
2 degree of swelling was estimated using the formula given before. To increase the accuracy of
3 the results, this process was performed three times.
4

5 **3.2.3 Swelling trend in ionic solutions.**

6
7 The evaluation of electrolyte solution swelling was done. In particular, prepared electrolyte
8 solutions containing NaCl and CaCl₂ at different concentrations (0.2, 0.4, 0.6, 0.8, and 1.0 M)
9 were made in accordance with known procedures. Utilising the same technique described in
10 Section 3.2.1, the swelling indices of the hydrogels made in various electrolyte solutions were
11 calculated.
12
13
14
15

16 **3.3 Thermogravimetric analysis**

17
18 TGA of hydrogels was carried out on Thermal analysis instrument SDT build 95 module DSC-
19 TGA standard, USA, with nitrogen flow of (15 ml/min). The temperature range was kept at 20
20 °C per-min from ambient room temperature to 600 °C.
21

22 **3.4 *In-vitro* biodegradation**

23
24 CPG samples were cross-linked with fixed concentration of 3-APDEMS and different ratan-jot
25 extract concentrations before being dipped into a PBS solution at 37 °C. At certain intervals (1,
26 2,3,4, 5 and 6 days), the degradation of the samples was monitored. The samples were removed
27 from the solution, thoroughly dried with blotting paper to eliminate any excess solution,
28 weighed, and afterward submerged in new PBS solution once more. To avoid any
29 contamination from bacteria or fungi, all studies were conducted in sterilised environments.
30 Using the following equation (2), the biodegradability of the hydrogel samples was calculated
31
32
33
34
35
36
37

$$38 \quad Biodegradation (\%) = \frac{W_d - W_i}{W_i} \times 100 \quad (2)$$

39
40 where W_d is the weight of the CPG samples following degradation and W_i is the weight of the
41 CPG specimens at their initial composition [32, 33].
42
43

44 **3.5 Antimicrobial profile**

45
46 CPGs were tested against Escherichia coli (*E. coli*) and B.Subtilis to determine their
47 antibacterial efficacy. The sterile Luria-Bertani (LB) medium was used to monitor the growth
48 of the bacterial strain. It was made by dissolving 10 g of tryptone, 5 g of yeast, and 10 g of NaCl
49 in 800 ml of distilled water while keeping the pH neutral. Following volume adjustment to 1000
50 ml, the solution was autoclave sterilized for one hour. During the sample preparation process,
51 a hydrogel sample (5 × 5 mm) was added after mixing 20 ml of LB media and 20 ml of bacterial
52 strain (*E. coli* or *B.Subtilis*). The control group underwent the same process again. Using a
53
54
55
56
57
58
59
60
61
62
63
64
65

1 spectrophotometer (Double beam, PerkinElmer, Model Lambda25, USA) set to measure optical
2 densities at 600 nm, the antibacterial efficacy was evaluated [34].

3 **3.6 Cytotoxicity Evaluation *in-vitro***

4
5 Using the brine shrimp lethality assay, a typical method for preliminary toxicity screening, in
6 vitro cytotoxicity study was carried out. Brine shrimp eggs were incubated for 48 hours at room
7 temperature in sterile sea water with constant aeration in order to conduct the experiment.
8
9 Active nauplii were taken after hatching and moved to a deep well microliter plate from the
10 brighter area of the hatching vessel. Each well of the plate was 1.8 cm in diameter, 2 cm deep,
11 and contained 0.2 ml of saltwater. In the wells containing active nauplii, hydrogel samples were
12 inserted in triplicate and the immature larvae were counted. The experiment involved keeping
13 the well plate at normal temperature and in the dark. Following a 24-hour observation period,
14 observations of surviving nauplii were made under a microscope (GXM, XPL33230; GT
15 Vision, Haverhill, UK) and tallied to determine mortality using Equation (3)
16
17
18
19
20
21
22

$$23 \quad M(\%) = \frac{A-B-N}{G-N} \times 100 \quad (3)$$

24
25
26 Where: After 24 hours, M is the proportion of dead larvae.

27 A is the quantity of dead larvae after 24 hours.

28 B represents the typical number of dead larvae in the control samples after a day.

29 G = the total number of larvae,

30 N = the number of dead larvae before the test.

31
32
33 This formula made it possible to calculate the proportion of dead larvae after 24 hours while
34 taking into account the control samples and beginning larval population [35].

35 **3.7 Porosity**

36
37 Using the solvent displacement method, the synthetic hydrogels' porosity was evaluated. As a
38 standard, 100% ethanol was employed as the displacing solvent. An electronic Vernier calliper,
39 the Fowler 6/150 mm Pro-Max Electronic Calliper 54-200-777-1, was used to measure the
40 length, width, and volume of dry hydrogel films. To successfully permeate the hydrogel pores,
41 pre-weighed hydrogel samples were submerged in the displacement solvent for 24 hours. The
42 samples that had been soaked were taken out of the solvent after 24 hours and weighed again.
43 Each sample went through this procedure three times. Equation 4 was used to calculate the
44 percentage of porosity [36].
45
46
47
48
49
50
51
52
53

$$54 \quad \text{Porosity \%} = \frac{M2-M1}{\rho V} \times 100 \quad (4)$$

1 Here, M_1 is the weight of sample before dipped in ethanol and M_2 is the weight of the
2 hydrogel sample after it has been soaked in ethanol. V is the volume of sample and ρ is the
3 density of ethanol.
4

5 **3.8 Scanning electron microscopy**

6 Scanning electron microscopic analysis (SEM) was used for Surface morphology of the
7 hydrogel. Hydrogels were inspected through SEM, Model JEOL/EO JSM 6480 (LA) Akishima,
8 Tokyo, Japan. At different magnification the SEM images of hydrogels were recorded. A 48-
9 hour freeze-drying procedure in liquid nitrogen under vacuum conditions was used to retain the
10 hydrogel's porous cross-linked structure without compromising it. Approximately 0.2 mm was
11 the thickness of the samples.
12
13
14
15
16
17

18 **3.9 Contact angle**

19 The wettability of the hydrogel surfaces after hydration was evaluated using the Contact Angle
20 (CA) measurement. We used a Dataphysics Model OCA20 (Filderstadt, Germany) to do this
21 assessment at room temperature. Before being placed on a glass cover slide, the hydrated
22 hydrogel samples were divided into 2 cm² pieces. Using a micrometric syringe, ten microliters
23 of deionized water were injected onto the sample surface. After taking a still picture, the inbuilt
24 software was used to calculate the contact angle. We recorded the average values of each sample
25 after it was tested ten times ($n = 10$).
26
27
28
29
30
31

32 **3.10 Drug release profile**

33 Phosphate buffer saline (PBS) solution of pH 7.4 was used to study drug release. In 500 ml of deionized
34 water, 4.0 g of NaCl, 0.12 g of KH₂PO₄, 0.1 g of KCl, and 0.72 g of Na₂HPO₄ were mixed to make the
35 PBS solution. At 37 °C, 100 ml of the PBS solution was used to submerge the drug-loaded hydrogel.
36 In order to keep the beakers total volume at 100 mL, 5.0 ml of the solution was taken out and replaced
37 every 10 minutes with an equal amount of brand-new PBS solution. A UV-Vis spectrophotometer
38 (more precisely, a double-beam Perkin Elmer Model Lambda 25 USA) with a wavelength of 205 nm
39 was used to analyse the samples over the course of three hours. For comparison, ampicillin sodium
40 reference solution with a 100 ppm concentration was also made.
41
42
43
44
45
46
47
48
49
50

$$51 \text{ Cumulative release (\%)} = \left(\frac{M_t}{M_0} \right) 100\% \quad (5)$$

52 In this context, M_t stands for the amount of ampicillin that was liberated from the hydrogel at a given
53 time t , whereas M_0 stands for the initial amount of ampicillin that was injected into the hydrogels [37].
54
55
56
57
58
59
60
61
62
63
64
65

4. Results and discussion

4.1 FTIR

FTIR spectra of all the hydrogel samples (CPG, CPG-3AR1, CPG-3AR2, CPG-3A) are given in Figure 2. For chitosan the absorption peaks of amide I was confirmed at 1674 cm^{-1} . The bands detected at 890 cm^{-1} and 1167 cm^{-1} were due to the existence of chitosan pyranose ring and saccharine. The symmetric and asymmetric C-H stretching in chitosan, gum arabic showed peaks at $2916\text{--}2873\text{ cm}^{-1}$. The hydrogen bond between polymeric chains, both intra- and intermolecular bonds, were confirmed by the broad peak value at $3556\text{--}3080\text{ cm}^{-1}$ that confirms the -OH stretching of all prepared hydrogels. The stretching vibration of C-N of PVP within the hydrogel networks are observed at peaks $1200\text{--}1400\text{ cm}^{-1}$. The Si-N peak appeared in the range of $934\text{--}940\text{ cm}^{-1}$. Carbonyl peak range (1655 cm^{-1} - 1649 cm^{-1}) confirmed that it shifted to lower wavenumber (1649 cm^{-1}) because of the formation of hydrogen bonding. The presence of Si-O-Si and Si-O-C that confirmed the crosslinking due to silanol groups showed the peaks, at of $1128\text{--}1016\text{ cm}^{-1}$ [38, 39].

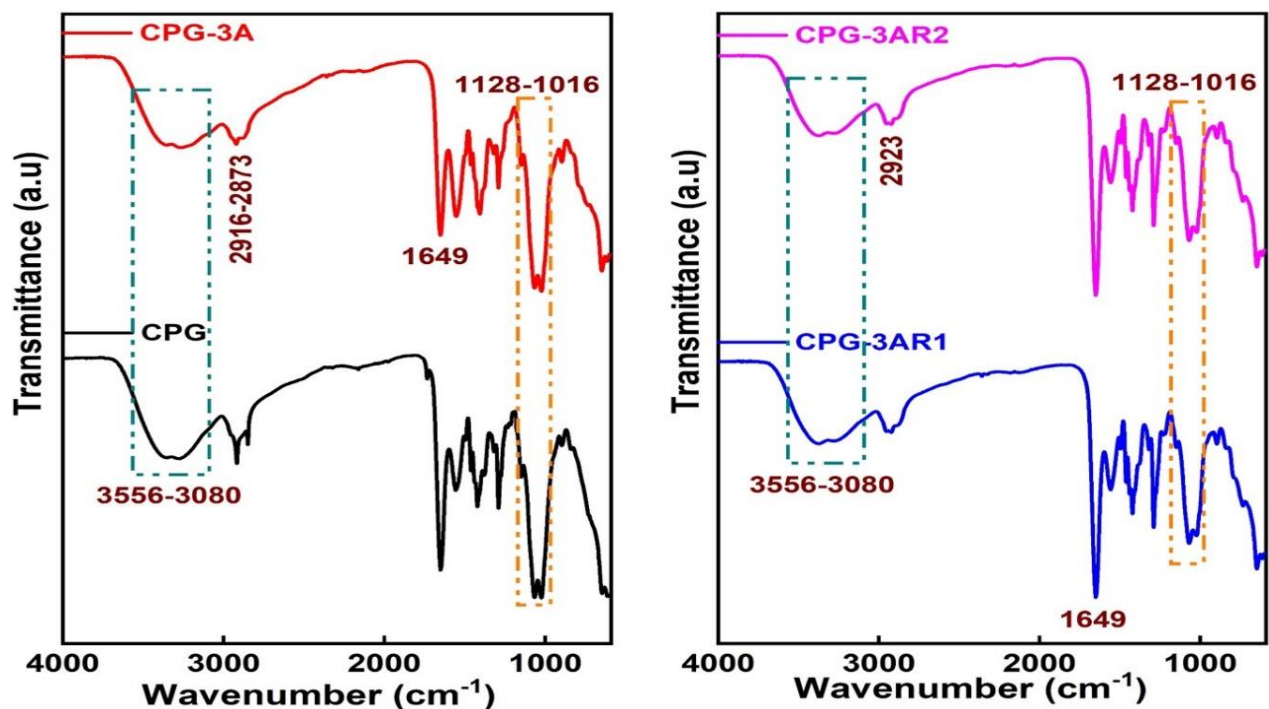


Fig.2 FTIR spectra of the CPGs hydrogels.

4.2 Swelling studies

4.2.1 Swelling trend in distilled water

The hydrogels swelling in water over time is illustrated in Figure 3. All the hydrogel samples exhibited a smooth progress of swelling over time but equilibrium time of all hydrogels was

1 different. This is crystal clear and can be observed from Figure 3. that crosslinking is inversely
2 proportional to swelling. Hydrogels showed low swelling with the addition of cross linker.
3 Addition of cross linker decreased the water entry as the cross linker not only increased the
4 number of pores but also decreased the pore size due to development of a number of inter and
5 intramolecular interactions. Consequently, it decreases the swelling of hydrogels with increase
6 in equilibrium time. The controlled sample swelling increased with the passage of time but it
7 showed less stability than other cross-linked hydrogels so it gets dissolved early. The
8 equilibrium time for controlled (CPG) hydrogel was observed 150 minutes and exhibited the
9 highest swelling (42 g/g) because of the absence of cross linker and its structure was less dense
10 than other cross-linked structures. CPG-3A showed abrupt increase in swelling at 180 minutes
11 it showed swelling 50.9 g/g and the equilibrium swelling time of CPG-3A was 210 min and its
12 swelling was 54.5 g/g. Because of the presence of cross linker, it showed stability than all
13 CPGs hydrogels. While swelling time was displayed by CPG-3AR1 and that of CPG-3AR2
14 was 180 min with swelling values 43.05 g/g and 44.95 g/g, respectively. Their equilibrium
15 time decreases than CPG-3A because of the presence of ethanolic extract of ratan-jot that causes
16 hydrolysis in hydrogels. On the other hand CPG-3AR2 showed more smooth linear curve rather
17 than CPG-3AR hydrogel may be due to highest volume of ethanolic extract in it[14].
18
19
20
21
22
23
24
25
26
27
28
29
30
31
32
33
34
35
36
37
38
39
40
41
42
43
44
45
46
47
48
49
50
51
52
53
54
55
56
57
58
59
60
61
62
63
64
65

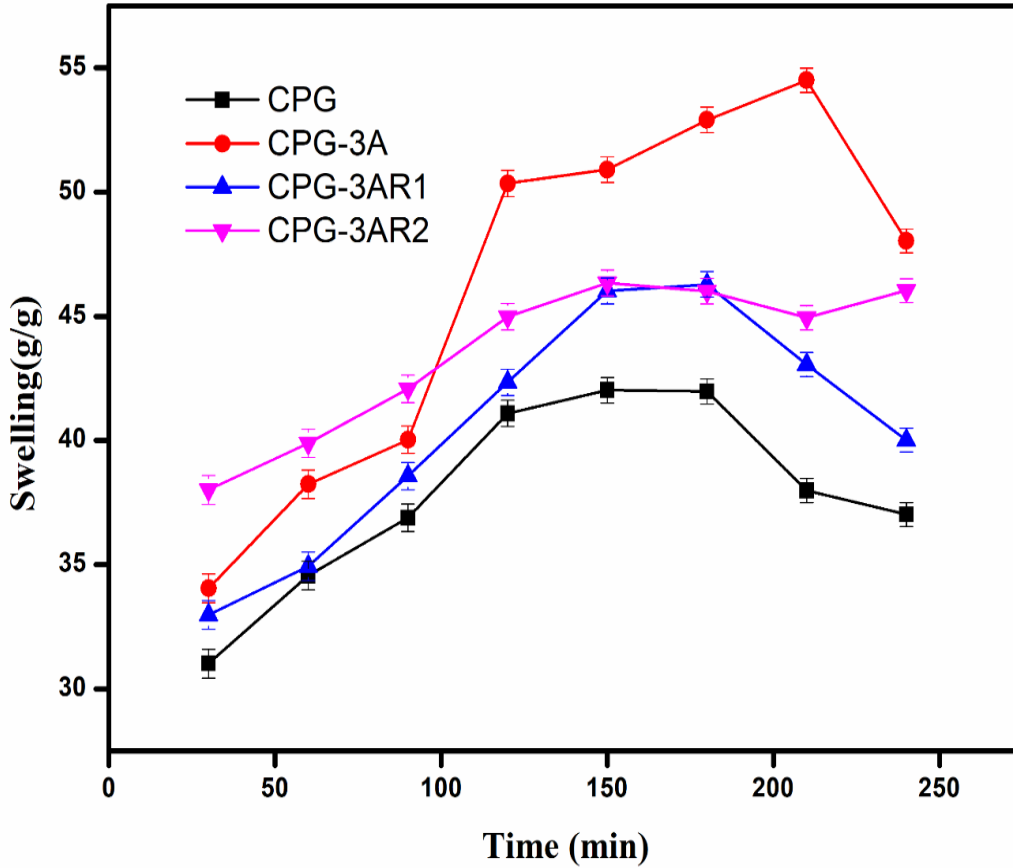


Fig.3 Swelling response of the prepared CPGs in distilled water.

4.2.1.1 Water diffusion method

The solvents migration from the surrounding extracellular matrix into the hydrogels internal structure affects the hydrogel's ability to expand. Researchers frequently use the following equation to shed light on the water diffusion mechanism that causes this swelling phenomenon:

$$F = kt^n \quad (6)$$

Understanding the transport of solvent inside hydrogels depends heavily on the swelling rate constant (k), F is the fractional swelling represented by the ratio of W_{eq} to W_t and the swelling exponent n [40]. Researchers may determine the values of n and k by computing the swelling data of hydrogels in distilled water. The value of n offers information on the solvent transport method in hydrogels. A Fickian Transport Mechanism indicates if $n \leq 0.5$, whereas a non-Fickian Mechanism indicates if $n \geq 0.5$ but less than 1.

By using swelling values of developed hydrogels (CPG, CPG-3A, CPG-3AR1, CPG-3AR2) a relationship between $(\ln t)$ and $(\ln F)$ is shown in Figure 4. In Table 2 the values of diffusion parameter are calculated and given. From the given data, it was determined that in fabricated

hydrogels CPG exhibited Non-Fickian diffusion mechanism as the n value was greater than 0.5. While all remaining hydrogels exhibited Fickian diffusion mechanism as the n value was less than 0.5.

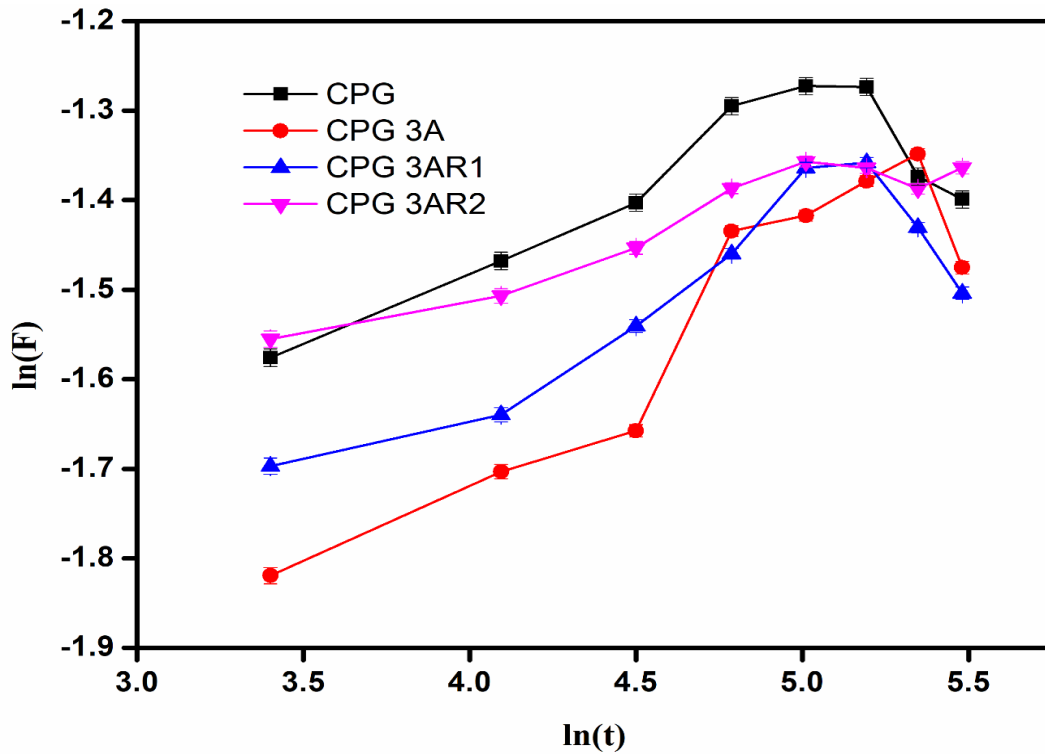


Fig. 4 CPGs hydrogels ln(F) vs. ln(t) plots.

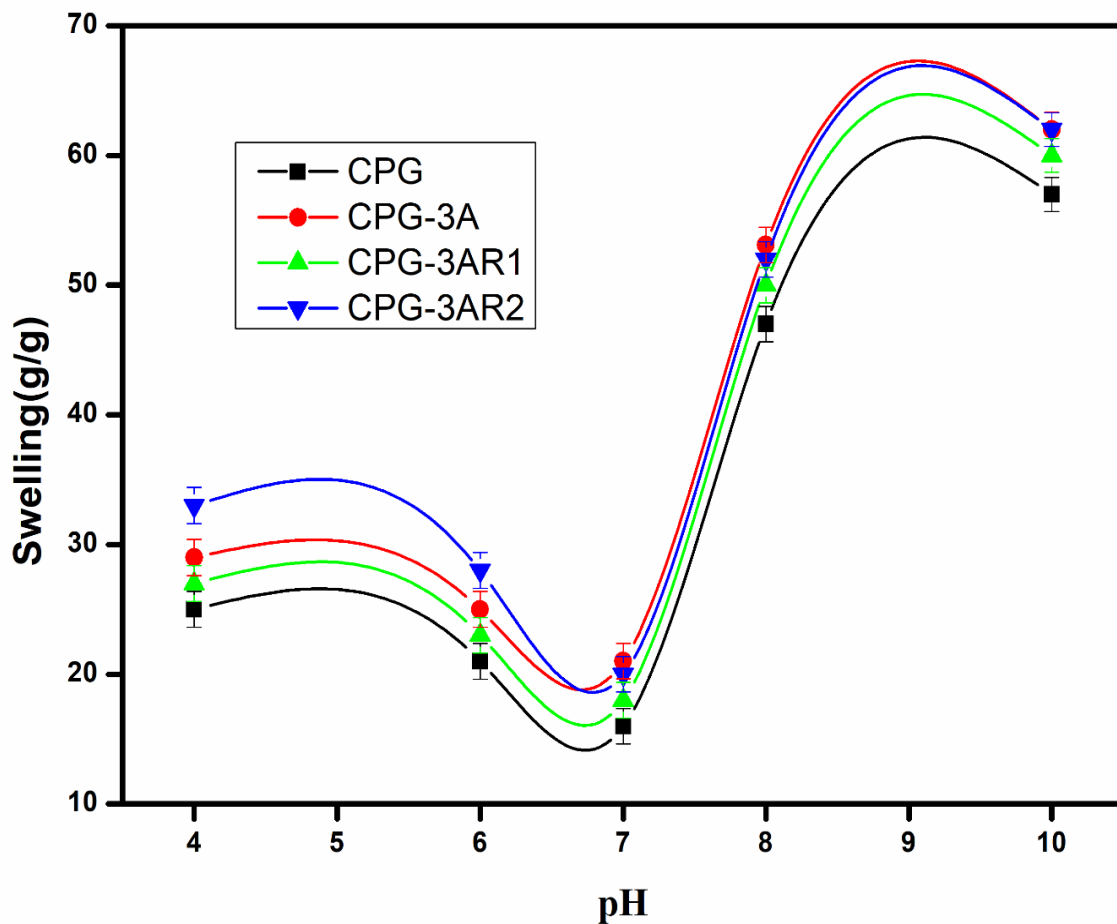
Table.2 Diffusion parameter of the CPGs hydrogels

Parameters	CPG	CPG-3A	CPG-3AR1	CPG-3AR2
n	0.814	0.262	0.205	0.125
Intercept	-2.209	-2.747	-2.436	-1.999
K	0.109	0.064	0.087	0.135
Regression(%)	96	91.9	91.9	92.9

4.2.2 Swelling in pH solutions

To investigate the behaviour of the generated hydrogel, a series of buffers with various pH values (10, 8, 7, 6, 4, 2 and 1.2) were created. Figure 5. shows how the hydrogel films swell over time in different buffers. It was shown that all the samples show pronounced swelling in an alkaline environment but this trend decreased in a neutral and acidic pH. Interestingly, the hydrogels started to swell once again around pH 8 to 10. The CPG (Control) sample exhibited the most swelling out of all the samples, which can be attributed to the large voids inside its

1 polymer network because it is uncrosslinked. As a result of greater covalent and physical
 2 bonding in other hydrogel samples, the network was denser and more compact, which reduced
 3 swelling. At pH values of 4, 6 and 7 the swelling response of all fabricated hydrogels was stable.
 4 The $-NH_2$ of chitosan and carboxylate group of gum arabic were the main interaction groups in
 5 the produced hydrogels. Notably, at pH 1.2 and 2 the hydrogels rapidly disintegrated
 6 completely. The high protonation of the chitosan's amino groups ($-NH_2$) into ammonium ions
 7 ($-NH_3^+$) is the reason that causes the high swelling in lower acidic media. As the pH increases
 8 swelling decreases because of amine group deprotonation. Chitosan amine group ($-NH_3^+$)
 9 started to deprotonate again when exposed to high pH environments. Resultantly, at pH 4, 6,
 10 and 7 there develop physical networks in CPGs hydrogels. While at higher pH like 8,10
 11 hydrogels showing its greatest expansion in alkaline pH solutions due to carboxylate group of
 12 gum arabic[41, 42].
 13
 14
 15
 16
 17
 18
 19
 20
 21

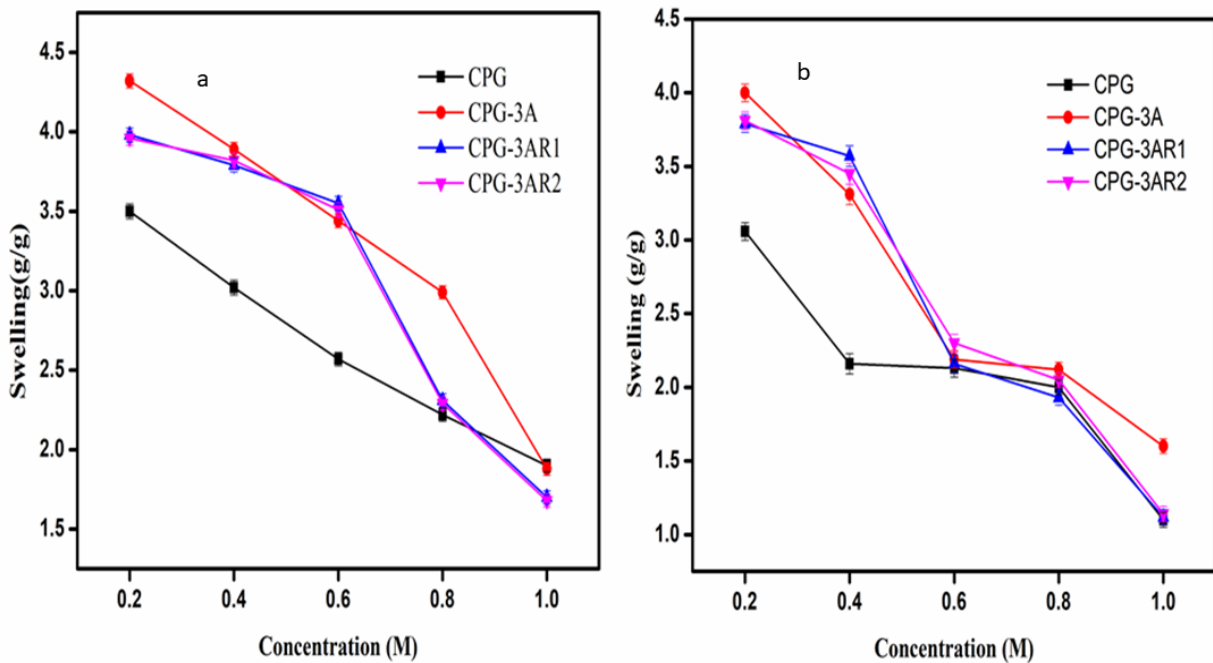


22
 23
 24
 25
 26
 27
 28
 29
 30
 31
 32
 33
 34
 35
 36
 37
 38
 39
 40
 41
 42
 43
 44
 45
 46
 47
 48
 49
 50
 51
 52
 53
 54 **Fig.5** Swelling indices of the CPGs in buffer solutions.

55 56 **4.2.3. Swelling in ionic solutions**

57 A wide variety of electrolytes with complex compositions can be found in the human body. As
 58 typical electrolytes for the investigation, NaCl and CaCl₂ were used. Because Na⁺ ions are
 59
 60
 61
 62
 63
 64
 65

1 monovalent and Ca^{++} ions are divalent, their charge-to-size ratios differ, substantially. The kind
 2 and concentration of salt used will determine how much hydrogels swell in ionic solutions.
 3 Using solutions with various concentrations of NaCl and CaCl_2 , the swelling behaviour of the
 4 CPGs series was assessed. Both salts have the same anions (Cl^-), but they have different cations
 5 (Na^+ and Ca^{2+}). According to Peppas et al. report from 2000, the concentration of these salts
 6 significantly affected how much the hydrogel swelled. Complex structures took place at lower
 7 salt concentrations, which caused the holes in the hydrogel to widen. According to Wang et al.
 8 explanation, as the amount of salt grew, the osmotic pressure between the external solution and
 9 the hydrogel dropped, hence limiting the extent of hydrogel swelling. Each hydrogels
 10 equilibrium time for the CPGs series swelling was calculated, as shown in Figure 6 [43].
 11
 12
 13
 14
 15
 16
 17
 18
 19
 20



21
22
23
24
25
26
27
28
29
30
31
32
33
34
35
36
37
38
39
40
41
42
43 **Fig.6** CPGs swelling indices in ionic solutions of CaCl_2 (b) and NaCl (a).
44

45 **4.3 Thermogravimetric analysis (TGA)**

46 Utilizing TGA, it was determined how the crosslinker affected the produced hydrogels thermal
 47 stability with a focus on the effect of 3-APDEMS concentration. Figure 7. shows 4 separate
 48 stages of thermal degradation together with the weight loss behaviour of the hydrogel samples.
 49 At first, weight loss up to 100°C was noticed, which was attributed to moisture loss and at about
 50 200°C , the degradation process occurs. At temperature 320°C , side chains or functional groups
 51 began to separate. At 470°C , more deterioration of the primary polymers backbone was seen.
 52 In the last stage, up to 500°C no weight loss was observed indicating residual or ash contents.
 53 All hydrogels completely degraded after 470°C showing similar pattern of degradation.
 54
 55
 56
 57
 58
 59
 60
 61
 62
 63
 64
 65

1
2 Although, it can be seen from the graph that thermal stability increases with the addition of
3 cross linker amount. The thermogram of CPG hydrogel with no cross linker showed 22%
4 weight loss at 240 °C. while at 400°C 50% weight loss was observed respectively. While for
5 CPG-3A, weight loss was 20%.at 240 °C whereas it was 50% at 404°C. On the other hand, the
6 CPG-3AR1, CPG-3AR2 both showed 21 %, weight loss at 240°C but CPG-3AR2 showed 50%
7 weight loss at 403°C while CPG-3AR1 showed 50% weight loss at temperature 401°C. It is
8 therefore, crystal clear that CPG-3AR among all crosslinked hydrogels is more thermally stable.
9 At 470°C the remaining residues of all hydrogels were CPG 23%,CPG-3A 26.52%, CPG-
10 3AR1 24.18% and CPG-3AR2 24.29% respectively [35, 42, 44].
11
12
13
14
15

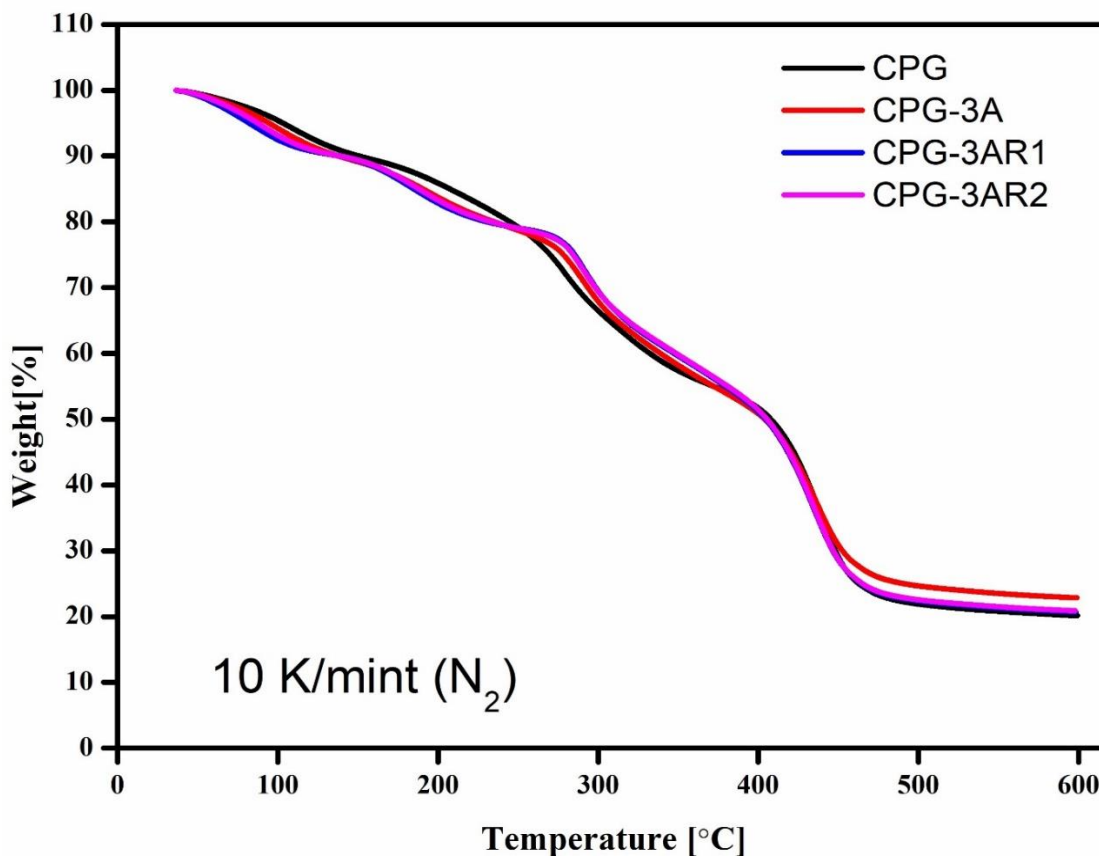


Fig.7 TGA thermograms of the CPGs hydrogels.

4.4 Scanning electron microscopy (SEM)

Figure 8 shows the morphology of the hydrogels made from chitosan, PVP and gum arabic. Without a crosslinker, the hydrogels showed surface abnormalities, including observable depressions (Figure.8). However, the hydrogels showed a more uniform and smooth surface when 3-APDEMS was introduced as a crosslinker (SEM pictures). These photos unmistakably show that the prepared hydrogels have a distinct porous structure, the crosslinker and ethanolic ratan-jot extract addition significantly contributing to the creation of pores in CPG-

1
2
3
4
5
6
7
8
9
10
11
12
13
14
15
16
17
18
19
20
21
22
23
24
25
26
27
28
29
30
31
32
33
34
35
36
37
38
39
40
41
42
43
44
45
46
47
48
49
50
51
52
53
54
55
56
57
58
59
60
61
62
63
64
65

3A, CPG-3AR1 and CPG-3AR2. These micrographs show that the addition of a particular amount of crosslinker (50 μL) caused the creation of many pores that were uniformly spaced across the surface (Figure .9). In fact, the extra OH groups produced by the addition of the right quantity of crosslinker as well as extract encouraged the growth and expansion of the hydrogel network between the polymer chains. The improved water absorption seen in CGPs gels with a crosslinker likely results from this improvement, which also makes the gels appropriate for gas exchange and encapsulating biological agents [34] .

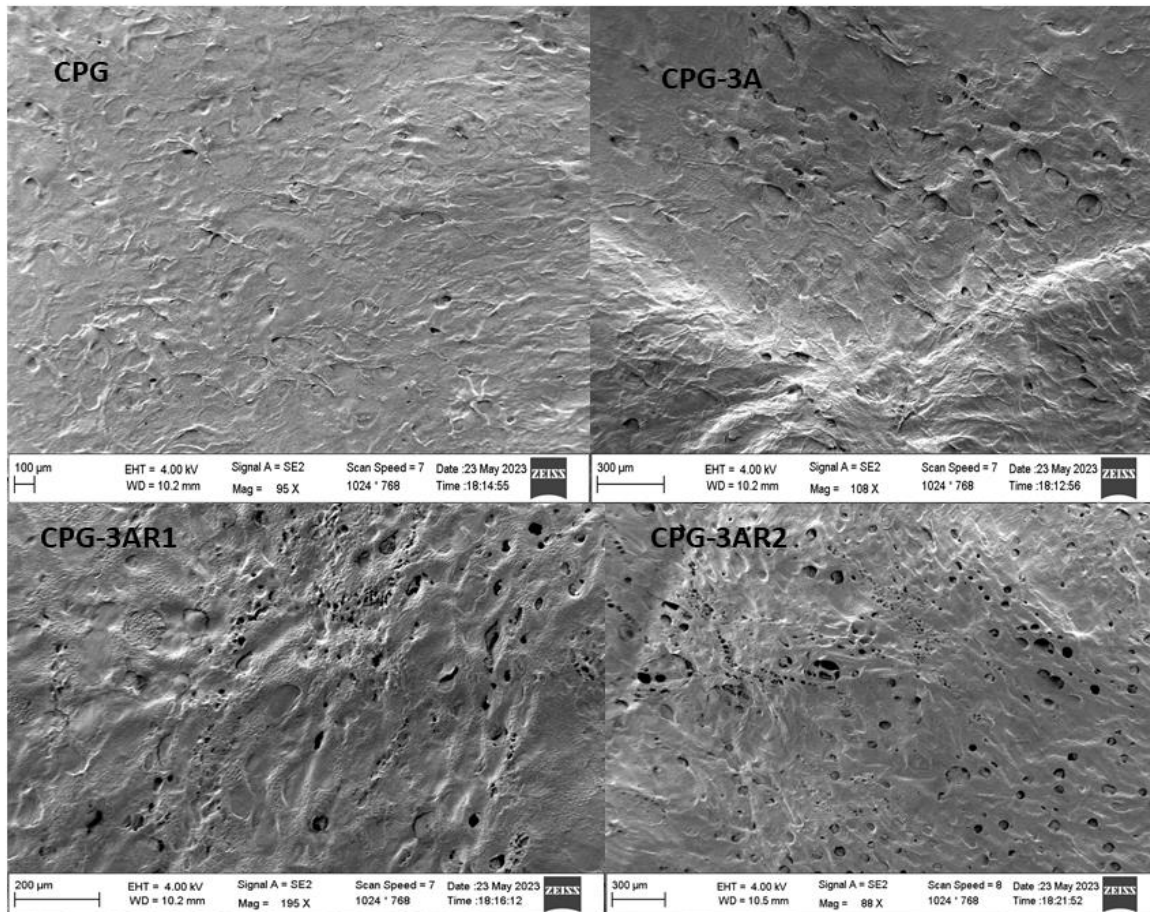


Fig.8 SEM micrographs of CPG (control), CPG-3A, CPG-3AR1 and CPG-3AR2.

4.5 *In-vitro* biodegradation analysis

Figure 9. illustrates the relationship between incubation period and degradation by showing the biodegradation profile of the CPGs. It has been noted that the crosslinking agent increases the stability of the hydrogels and that the rate of degradation increases without any concentration of 3-APDEMS. When the concentration of 3-APDEMS is utilised, the degradation rate gradually drops over the time. Furthermore, degradation also rises when ratan-jot extract is added because it results in hydrolysis in the hydrogel. Although, gum Arabic is natural polymer but here, the degrading behaviour is mostly related to the presence of CS, a biopolymer that

breaks down into oligosaccharide units of various lengths and dissolves glycosidic linkages. This degradation is basically caused by the dissociation of secondary and primary interactions in fabricated hydrogel. These interactions developed due to CS,GA,PVP and 3-APDEMS functional groups (-OH,-NH₂).Smaller polymeric chains are created from these weak connections and are subsequently broken down by mtabolic processes [45].

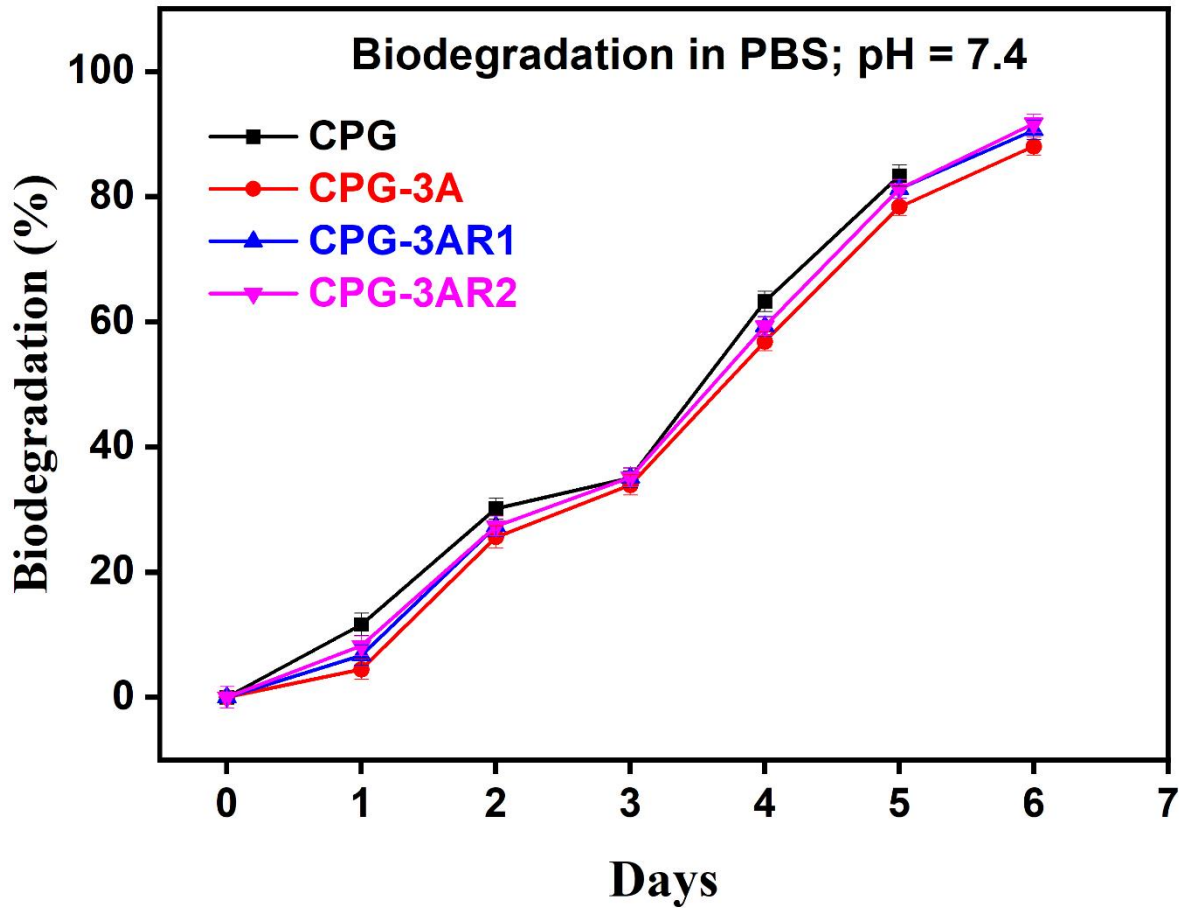
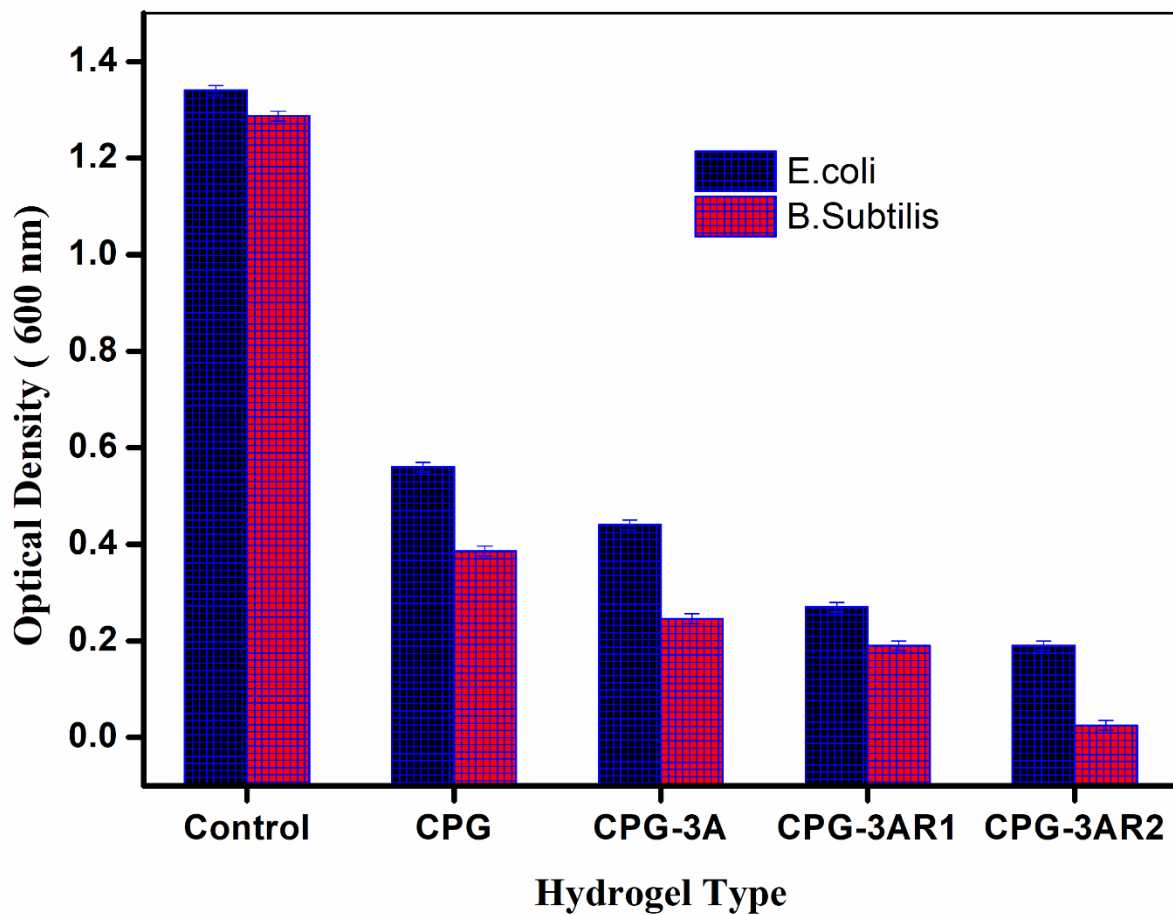


Fig.9 Degradation (%) of the CPGs in the PBS solution

4.6 Microbial resistance

Figure 10. presents the results of the liquid diffusion method used to evaluate the hydrogels antibacterial properties. The control solutions absorbance value was found to be 1.34 for *E.Coli* and 1.287 for *B.Subtilis* . On the other hand, the test sample absorbance values were less than 1.34 and 1.287 which suggests efficient inhibition. The inhibition of bacterial growth is mainly caused by 3-APDEMS crosslinker and ratan-jot extracts. Interestingly, CPG-3AR2 demonstrated an especially remarkable capacity to inhibit bacteria's growth. The negatively charged bacterial cell wall interacted with the test samples, which contained cationic (positively charged) chitosan. Due to the interaction, the *E.Coli* cell wall was disrupted, the bacterial cell was penetrated and the growth of the bacteria was inhibited by preventing the conversion of

1 DNA into RNA. Through hydrogen bonding and physical interactions with the bacterial cell
2 wall, PVP and GA play a critical role in controlling the growth of gram positive bacteria. The
3 hydroxyl groups in GA, the C=O and NH groups in PVP make interactions with bacterial cell
4 wall. These interactions cause the bacterial cell walls structural integrity to be weakened, which
5 prevents bacteria from growing. On the other side, because of double quantity of antibacterial
6 resistant ratan-jot extract in this gel, it shows excellent antibacterial activity. The CPGs
7 demonstrated greater antibacterial activity against B. subtilis because of its thick peptidoglycan layer,
8 which makes it more vulnerable to the antimicrobial chemicals inside the hydrogel. E. coli, on the other
9 hand, has an outer membrane made of lipopolysaccharides that acts as a barrier to protect it from
10 antibacterial substances. This discrepancy in antibacterial efficacy is explained by this structural
11 difference [46, 47].
12
13
14
15
16
17
18
19
20



51
52 **Fig.10** Antibacterial resistance of CPGs hydrogels.

53 4.7 Cytotoxicity analysis

54
55 Analysing cytotoxicity is a useful technique for identifying potential problems with local tissue
56 response. It enables assessment of cell toxicity and offers information on how cells and tissues
57 react. By using the equation 3 from Section 3.6 and looking at both living and dead nauplii
58
59
60
61
62
63
64
65

under a light microscope, in-vitro cytotoxicity examination of the hydrogel samples was carried out. Numerous reasons, including chemical cytotoxicity, dissolved oxygen deficit in sea water and the development of a viscous film on the nauplii gills, can be blamed for the death of nauplii. The low proportion of mortality seen at lower fix cross linker doses in this investigation indicates that the likelihood of nauplii dying from toxicity is extremely low (Table. 3). It is also important to note that when the concentration of ratan-jot extract exceeds to 300 μ L, the percentage of nauplii death also decreases by diminishing the toxic effects due to prevention of bacterial growth, retaining the sterile environment and cellular growth. The hydrogel samples utilised in the study were made with CS, GA, PVP, 3-APDEMS and ratan jot extract all of which are FDA-approved and recognised as being biocompatible. This is very important to keep in mind that the development of viscous layers on the gills of the nauplii may be responsible for this low mortality. These layers may prevent oxygen from passing through, killing the nauplii in the process [47, 48].

Table.3 Percentage of *A. Salina* deaths following 24-hour exposure to CPGs

Types of Hydrogels	Mortality (%)
CPG	1.72
CPG-3A	1.56
CPG-3AR1	1.51
CPG-3AR2	1.47

4.8 Porosity

In the context of hydrogel applications for drug release, porosity is essential since it improves the hydrogel matrix ability to absorb pharmaceuticals and makes their dispersion more uniform. This study focused on porosity evaluation, particularly with regard to CPG hydrogels. In Table. 4. the outcomes of porosity are shown, which indicates that the presence of cross-linker along with the higher concentration of ethanolic ratan-jot plant extract, both these lead to the hydrogels increased porosity. 3-APDEMS is essential in increasing porosity, the crosslinker encouraging the creation of connected channels. The increased concentration of hydroxyl groups in CPG hydrogels facilitates the formation of additional hydrogen and covalent bonds. As a result, this network structure strengthening is responsible for the initial rise in porosity.

Hydrogel expansion further encouraged by the addition of ethanolic ratan-jot plant extract. By increasing the plant extract concentration, more gaps are created inside the structure that causes

1 hydrogels to expand more. Remarkably, the ethanolic ratan-jot extract and 3-APDEMS both
2 played a significant role in enhancing the porosity of CPG hydrogels from 53% to 58% [49].
3
4
5
6

7 **Table.4** Porosity of prepared hydrogels.
8

9 Sample code	10 Porosity (%)
11 CPG	53.07+0.87
12 CPG-3A	57.03+0.71
13 CPG-3AR1	58.41+0.21
14 CPG-3AR2	58.89+1.02

19 **4.9 Contact angle**

20 Curious discoveries were made when CPGs hydrogels contact angles were studied. These are
21 shown in Figure 11. CPG(control) had the largest contact angle (73°) among all the CPGs
22 hydrogels when CPGs hydrogels with different concentrations of ratan-jot extract and specific
23 amount of cross-linker were compared. Contact Angle values decreased as a result of the
24 addition of 3-APDEMS as well as plant extract concentration. The contact angle approaches
25 0° when water droplets spread out across the hydrogel sheet due to strong adhesion. Angles of
26 contact between 0° and 90° indicating that the hydrogel is hydrophilic, while angles larger than
27 90° indicate that it is hydrophobic. Results shows that all fabricated hydrogels are
28 hydrophilic[50, 51].
29
30
31
32
33
34
35
36
37
38
39
40
41
42
43
44
45
46
47
48
49
50
51
52
53
54
55
56
57
58
59
60
61
62
63
64
65

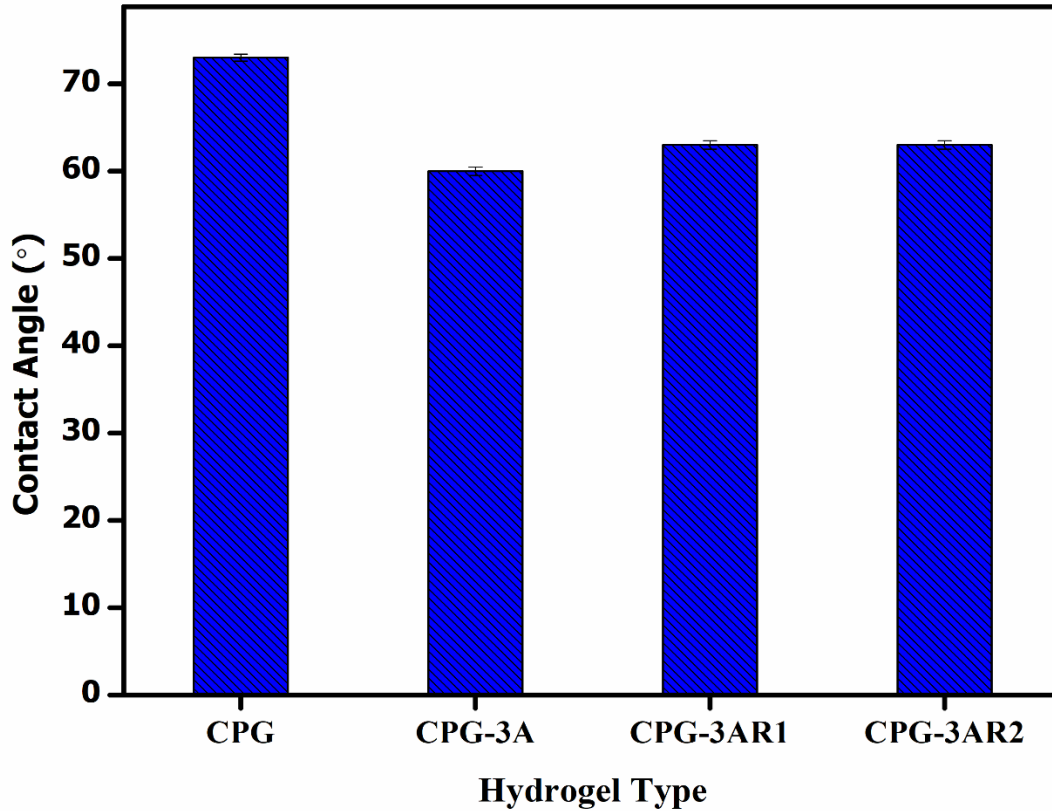


Fig.11 Hydrophilicity response of the CPGs hydrogels.

4.10 Drug release analysis and its kinetics

Using CPG-3AR2 as the carrier, the release % of ampicillin sodium was investigated over a time in a PBS solution (pH 7.4) at 37°C. Notably, the CPGs hydrogels showed noticeable swelling in an acidic as well as in basic environment showing that they may release the medication quickly in that setting. The drug release from the loaded samples was, therefore, assessed using a pH 7.4 (PBS) solution. This decision was made due to the reason that regulated release would be difficult to achieve if the medicine was administered orally because of how quickly it would be released in the stomach acidic environment. Contrarily, medicine release was regulated at blood pH levels, favouring injectable administration. In about 2 hour and 40 minutes, the drug release efficiency was precisely attained, reaching 80.82% and at about 180 minutes its release was 98.717%. (Figure 12). In study 2024, Andlib et al. created a chitosan-based carrier with a 90-minute drug release rate of over 98.236% [37]. The value of the exponent coefficient (n) in equation (6) plays a critical role in defining the diffusion way by which the medication is released from the hydrogel. The value of n for CPG-3AR2 hydrogel observed as 0.63 confirming the Non-Fickian diffusion process.

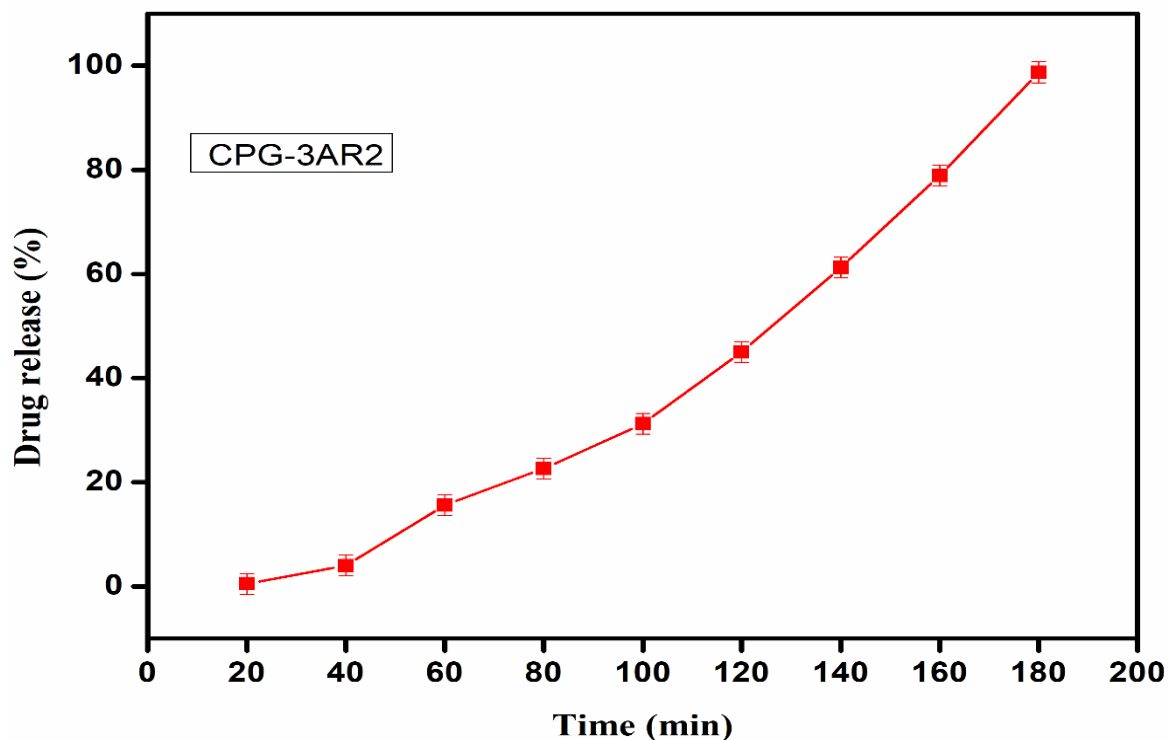


Fig.12 Drug release profile of engineered CPG-3AR2 sample in PBS solution

5. Conclusions

Through solution casting method, a new pH-sensitive cross-linked hydrogels were made by utilising biopolymers. Chitosan (CS), gum arabic(GA), polyvinylpyrrolidone (PVP) and 3-aminopropyl-diethoxymethylsilane (APDEMS) were expertly combined with anti-inflammatory ratan-jot extract to create these unusual hydrogels. FTIR spectroscopy was used to verify that the hydrogel components successfully interacted with one another. The CPGs gels with excellent biodegradation, pH sensitivity, antibacterial as well as cytotoxic behaviour makes it a good option for injectable drug delivery application. To determine the significance of the produced CPGs, the controlled release behaviour of CPG-3AR2 loaded with Ampicillin sodium was checked, attaining release rates of 98.717% in PBS, respectively, over 180 minutes. CPG showed the largest swelling capability, reaching 54.5g/g. However, the level of edema in distilled water reduced as the amount of 3-APDEMS rose. CPG-3A had the greatest thermal stability of all the samples. These hydrogels did not demonstrate hazardous effects on cell growth, according to an in vitro cytotoxicity analysis, which allowed cells to behave normally and follow their usual life cycles. The developed hydrogels are very promising for the controlled release of drug but however these are only studied with ampicillin sodium as a model drug for drug

1
2
3
4
5
6
7
8
9
10
11
12
13
14
15
16
17
18
19
20
21
22
23
24
25
26
27
28
29
30
31
32
33
34
35
36
37
38
39
40
41
42
43
44
45
46
47
48
49
50
51
52
53
54
55
56
57
58
59
60
61
62
63
64
65

release experiment. Also the controlled release time of ampicillin sodium from the hydrogel is 180 minutes. We have performed only in in-vitro analysis but for more clinical and in-vivo studies more analysis will be performed in future.

References

1. Sur, S., et al., *Recent developments in functionalized polymer nanoparticles for efficient drug delivery system*. Nano-Structures & Nano-Objects, 2019. **20**: p. 100397.
2. Huang, H., et al., *Thermo-sensitive hydrogels for delivering biotherapeutic molecules: A review*. Saudi Pharmaceutical Journal, 2019. **27**(7): p. 990-999.
3. Pacheco, C., et al., *Recent advances in long-acting drug delivery systems for anticancer drug*. Advanced Drug Delivery Reviews, 2023. **194**: p. 114724.
4. Huang, H., et al., *Thermo-sensitive hydrogels for delivering biotherapeutic molecules: A review*. Saudi Pharmaceutical Journal, 2019.
5. Zhang, Q., et al., *Recent advances in protein hydrogels: From design, structural and functional regulations to healthcare applications*. Chemical Engineering Journal, 2023. **451**: p. 138494.
6. Malik, M.K., et al., *Significance of chemically derivatized starch as drug carrier in developing novel drug delivery devices*. The Natural Products Journal, 2023. **13**(6): p. 40-53.
7. Fan, X., et al., *Mussel-induced nano-silver antibacterial, self-healing, self-adhesive, anti-freezing, and moisturizing dual-network organohydrogel based on SA-PBA/PVA/CNTs as flexible wearable strain sensors*. Polymer, 2022. **256**: p. 125270.
8. Luo, Y., et al., *From crosslinking strategies to biomedical applications of hyaluronic acid-based hydrogels: A review*. International Journal of Biological Macromolecules, 2023. **231**: p. 123308.
9. Yu, W., et al., *Hydrogel-mediated drug delivery for treating stroke*. Chinese Chemical Letters, 2023: p. 108205.
10. Barberi, G., et al., *Thermosensitive and mucoadhesive Xanthan gum-based hydrogel for local release of anti-Candida peptide*. Journal of Drug Delivery Science and Technology, 2024. **100**: p. 106054.
11. Hernandez Rivera, G., et al., *PVA-gelatine based hydrogel loaded with astaxanthin and mesoporous bioactive glass nanoparticles for wound healing*. Journal of Drug Delivery Science and Technology, 2024: p. 106235.
12. Li, T., et al., *Biocompatible puerarin injectable-hydrogel using self-assembly tetrapeptide for local treatment of osteoarthritis in rats*. Journal of Drug Delivery Science and Technology, 2022. **78**: p. 103909.
13. Zulaikha, W., M. Zaki Hassan, and S.a. Abdul Aziz, *Nanoparticle-embedded hydrogels as a functional polymeric composite for biomedical applications*. Materials Today: Proceedings, 2023.
14. Qureshi, M.A.u.R., N. Arshad, and A. Rasool, *Graphene oxide reinforced biopolymeric (chitosan) hydrogels for controlled cephadrine release*. International Journal of Biological Macromolecules, 2023. **242**: p. 124948.
15. Shariatinia, Z. and A.M. Jalali, *Chitosan-based hydrogels: Preparation, properties and applications*. International Journal of Biological Macromolecules, 2018. **115**: p. 194-220.
16. Mohite, P., et al., *Chitosan-Based Hydrogel in the Management of Dermal Infections: A Review*. Gels, 2023. **9**(7): p. 594.
17. Sudheer, S., S. Bandyopadhyay, and R. Bhat, *Sustainable polysaccharide and protein hydrogel-based packaging materials for food products: A review*. International Journal of Biological Macromolecules, 2023. **248**: p. 125845.

18. Ahmad, S., et al., *Antimicrobial gum based hydrogels as adsorbents for the removal of organic and inorganic pollutants*. Journal of Water Process Engineering, 2023. **51**: p. 103377.
19. Amaya-Chantaca, N.J., et al., *Semi-IPN hydrogels of collagen and gum arabic with antibacterial capacity and controlled release of drugs for potential application in wound healing*. Progress in Biomaterials, 2023. **12**(1): p. 25-40.
20. Cai, L., et al., *Polypeptide-based self-healing hydrogels: Design and biomedical applications*. Acta Biomaterialia, 2020. **113**: p. 84-100.
21. Nisar, S., et al., *5 - Recent advances in natural polymer based hydrogels for wound healing applications*, in *Advances in Healthcare and Protective Textiles*, S. ul-Islam, A. Majumdar, and B. Butola, Editors. 2023, Woodhead Publishing. p. 115-149.
22. Kurakula, M. and G.K. Rao, *Moving polyvinyl pyrrolidone electrospun nanofibers and bioprinted scaffolds toward multidisciplinary biomedical applications*. European Polymer Journal, 2020. **136**: p. 109919.
23. Gupta, B., et al., *Cellulosic polymers for enhancing drug bioavailability in ocular drug delivery systems*. Pharmaceuticals, 2021. **14**(11): p. 1201.
24. Franco, P. and I. De Marco, *The Use of Poly(N-vinyl pyrrolidone) in the Delivery of Drugs: A Review*. Polymers, 2020. **12**(5): p. 1114.
25. Rasekh, M., et al., *Electrospun PVP–indomethacin constituents for transdermal dressings and drug delivery devices*. International Journal of Pharmaceutics, 2014. **473**(1-2): p. 95-104.
26. Demeter, M., et al., *Biocompatible and antimicrobial chitosan/PVP/PEO/PAA/AgNP composite hydrogels synthesized by e-beam cross-linking*. Radiation Physics and Chemistry, 2024. **216**: p. 111391.
27. Kanwal, M., et al., *Cytocompatible and stimuli-responsive chitosan based carrier with 3-aminopropyl(diethoxy)methylsilane for controlled release of cefixime*. Chemical Papers, 2023. **77**(9): p. 5571-5586.
28. Zahoor, S., et al., *Diabetic wound healing potential of silk sericin protein based hydrogels enriched with plant extracts*. International Journal of Biological Macromolecules, 2023. **242**: p. 125184.
29. Yahia, S., I.A. Khalil, and I.M. El-Sherbiny, *Dual antituberculosis drugs-loaded gelatin hydrogel bioimplant for treating spinal tuberculosis*. International Journal of Pharmaceutics, 2023. **633**: p. 122609.
30. Bisht, A., V. Kamboj, and A. Bisht. *Reviewing Medicinal Plants of Treasure Land: The Indian Himalayan Range*. in *Environmental Pollution and Natural Resource Management*. 2022. Cham: Springer International Publishing.
31. Farooq, A., et al., *Designing Kappa-carrageenan/guar gum/polyvinyl alcohol-based pH-responsive silane-crosslinked hydrogels for controlled release of cephadrine*. Journal of Drug Delivery Science and Technology, 2022. **67**: p. 102969.
32. Bashir, A., et al., *Co-concentration effect of silane with natural extract on biodegradable polymeric films for food packaging*. International Journal of Biological Macromolecules, 2018. **106**: p. 351-359.
33. Rehmat, S., et al., *Novel Stimuli-Responsive Pectin-PVP-Functionalized Clay Based Smart Hydrogels for Drug Delivery and Controlled Release Application*. Frontiers in Materials, 2022. **9**.
34. Jabeen, S., et al., *Development of a novel pH sensitive silane crosslinked injectable hydrogel for controlled release of neomycin sulfate*. International Journal of Biological Macromolecules, 2017. **97**: p. 218-227.
35. Gull, N., et al., *Inflammation targeted chitosan-based hydrogel for controlled release of diclofenac sodium*. International Journal of Biological Macromolecules, 2020. **162**: p. 175-187.

- 1
2
3
4
5
6
7
8
9
10
11
12
13
14
15
16
17
18
19
20
21
22
23
24
25
26
27
28
29
30
31
32
33
34
35
36
37
38
39
40
41
42
43
44
45
46
47
48
49
50
51
52
53
54
55
56
57
58
59
60
61
62
63
64
65
36. Qu, Q., et al., *Strength and targeted-sustained release properties of sodium alginate-polyacrylamide hydrogel for anti-wrinkle eye-patch*. Journal of Drug Delivery Science and Technology, 2024. **100**: p. 106065.
 37. Andlib, H., M. Shafiq, and A. Sabir, *Sodium Ampicillin release from biocompatible hydrogel with enhanced antibacterial characteristics*. Journal of Drug Delivery Science and Technology, 2024: p. 106086.
 38. Jadoon, A., et al., *Probing the role of hydrolytically stable, 3-aminopropyl triethoxysilane crosslinked chitosan/graphene oxide membrane towards Congo red dye adsorption*. Current Applied Physics, 2022. **40**: p. 110-118.
 39. Ghauri, Z.H., et al., *Development and evaluation of pH-sensitive biodegradable ternary blended hydrogel films (chitosan/guar gum/PVP) for drug delivery application*. Scientific Reports, 2021. **11**(1): p. 21255.
 40. Andlib, H., M. Shafiq, and A. Sabir, *Development of pomegranate peel extract amalgamated ternary hydrogel with synergistic antibacterial efficacy against Escherichia Coli (E. Coli)*. 2024.
 41. Felinto, M.C., et al., *The swelling behavior of chitosan hydrogels membranes obtained by UV- and γ -radiation*. Nuclear Instruments and Methods in Physics Research Section B: Beam Interactions with Materials and Atoms, 2007. **265**(1): p. 418-424.
 42. Feyissa, Z., et al., *Fabrication of pH-Responsive Chitosan/Polyvinylpyrrolidone Hydrogels for Controlled Release of Metronidazole and Antibacterial Properties*. International Journal of Polymer Science, 2023. **2023**: p. 1205092.
 43. Risbud, M., et al., *pH-sensitive freeze-dried Chitosan-polyvinyl hydrogels as controlled release system for antibiotic delivery*. Journal of controlled release : official journal of the Controlled Release Society, 2000. **68**: p. 23-30.
 44. Sabbagh, H.A.K., et al., *A statistical study on the development of metronidazole-chitosan-alginate nanocomposite formulation using the full factorial design*. Polymers, 2020. **12**(4): p. 772.
 45. Azaza, Y.B., et al., *Chitosan/collagen-based hydrogels for sustainable development: Phycocyanin controlled release*. Sustainable Chemistry and Pharmacy, 2023. **31**: p. 100905.
 46. Sarmah, D., et al., *Self-cross-linked starch/chitosan hydrogel as a biocompatible vehicle for controlled release of drug*. International Journal of Biological Macromolecules, 2023. **237**: p. 124206.
 47. Gull, N., et al., *In vitro study of chitosan-based multi-responsive hydrogels as drug release vehicles: a preclinical study*. RSC Advances, 2019. **9**(53): p. 31078-31091.
 48. Suneka, S. and T. Manoranjan, *Brine shrimp lethality assay with selected medicinal plants extracts*. Vignanam Journal of Science, 2021.
 49. Pan, H., et al., *Non-stick hemostasis hydrogels as dressings with bacterial barrier activity for cutaneous wound healing*. Materials Science and Engineering: C, 2019. **105**: p. 110118.
 50. Ahmad, F., et al., *An eco-friendly hydroentangled cotton non-woven membrane with alginate hydrogel for water filtration*. International Journal of Biological Macromolecules, 2024. **256**: p. 128422.
 51. Hafeez, S., et al., *Fabrication of pectin-based stimuli responsive hydrogel for the controlled release of ceftriaxone*. Chemical Papers, 2023. **77**(4): p. 1809-1819.